Trafficking of Polarized Membrane Proteins in Developing and Mature Hippocampal Neurons

By

Jennifer Dawn Petersen

A Dissertation

Presented to the Neuroscience Graduate Program

and the Oregon Health & Science University

School of Medicine

in partial fulfillment of

the requirements for the degree of

Doctor of Philosophy

April 2009

School of Medicine
Oregon Health & Science University

CERTIFICATE OF APPROVAL

This is to certify that the Ph.D. dissertation of

Jennifer Dawn Petersen

has been approved

Gary Banker	Mentor
Peter Gillespie	Committee Member
John Adelman	Committee Member
Wolfhard Almers	Committee Member
Philip Copenhaver	Committee Member

TABLE OF CONTENTS

LIST OF FIGURES

Chapter 2

Chapter 3

LIST OF SUPPLEMENTAL MOVIES

LIST OF ABBREVIATIONS

ANF	atrial natriuretic factor
APP	amyloid precursor protein
BDNF	brain derived neurotrophic factor
CA-Kinesin-1	constitutively active Kinesin-1
CCD	charged-coupled device
C. elegans	the nematode, *Caenorhabditis elegans*
COS	cell line derived from kidney of the African green monkey
CK2	protein kinase CK2 (formerly called Casein Kinase 2)
CNS	central nervous system
DIV	days *in vitro*
EM	electron microscopy
GFP	green fluorescent protein
EB3	end-binding protein 3
GPI	Glycosyl-phosphosphatidylinositol
GSK3	glycogen synthase kinase 3
IDA-1	*C. elegans* ortholog of mammalian phogrin
IκBα	inhibitor of κB-α
IKK	inhibitor of κB kinase
imac	gene encoding the mammalian KIF1A ortholog in *Drosophila*
ISG	immature secretory granule
JIP	JNK-interacting protein
JNK	c-Jun N-Terminal kinase
KHC	kinesin heavy chain
KIF	kinesin superfamily protein
KLC	kinesin light chain
KCNQ	voltage gated potassium channel
Lys	the amino acid lysine
MAP	microtubule associated protein
mCherry	monomeric Cherry red fluorescent protein
MDCK	Madin-Darby canine kidney
mRFP	monomeric red fluorescent protein
Na_v	voltage-dependent sodium channel
NF-κB	nuclear factor κ-light-chain-enhancer of activated B cells
NgCAM	neuron-glia cell adhesion molecule
NPY	neuropeptide Y
NrCAM	NgCAM-related cell adhesion molecule
PC12	tumor cell line from rat adrenal medulla chromaffin cells
pIκBα	phosphorylated inhibitor of κB-α
PNS	peripheral nervous system
PTM	post translational modification
SEPT2	septin 2
shRNA	short hairpin RNA
siRNA	small interfering RNA
SLMV	synaptic-like micro-vesicle

ss	signal sequence
tdTomato	tandem Tomato red fluorescent protein
TfR	transferrin receptor
TGN	*trans* Golgi network
TTCP	tubulin tyrosine carboxypeptidase
TTL	tubulin-tyrosine ligase
unc	genes associated with uncoordinated behavior in *C. elegans*
VSV-GtsO45	temperature-sensitive vesicular stomatitis virus G-protein
YFP	yellow fluorescent protein

Acknowledgements

First and foremost, I would like to extend a heartfelt thanks to my mentor Dr. Gary Banker for accepting me into his lab as a graduate student, and providing me with extensive training in live-cell imaging of neurons. Gary's high standards for experimental rationale, image quality, data analysis, and interpretation of results have pushed me to grow intellectually and will improve the quality of my work for the rest of my life. Also integral to my success as a graduate student was the mentoring I received from Dr. Stefanie Kaech. Her breadth of knowledge in neuronal cell biology and microscopy has made working with her a rich learning experience. I would also like to thank Julie Luisi Harp and Barbara Smoody for their technical support in providing genetic constructs and cultured neurons, respectively, as well as their friendship throughout my time in the lab. Thanks also to the post-docs in the lab—Chun-fang Huang, Cheng Fang, and Bernard Sampo—all of whom offered much guidance and encouragement throughout my tenure as a student. Fellow graduate students Brian Jenkins, Greta Glover, Catherine Jacobson, and Sonal Das also helped me along the way, and I thank them for their camaraderie. Thanks also to my thesis advisory committee chair Dr. Peter Gillespie, as well as the other members of my committee: Wolf Almers, John Adelman, and Philip Copenhaver, each of whom was a much appreciated source of counsel and encouragement. A special acknowledgement is also owed to my long-time mentor and friend, Dr. Thomas S. Reese who taught me to greet both science and life with intensity, imagination, and the highest of expectations. Countless thanks are also owed to my friends, especially Jill Wentzell, Jennifer Horn, Anna Malyala, Catherine Jacobson, Emily Pratt, Helen Tanner, and Mary Ann and Alfred Killilea who bring joy to my life and provide strong shoulders to lean on when needed. Thanks also to my dog Sky who has shared this Oregon adventure with me and made every day brighter. Finally, thanks to my parents Gail and Hal, my brother Jeff, my grandmother Madalene Gregory, and the rest of my family for the encouragement and support that enabled me to successfully complete this doctorate.

Abstract

This dissertation presents studies concerning two specific aspects of protein trafficking in neurons. First, live-cell imaging of GFP-tagged dendritic proteins in cultured hippocampal neurons was used to study the selective transport of dendritic proteins, which are specifically blocked from entering the axon. This selective transport is likely the primary mechanism by which dendritic proteins are restricted to the somatodendritic domain, and is therefore critical to neuronal function. The block of dendritic transport into the axon was found to have two components; selective entry, which reduced the probability that a dendritic vesicle would enter the axon, and the transport filter, which blocked dendritic vesicles that did enter the proximal axon from advancing more than a few microns into the axon. In mature neurons the transport filter aligned with the cell-body proximal edge of the initial segment, a specialized domain of the axon that forms the boundary between axonal and somatodendritic domains. However, the transport filter was detected in the axons of newly formed axons of stage 3 cells, before the initial segment developed. Furthermore, selective dendritic transport was detected in neurites of stage 2 neurites, at which time it was dynamically regulated. Second, live-cell imaging was used to study the transport of two types of axonal proteins—synaptic vesicle proteins and dense core granule proteins—both of which must be transported into the far reaches of the axon to support synaptic and trophic signaling. A Kinesin-3 family member, KIF1A, has been implicated in the transport of both of these proteins in the axon. Two-color live-cell imaging showed that upon Golgi departure synaptic vesicle and dense core granule proteins, as well as axonal plasma membrane proteins are initially transported in a common transport tubule. KIF1A did not associate with this transport tubule but did label spherical dense core granule-containing organelles at later time points, suggesting that more specialized vesicle populations that arise from the common tubule are moved by KIF1A. These studies have revealed important new aspects of dendritic and axonal transport, which will be useful in future studies that seek to understand the regulation of protein trafficking in neurons.

Chapter 1

Introduction

Overview

The elaborate morphology of axons and dendrites, and their distinct functional roles, pose particular challenges to the protein trafficking machinery of nerve cells. Numerous cell components, such as pre- and postsynaptic proteins, signaling molecules, cytoskeletal elements, RNA complexes, and mitochondria, to name but a few, must be differentially localized to either the dendrites to support signal reception and integration or the axon to enable action potential propagation and synaptic transmission. Establishment and maintenance of this polarized distribution of protein machineries to the dendritic or axonal domains is fundamental to neuronal function.

While some protein synthesis occurs locally in the dendrites, most proteins destined for the dendrites (dendritic proteins) are synthesized in the cell body. The axon lacks significant protein synthesis machinery, thus practically all synthesis of axon-targeted proteins (axonal proteins) occurs in the cell body. Therefore, both dendritic and axonal proteins must be transported great distances from the cell body into the axon and dendrites. This is particularly true for axonal proteins because the axon can be centimeters to even a meter in length in some human motor neurons, while dendrites are usually on the order of hundreds of micrometers to a few millimeters long. Axonal and dendritic proteins must also be rapidly transported in the retrograde direction, back to the cell body, for functions such as retrograde signaling to the nucleus or to dispose of proteins that have been targeted for degradation. Thus the transport system of neurons faces two important challenges: to differentially traffic axonal and dendritic

proteins to their distinct cellular domains, and to do so quickly and efficiently despite the long distances that need to be traversed, particularly in the axon.

My thesis addresses these two aspects of the transport challenge in neurons. In Chapter 2, I present a study on the selective transport of dendritic proteins. By an unknown mechanism, the transport of dendritic proteins is selectively blocked in the proximal axon, while proteins that belong in the axon are transported through this area without hindrance. Interestingly, the boundary between the axonal and somatodendritic domains is also located in the proximal axon and is marked by a specialized structure called the axon initial segment. I will examine the potential role of the initial segment in the selective transport of dendritic proteins and determine when selective transport of dendritic proteins arises during neuronal development. Chapter 3 presents a model of how newly synthesized axonal proteins are efficiently transported to the far reaches of the axon to support axonal function, with specific regard to synaptic vesicle proteins and dense core granule proteins.

To begin, I will describe the basic cellular machinery involved in protein and organelle transport in neurons beginning with molecular motors that shuttle axonal and dendritic cargo throughout the neuron and the cytoskeletal tracks they use as superhighways for fast, efficient transportation. I will then elaborate on the phenomenon of selective transport in neurons and introduce the initial segment and its involvement in maintaining an organized boundary domain between the axonal and somatodendritic domains. Finally, I will discuss the transport of axonal proteins, which must be trafficked efficiently and continuously

to the far reaches of the axon, a particularly daunting task considering that the length of the axon can be a thousand times the diameter of the cell body.

Microtubule-based molecular motors for protein transport

There are two superfamilies of motor proteins that carry out microtubule-based transport of proteins and organelles in eukaryotic cells. These motors are called kinesins and dyneins (Vale, 2003). Both motors use microtubules, which are polarized filamentous components of the neuronal cytoskeleton, as tracks along which to walk while they simultaneously bind and drag cargo. Cargos can be in the form of protein complexes such as RNA granules, organelles such as mitochondria, or membrane-bound vesicular carriers that contain membrane proteins or soluble peptides such as trophic factors.

There are a total of 45 different kinesin-encoding genes in humans, 38 of which are expressed in the brain (neurons and glia). Of these 38 neuronally expressed kinesins, about a dozen are responsible for all the long-range transport of organelles in neurons, while the others function in processes such as mitosis (Miki et al., 2005). With discovery of numerous kinesins in recent years came a need for a standardized nomenclature and grouping into families, based on sequence homology (Lawrence et al., 2004). Thus, there are 14 different kinesin families, each with multiple members. Kinesins from all but one family, (Kinesin-14 family), move selectively toward the plus-end of microtubules, (see below for details) which are typically oriented toward the cell periphery. Thus kinesins are referred to as anterograde motors.

There are 15 different dynein genes in human genome. In contrast to kinesins, dyneins move toward the minus-end of microtubules, which orient toward the cell body, and are thus called retrograde motors (Vallee et al., 2004). Of the 15 different dyneins, only one, cytoplasmic dynein, is responsible for all the long-range retrograde transport in neurons. The other 14 dyneins function in axonemal transport in cilia or flagella. Dynein motors are composed of a complex of at least 8 subunits. The subunits of the dynein complex associate with a second multi-subunit complex called dynactin, which targets the dynein complex to specific sites such as the kinetochore during cell division (Vallee et al., 2004). This thesis focuses on the anterograde transport of dendritic and axonal proteins.

Composition and orientation of microtubule tracks in neurons

The ability of kinesins to walk with directionality depends on the existence of a polarized substrate along which to move, and this substrate is the microtubule cytoskeleton of the cell. Microtubules are composed of numerous α- and β-tubulin subunit dimers, which polymerize end-to-end to form an asymmetrical protofilament terminating with a β-tubulin subunit at one end and an α-tubulin subunit at the other. Thirteen protofilaments bind in a staggered, parallel orientation to form a 24 nm-wide helical cylinder, which is the microtubule. The end of the microtubule composed of protofilaments that terminate with β-tubulin subunits is referred to the plus-end of the microtubule, while the other end, which terminates with α-tubulin subunits, is the minus-end.

It was quickly recognized that knowing how the microtubules were oriented in neurons would be fundamental to understanding the regulation of transport. Insights about microtubule orientation were first obtained using an electron microscopy technique called the hook-assay (McIntosh and Euteneuer, 1984) and more recently by live-cell imaging of fluorescently tagged microtubule plus-end binding proteins (Tirnauer and Bierer, 2000). The hook assay, applied to postganglionic sympathetic fibers from cat, originally demonstrated that in mature neurons, all the microtubules in the axon are oriented the same way, with their plus-ends pointing toward the distal axon (Heidemann et al., 1981). A second study using the hook assay to study microtubule polarity in cultured hippocampal neurons confirmed this finding and went on to examine microtubule organization in dendrites (Baas et al., 1988). They found that throughout most of the length of dendrites, microtubule polarity is mixed, with both plus and minus ends pointing toward dendritic tips; near the distal tips of dendrites, however, all the microtubules are unidirectional, with their plus end toward the dendrite tip (sometimes called plus-end out) (Baas et al., 1988). A recently developed technique, the live-cell imaging of GFP-tagged microtubule plus-tip binding proteins, such as EB3 (Nakagawa et al., 2000), has been used to verify the findings of the earlier hook assay studies. EB3-tagged with GFP accumulates on the plus-end of actively polymerizing microtubules, and falls off when polymerization ends. Thus, in live-cell imaging recordings, EB3-GFP ‘comets’ or ‘dashes’ moving in the direction of polymerization indicate the microtubule plus end (Stepanova et al., 2003). Analysis of EB3-GFP comet direction in live-cell

recordings in cultured hippocampal and Purkinje neurons showed that in the axon, microtubules polymerized almost exclusively away from the cell body, indicating a unidirectional population of microtubules. In proximal dendrites the direction of EB3-GFP comets was mixed, with half moving towards the cell body and half towards the dendrite tips, indicating a mixed population of microtubule polarity in the dendrites. In the distal dendrites, however, EB3-GFP comets indicated a uniform population of plus-end out microtubules. These results are in complete agreement with the earlier hook assay results (Stepanova et al., 2003).

Microtubules are not static structures. They dynamically polymerize and depolymerize; a process that is regulated by a complicated interplay of plus-end capping proteins and the binding of microtubule-associated proteins (MAPs), which can stabilize microtubules. Microtubules can also be posttranslationally modified in ways that affect stability and interaction with kinesins. These aspects of microtubules and their impact on intracellular trafficking are discussed in a subsequent section.

Fundamentals of kinesin structure and function

The first kinesin identified was isolated from squid axoplasm and vertebrate brain (Brady, 1985; Vale et al., 1985). Originally called conventional kinesin, or just kinesin, by today's nomenclature system, it is a Kinesin-1 family member. Since its discovery, the structure of kinesin, its mechanism of motility, and its cargo binding have been extensively studied (Hirokawa and Noda, 2008). While there are some variations in structure and function between kinesin families, many of

the fundamentals apply to all kinesins. Therefore I will review the basic features of Kinesin-1.

Functional domains of kinesin motor proteins

Like most kinesins, Kinesin-1 functions as a dimer of kinesin heavy chains (KHCs), each with an accessory kinesin light chain (KLC). KHC is a rod shaped molecule with a globular N-terminal motor domain followed by a flexible neck linker, stalk domain, and C-terminal cargo binding domain (Hirokawa et al., 1989; Scholey et al., 1989; Yang et al., 1989; Morii et al., 1997; Tripet et al., 1997; Seiler et al., 2000). The motor domain is highly conserved amongst all kinesins; however the stalk and cargo binding domains are highly divergent, each specialized to bind to a specific and diverse set of cargo molecules.

Kinesin dimerization promotes processivity

Dimerization of kinesins is fundamental to their ability to walk long distances, at a fast rate (Hancock and Howard, 1998). They dimerize at a coiled-coil domain located in the stalk, bringing two motor domains together at the N-terminus and two cargo domains together at the C-terminus (Huang et al., 1994). Each motor domain contains two binding sites: a microtubule binding domain and a nucleotide binding pocket that binds and hydrolyzes ATP (Yang et al., 1989; Woehlke et al., 1997). The motor domains bind and walk along microtubules in a hand-over-hand motion, with one motor remaining bound to the microtubule while the other takes a step. The stepping motion is powered by cycles of ATP binding and hydrolysis that induce conformational changes in the flexible neck linker,

causing it to swing the trailing motor domain forward, past the leading microtubule-bound motor domain, to the next binding site along the microtubule making a forward step (Asbury, 2005). This mechanism prevents diffusion of kinesin away from the microtubule between steps, resulting in a highly processive motor, meaning it is capable of taking many steps before dissociating from the microtubule. It also enables directional stepping along microtubules toward the plus-end and imparts specificity of anterograde movement to kinesin motor proteins (Gennerich and Vale, 2009).

Kinesin cargo binding specificity

The cargo binding domain of kinesins share little sequence homology, reflecting their different cargo binding specificities. Additionally, the tails of kinesins can associate with accessory molecules that themselves bind distinct sets of cargo. In this manner, kinesins expand their cargo binding repertoire. Kinesin-1 motor proteins serve as an example. The cargo binding domain of Kinesin-1 is located at the C-terminus and can directly bind cargo. Alternatively, the KLC accessory proteins, of which there are three types in mammals (Rahman et al., 1998), associate with the C-terminus of Kinesin-1 and bind sets of cargos that are distinct from KHC (Diefenbach et al., 1998).

Cargo binding options are further expanded if the tail of kinesin associates with scaffolding proteins as cargo, which themselves have multiple protein interaction domains. For example the c-Jun N-terminal kinase (JNK)-interacting proteins, or JIP family of scaffolding molecules (Bowman et al., 2000; Byrd et al., 2001; Verhey et al., 2001) can serve as cargo. JIPs bind kinases of the JNK pathways

(Kelkar et al., 2000). Recruitment of these kinases to the motor complex may in turn regulate the motors binding to other cargos (Verhey et al., 2001; Stagi et al., 2006; Horiuchi et al., 2007).

In mammals, there are three Kinesin-1 family members (KIF5A, 5B, and 5C) (Aizawa et al., 1992; Kanai et al., 2000), three different KLCs (Rahman et al., 1998; Vale, 2003), and three JIPs (JIP1, JIP2, and JIP3) (Ito et al., 1999). The different Kinesin-1 family members heterodimerize and bind light chains in various combinations (Rahman et al., 1998), creating motors with different cargo specificities and motors that are regulated in different ways (Vale, 2003). This multiplicity of subunit association may explain why Kinesin-1 has been associated with the transport of a diverse set of cargo proteins, including vesicular cargo, protein complexes, and organelles, in both the axon and dendrites.

The polarized transport of axonal and dendritic proteins

The discovery of GFP and additional fluorescent proteins that can be used as tools to label proteins in living cells and visualize their transport in real time has revolutionized the study of protein trafficking (Chamberlain and Hahn, 2000). In cultured neurons, live-cell imaging of fluorescently tagged axonal and dendritic proteins has revealed dramatic differences in the transport pattern of vesicle populations containing these proteins, showing that kinesin-based transport in neurons is a highly complex and regulated process, about which we have many more questions than answers (Burack et al., 2000). Live-cell imaging of fluorescently-tagged axonal and dendritic proteins shows that the first step

toward achieving a polarized distribution of axonal and dendritic membrane proteins occurs at the level of the *trans* Golgi network, where proteins destined for the axon and dendrite are sorted away from each other and bud from the Golgi in distinct transport vesicle populations (Craig and Banker, 1994; Keller and Simons, 1997; Glover, 2005).

Axonal vesicles transport into axons and dendrites

Live-cell imaging also shows that transport vesicles labeled with GFP-tagged axonal proteins traffic throughout the cell, including the dendrites as well as the axon (Burack et al., 2000). Two studies used antibody uptake experiments to determine if vesicles containing axonal proteins fused with the dendritic plasma membrane (Sampo et al., 2003; Wisco et al., 2003). They found that the enrichment of axonal proteins in the axonal cell surface is a function two processes of selectivity that occur at the plasma membrane. As some vesicles containing axonal membrane proteins fuse selectively with the axonal plasma membrane, antibody staining never revealed any endocytosed axonal proteins in the dendrite. As other vesicles containing axonal proteins are competent to fuse in the dendritic domain, but the axonal proteins that reach the dendritic surface are quickly removed by endocytosis, immunostaining revealed endosomes containing these axonal proteins in the dendrites (Sampo et al., 2003; Wisco et al., 2003).

Although vesicles containing axonal proteins traffic into the dendrites as well as the axon, they are more likely to enter the axon, suggesting that a cellular mechanism exists that directs this transport (Nakata and Hirokawa, 2003). A

study using cultured hippocampal neurons to visualize the post-Golgi transport of a GFP-tagged axonal protein (temperature-sensitive vesicular stomatitis virus G-protein, VSV-GtsO45) observed that tubular post-Golgi vesicles containing axonal proteins preferentially entered the axon rather than dendrites in 60% of cells. On average, the axonal vesicles entered the axon with a 3.8-fold bias over dendrites (Nakata and Hirokawa, 2003). A second study also documented a 2-fold bias for vesicles containing axonal proteins to enter the proximal axon compared to dendrites (Burack et al., 2000).

Dendritic vesicles are selectively blocked from entering the axon

A dramatically different trafficking pattern is revealed when the transport of dendritic proteins is visualized. Vesicles containing dendritic proteins transport in and out of dendrites, as one would expect, but their transport into the axon is completely blocked somewhere in the proximal axon (Burack et al., 2000; Silverman et al., 2001). Thus, in contrast to the transport of axonal proteins, dendritic proteins are selectively transported only in the dendrites and do not transport into the distal axon. The selective transport of dendritic proteins is likely the primary mechanism by which dendritic proteins are polarized to the somatodendritic domain (Burack et al., 2000).

Selective dendritic transport may be particularly critical to neuronal polarity and therefore function. If dendritic transport vesicles transported into the axon, their return to the cell body would depend on dynein because the microtubules in the axon are uniformly plus-end out, toward the distal axon. Keeping in mind that the axon accounts for ~90% of the cytoplasmic volume of a neuron (Setou et al.,

2004), the axon could be a sink into which a large proportion of dendritic transport vesicles would be irretrievably siphoned if their transport was not blocked.

The transport of axonal transport vesicles into the dendrites could be viewed as a waste of time and energy for the trafficking system; alternatively, it may serve as kind of insurance policy for the neuron. In studies of axonal regeneration, it has been shown that when the axon of mature neurons is cut close to the cell body, axonal identity is lost and the cell will re-specify an axon, much like it did during the initial development of polarity. Interestingly, the new axon sometimes forms from the tip of a mature dendrite, and not necessarily from the stump of the original axon. This shows that even mature neurons retain the ability to specify an axon and can do so from mature dendrites (Gomis-Ruth et al., 2008). The ability of axonal transport vesicles to transport into the dendrites may be important to retaining the plasticity of mature neurons to re-polarize in the event of axon severing. This could be essential to the repair of neuronal connections in case of injury.

Possible mechanisms of selective dendritic transport

Understanding the cellular mechanism by which the transport of dendritic vesicles in the axon is selectively blocked and how axonal proteins are coaxed to enter the axon with a bias will reveal important aspects of how kinesin-based transport is regulated. We know from live-cell imaging studies that dendritic vesicles enter the axon, but their anterograde movement soon becomes blocked, therefore the molecular mechanism responsible for selectively blocking dendritic

transport must be localized in the proximal axon (Burack et al., 2000). Two molecular mechanisms could account for selective dendritic transport. First, microtubules can be modified by posttranslational modifications which could create biochemical differences in the microtubule tracks near the base of the axon that derail motors moving the dendritic cargo, or enhance transport of axonal vesicles (Westermann and Weber, 2003). Second, signaling molecules, such as kinases, could be localized to the proximal axon that could regulate the motor, either causing its inactivation or dissociation from the cargo by phosphorylation (Morfini et al., 2001).

Microtubule modifications that enhance kinesin transport

The binding of kinesin to microtubules is regulated by the reversible modification of polymerized microtubules by posttranslational modifications (PTMs) and binding of microtubule-associated proteins (MAPs) (Lakamper and Meyhofer, 2006). Numerous isotypes of α- and β-tubulin are expressed in neurons, and are subject to multiple forms of PTMs, including acetylation, polyglutamylation, detyrosination, polyglycylation, phosphorylation, and palmitoylation (Westermann and Weber, 2003). All but acetylation occur on the carboxy-terminal tail of tubulin, which is a 10 (α-tubulin) or 18 (β-tubulin) amino acid-long, negatively charged, highly flexible domain oriented toward the outside surface of the microtubule polymer (Nogales et al., 1998). The tails have high degree of sequence variation between the otherwise identical tubulin isotypes, thus the C-terminal tails are ‘isotype defining’ domains of tubulin (Sullivan and Cleveland, 1986). Kinesin motor proteins and MAPs bind tubulin at different domains on the

C-terminal tail, thus it was suspected that modifications to the tail could influence kinesin and MAP binding.

In most cells, microtubules fall into two categories, highly dynamic, ‘unstable’ microtubules with half-lives of 5-10 minutes, and ‘stable’ microtubules, with half-lives of several hours. PTMs occur on the long-lived microtubules, and serve as markers of stable microtubules, although PMTs themselves do not contribute to microtubule stability (Rosenbaum, 2000). Neurons have a greater proportion of stable microtubules than dividing cells, particularly in the axon, and many of the PTMs are enriched on axonal microtubules compared to microtubules in the neuronal cell body and dendrites. Three axonally enriched PTMs—acetylation, polyglutamylation, and detyrosination—have been found to influence the binding of kinesin, and in some cases MAPs, and may explain how dendritic transport vesicles are prevented from entering the axon, while axonal transport vesicles enter the axon with a bias.

Acetylation of microtubules

Acetylation, which occurs on a conserved lysine (Lys40) near the amino-terminus of α-tubulin, but not β-tubulin, increases binding of kinesin to microtubules (Reed et al., 2006). In binding assays, kinesin bound with lower affinity to microtubules purified from *Tetrahymena* expressing an acetylation-incompetent form of mutant α-tubulin, compared to wildtype. Similarly, in a microtubule gliding assay, the mutant microtubules moved at reduced speeds compared to wildtype, suggesting that acetylation influences the enzymatic activity of kinesin (Reed et al., 2006) .

Furthermore, the transport of a kinesin-1 cargo, JIP1 was altered after pharmacological treatment of hippocampal neurons and CAD cells (a neuronal cell line) with tubacin, a drug that specifically blocks the α-tubulin deacetylase, causing a global increase in cellular acetylation levels. JIP1 and Kinesin-1 accumulate selectively in a subset of neurites under normal conditions, possibly reflecting a preference of transport of kinesin-1 into neurites with higher acetylation levels. Following tubacin treatment, and hyperacetylation of microtubules in all neurites, JIP1 accumulated in all neurite tips, suggesting a loss of selective kinesin-1 transport (Reed et al., 2006). This effect on kinesin transport was surprising, because lys40 is oriented inside the microtubule lumen of the α-tubulin subunit, while kinesin binds on the outside of the microtubule surface, and mainly to β-subunits (Marx et al., 2006). It is possible that acetylation changes the conformation of the tubulin polymer in a way that influences the binding of kinesin (Reed et al., 2006).

Polyglutamylation of microtubules

Polyglutamylation, the addition of a chain of 1-6 negatively charged glutamyl units to a glutamate in the C-terminal tail of both α and β-tubulin, is the most abundant tubulin PTM in neurons, present on 50% of neuronal tubulin (Edde et al., 1990). *In vitro* blot-overlay studies of MAP binding discovered that both tau and MAP2 binding affinity was increased for polyglutamylated tubulin with chains of 1-3 glutamyl units (Boucher et al., 1994). Beyond a chain length of 3, the affinity for tau and MAP2 binding dropped suggesting a modulation of MAP binding by the length of polyglutamylation chain. The authors suggest that

addition of each glutamyl unit induces a progressive conformational change in the C-terminal tail that regulates MAP binding (Boucher et al., 1994). Subsequent studies showed the same affect of polyglutamylation chain length and the binding of Kinesin-1 motor domain; the affinity of the motor domain for microtubule binding was enhanced for chains 1-3 glutamyl units in length, but reduced for longer chain lengths (Larcher et al., 1996). The effect of chain length could not be generalized to all MAPs. Two additional MAPs, MAP1A and MAP1B, were tested for binding to polyglutamylated microtubules, and while MAP1B showed the same binding behavior of MAP2, tau and kinesin, MAP1A binding affinity remained high for microtubules with long polyglutamylation chains (Bonnet et al., 2001).

Interestingly, tau bound to microtubules has been shown to function as a roadblock to kinesin motors. The movement of beads coated with kinesin motors along microtubules was measured in the absence and presence of increasing concentrations of tau bound to the microtubules. The presence of tau resulted in bead movements of shorter run lengths, and the less force was required to pull the bead from the microtubule in the presence of tau (Vershinin et al., 2007). Similarly, single molecule imaging study showed GFP-tagged kinesin detached from microtubules when they encountered a patch of tau molecules bound the microtubule (Dixit et al., 2008). These studies suggest that regulated binding of tau to microtubules could be a means by which the binding of kinesins to microtubules is regulated. Increased concentrations of tau could be recruited to microtubules at sites along the axon where kinesin releases its cargo, such as at

the synapse (Dixit et al., 2008). Similarly, increased microtubule-bound tau could facilitate the handing off of cargo from kinesin, to myosin at the cell periphery (Vershinin et al., 2007).

Polyglutamylation also had an effect on the binding of a second kinesin, KIF1A (Ikegami et al., 2007). A study of the mutant mouse strain called ROSA22 which lacks an subunit of the enzyme complex required for polyglutamylation of α-tubulin showed that KIF1A binding to microtubules purified from ROSA22 mice was reduced compared to microtubules purified from control animals. KIF1A levels were reduced in neuronal processes of cultured hippocampal neurons and cerebellar slices of the ROSA22 mice suggesting a reduction in KIF1A translocation along microtubules with reduced α-tubulin polyglutamylation. Synaptic terminals of ROSA22 mice showed a 30% reduction in the number of synaptic vesicles consistent with reduced transport by KIF1A, furthermore, electrophysiological studies showed defects of synaptic transmission in hippocampal slices of ROSA22 mice (Ikegami et al., 2007) .

Detyrosination of microtubules

A third PMT, the detyrosination of α tubulins (but not β) has been shown to effect kinesin-microtubule interaction. The C-terminal tyrosine of α-tubulin can be removed (detyrosinated) by tubulin tyrosine carboxypeptidase (TTCP). Detyrosinated microtubules can be re-tryosinated by tubulin-tyrosine ligase (TTL). However, if the glutamic acid is removed from detyrosinated tubulin (by an unknown enzyme), an irreversible conversion to a form of tubulin called Δ2-

tubulin occurs, to which TTL cannot attach a tyrosine, thus removing the α-tubulin from the detyrosination/tyrosination cycle (Westermann and Weber, 2003). Detyrosinated microtubules are enriched in the axon, and kinesin has been shown to bind them with a higher affinity than tryosinated microtubules (Liao and Gundersen, 1998). A live-cell imaging study showed that GFP-tagged kinesin-1 labeled vesicles moved preferentially along a subset of microtubules in COS cells. By retrospective immunostain, these preferred microtubules were shown to be enriched for detyrosinated microtubules (Dunn et al., 2008).

All together, these data suggest that acetylation, polyglutamylation, and detyrosination increase the binding of some kinesins, (as well as MAPs in the case of polyglutamylation), and may serve as molecular road signs to direct kinesin based transport. It should be noted that these PTMs can co-exist in combination on the same microtubule, and exert potentially combined effects that differ from the effect of a single modification. They also may increase the binding of MAPs with can further influence the binding of kinesin. Furthermore, these modifications are rapidly reversible, and thus, could mediate dynamic changes in the regulation of kinesin transport (Westermann and Weber, 2003; Fukushima et al., 2009). A PTM or MAP localized to the proximal axon that inhibits transport of the motor moving dendritic cargo, while having no effect or even enhancing transport of axonal transport vesicles could account for the selective transport observed in cultured hippocampal neurons.

Kinesin regulation by phosphorylation

Another mechanism that could underlie selective transport of axonal and dendritic transport vesicles in neurons is direct enzymatic regulation of the motor transporting dendritic vesicles into the proximal axon by phosphorylation (Lee and Hollenbeck, 1995). In studies of Kinesin-1 phosphorylation, direct phosphorylation of KHC by c-Jun N-terminal kinase (JNK) was shown to inhibit kinesin binding to the microtubule (Morfini et al., 2006). Two different kinases, glycogen synthase kinase 3 (GSK3) and casein kinase 2 (CK2) have been shown to phosphorylate KLC, the cargo-binding accessory proteins to Kinesin-1, and cause dissociation from membrane-bound cargo organelles (Morfini et al., 2002; Pigino et al., 2009). From these studies of Kinesin-1 phosphorylation, it appears likely that phosphorylation is a means of regulating kinesin-based transport and may block entry of dendritic cargo vesicles to the axon, either by inhibiting binding of the motor carrying dendritic cargo to the microtubule in the axon, or by causing dendritic cargo to dissociate from the kinesin as it enters the axon. Identification of the kinesin(s) responsible for the transport of vesicles containing dendritic proteins will be essential to investigating this possibility.

Interestingly, there is a specialized molecular assembly in the base of the axon, called the axon initial segment, which could harbor kinases or other signaling molecules involved in motor regulation, or biochemical specializations of the microtubule track that prevent entry of dendritic cargo to the axon.

The axon initial segment: required for neuronal polarity

The axon initial segment is perhaps best known for its function as the site of action potential generation in the axon (Khaliq and Raman, 2006; Palmer and Stuart, 2006; Kole et al., 2008). However, in recent years the initial segment has gained further appreciation for its important role in maintaining neuronal polarity. The specialized membrane cytoskeleton of the initial segment not only anchors the high density of voltage-dependent sodium channels that underlie action potential generation, it also creates a physical barrier in the axon plasma membrane that prevents the diffusion of dendritic and axonal membrane proteins and lipids between axonal and somatodendritic domains (Kobayashi et al., 1992; Winckler et al., 1999; Nakada et al., 2003; Boiko et al., 2007; Hedstrom et al., 2008). Thus the initial segment marks the boundary between polarized domains of the neuron and is appropriately localized to play a role in the selective transport of vesicles containing dendritic proteins. Because Chapter 2 of this thesis examines this possibility, I will present a detailed description of the initial segment's composition, its primary structural features, its known functions in maintaining neuronal polarity, and how it could be involved in the selective transport of dendritic vesicles.

The axon initial segment: a specialized membrane domain

The initial segment membrane specialization is defined by the presence of ankyrinG, a member of the Ankyrin family of peripheral membrane proteins which link membrane proteins to the spectrin and actin cytoskeleton (Kordeli et al., 1995; Bennett and Baines, 2001). At the initial segment, ankyrinG recruits a

unique form of spectrin, called βIV-spectrin to the membrane (Berghs et al., 2000; Yang et al., 2007). This unique ankyrinG/βIV-spectrin-based membrane cytoskeleton is a hallmark of the initial segment.

AnkyrinG contains multiple protein and membrane interaction domains through which it binds specific types of ion channels and cell adhesion molecules at a very high density in the initial segment membrane and anchors them against the βIV-spectrin-based membrane cytoskeleton. Specifically, ankyrinG is required to cluster specific subtypes of ion channels at the initial segment including voltage dependent sodium channels (subtype $Na_v1.2$ in young animals and $Na_v1.6$ in adult) and potassium channels ($KCNQ_2$ and $KCNQ_3$) as well as two members of the L1 family of cell adhesion molecules, NrCAM and neurofascin 186 (Srinivasan et al., 1988; Davis et al., 1996; Hortsch, 1996; Zhou et al., 1998; Garrido et al., 2003; Lemaillet et al., 2003; Pan et al., 2006).

AnkyrinG is a required component of the initial segment

AnkyrinG is the lynchpin of the initial segment membrane complex, required for both initial segment formation during development and its maintenance in mature neurons. In region-specific cerebellar ankyrinG knockout-mice, initial segment components, such as βIV-spectrin, neurofascin 186, sodium channels, and KNCQ2/3 channels, failed to accumulate in the proximal axons of Purkinje neurons that lacked ankyrinG, showing that ankyrinG is necessary for their localization to the initial segment (Zhou et al., 1998; Jenkins and Bennett, 2001; Pan et al., 2006). When ankyrinG expression was silenced by shRNA in developing cultured hippocampal neurons that had yet to form initial segments,

other components of the initial segment failed to accumulate; even after 17 days in culture the initial segment failed to form (Hedstrom et al., 2007). However, when other components of the initial segment, including βIV-spectrin, voltage dependent sodium channels, or cell adhesion molecules, were systematically knocked down, the remaining components of the initial segment accumulated in the proximal axon and formed an initial segment in their absence (Hedstrom et al., 2007). These studies demonstrate that ankyrinG is the one initial segment protein that is required for its formation.

A third study knocked down ankyrinG in mature neurons using shRNA and found that after a week in culture, preexisting initial segments had disassembled (Hedstrom et al., 2008). ShRNA knockdown of βIV-spectrin, sodium channels, or neurofascin-186 did not lead to disassembly of the initial segment in mature neurons. Interestingly, upon dismantling of the initial segment, the axon gradually acquired dendritic identity, marked by the presence of MAP2 and dendritic membrane proteins on the surface of the former axon (Hedstrom et al., 2008). This experiment demonstrated that ankyrinG is required to maintain the initial segment membrane complex in mature neurons. Furthermore, loss of the initial segment in mature neurons resulted in a loss of neuronal polarity. The mechanism underlying the initial segment-dependent loss of neuronal polarity is not yet understood, but could be related to the loss of the diffusion barrier property of the initial segment (discussed below). Whether or not the selective transport of dendritic proteins is affected under these conditions needs to be investigated and is discussed in Chapter 2. In any event, these experiments

show that the initial segment plays an important role in maintaining neuronal polarity in mature neurons.

The initial segment forms a membrane diffusion barrier

The diffusion barrier in the initial segment was first detected by FRAP experiments in cultured rat cortical and spinal cord neurons using fluorescently tagged neurotoxin probes that selectively bind to sodium channels at excitable membrane domains (Angelides et al., 1988). By comparing fluorescence recovery rates in bleached areas in the cell body and distal axon with rates of recovery in the proximal axon, a reduced ability of sodium channels to diffuse in the area of the axon hillock/initial segment was detected (Angelides et al., 1988). In a later study, the membrane barrier in the initial segment was shown to reduce the diffusion of lipids in addition to membrane proteins. Fluorescently labeled lipids incorporated specifically into the axonal plasma membrane did not diffuse into the cell body even after prolonged periods of time (30-60 minutes). Additionally, FRAP of the proximal part of the axon of lipid-labeled axons showed only a 40% recovery of bleached lipid into the initial segment (Kobayashi et al., 1992).

Further evidence that a barrier to the diffusion of membrane proteins exists in the initial segment membrane was provided in a study that used optical tweezers to measure the tractability of beads coated with antibodies to axonally polarized membrane proteins, Thy-1 (a GPI-linked protein) and L1 (a transmembrane cell adhesion molecule), either in the initial segment or in the distal axon of mature cultured hippocampal neurons (Winckler et al., 1999). A ~10-fold reduction in

lateral mobility of membrane proteins was detected in the initial segment compared to those in the distal axon. This barrier was reversibly disrupted by treatment with the actin depolymerizing drug, Latrunculin-B, suggesting that the reduced mobility of membrane proteins in the initial segment is the result of direct or indirect tethering to the membrane cytoskeleton. Furthermore, prolonged disruption of the actin with Latrunculin-B in the presence of cycloheximide resulted in a loss of polarization of axonal and dendritic membrane proteins (Winckler et al., 1999).

A definitive study of the initial segment diffusion barrier and its correlation to the accumulation of ankyrinG and voltage dependent sodium channels was presented in a study that used various forms of single–molecule imaging to measure the mobility of individual lipid molecules in the axon plasma membrane during development of cultured hippocampal neurons. After recording diffusion rates of lipid molecules in the axon, the authors retrospectively stained the neurons for ankyrinG and directly showed that the lipids with low diffusion rates were in the area of ankyrinG staining. Furthermore, the degree to which mobility was suppressed correlated with the intensity of ankyrinG staining. Sodium channels labeled with Alexa wasp toxin β-pompilidotoxin were also immobilized in the initial segment of mature neurons. The authors also demonstrated that destabilization of the actin with latrunculin-A treatment decreased the immobile fraction of lipids and sodium channels in the initial segment membrane, while stabilization of actin with jasplakinolide treatment increased the immobile fraction (Nakada et al., 2003).

These results show that there is a barrier to the diffusion of both membrane proteins and lipid molecules in the membrane of the initial segment. Furthermore, the function of the diffusion barrier depends on the anchoring of a high concentration of membrane proteins in the initial segment membrane by ankyrinG. These membrane proteins serve as physical barriers to the diffusion of both membrane proteins and lipids and function in maintaining neuronal polarity (Nakada et al., 2003).

Unique ultrastructural features of the initial segment cytoplasm

Ultrastructural evidence suggests that the initial segment may have cytoplasmic specializations in addition to the specialized ankyrinG-based membrane complex. The initial segment is readily identified in electron microscopy thin-sections by the presence of a distinct membrane undercoating that likely corresponds to the unique cytoskeleton and dense membrane proteins at the initial segment membrane. In register with the appearance of the membrane undercoating that marks the initial segment, the microtubules running through the axon are bundled into fascicles that run parallel to the plasma membrane (Palay et al., 1968).

The microtubule fascicles begin to form in the axon hillock, and more microtubules join each fascicle as they approach the initial segment. Once in the initial segment, a typical pyramidal neuron has 3-7 fascicles, each containing 6-12 microtubules. The microtubules are held parallel to each, spaced 12 nm apart by distinct crossbars that resemble rungs of a ladder. Single microtubules were almost never observed in the initial segment. The fascicles then disappear at the

start of the first myelin sheath, and the microtubules become single and evenly spaced. Bundled microtubules of this description have not been observed anywhere else in the neuron and are completely unique to the initial segment (Palay et al., 1968; Peters et al., 1968).

Unique properties of the initial segment microtubules

The fasciculated microtubules in the initial segment appear more electron dense than microtubules in other parts of the neuron due to the presence of fine fibrous material associated with the microtubules (Palay et al., 1968). The identity of this fibrous material has yet to be determined, but it suggests the presence of a unique modification or protein associated with initial segment microtubules.

Initial segment microtubules have been shown to have unique binding properties. When the microtubule plus-end binding protein, EB1 (Tirnauer and Bierer, 2000), was highly over-expressed in cultured hippocampal neurons, it preferentially bound along the length of initial segment microtubules (Nakata and Hirokawa, 2003). Also, a rigor mutant form of Kinesin-1 that can bind but not be released from microtubules, preferentially bound to the microtubules in the initial segment (Nakata and Hirokawa, 2003) providing further evidence that the microtubules of the initial segment have unique biochemical features.

Shared features of the initial segment and nodes of Ranvier

Nodes of Ranvier, the small stretches of unmyelinated axon between myelin sheaths, are closely related to the initial segment (Salzer, 2003). Both are regions of excitable membrane, with dense accumulations of specific ion

channels that modulate the electrical properties of the cell; the initial segment setting the action potential threshold, and nodes of Ranvier responsible for propagating that action potential along the axon. A reflection of these similar functions is their protein composition. Nearly every protein enriched at the initial segment is also enriched at the nodes of Ranvier, including the specialized ankyrinG/βIV-spectrin membrane cytoskeleton, voltage dependent sodium channels, NrCAM and neurofascin-186 (Salzer, 2003). When viewed by thin section on the electron microscope, nodes of Ranvier also have a powdery sub-plasmalemmal density identical to that of the initial segment membrane, created by the ankyrinG/βIV-spectrin membrane cytoskeleton (Palay et al., 1968).

Surprisingly, the initial segment and nodes of Ranvier do not share the same mode of development (Dzhashiashvili et al., 2007). The initial segment forms by a cell-intrinsic program, thus the initial segment forms in neurons cultured in the absence of glia. Exogenously expressed ankyrinG accumulated in proximal axons of cultured dorsal root ganglion neurons, showing the presence of an initial segment specialization (Zhang and Bennett, 1998). Also, ankyrinG and other proteins accumulated at the initial segment and can be detected by immunostain of cultured hippocampal neurons (Winckler et al., 1999; Hedstrom et al., 2007). The formation of nodes of Ranvier, in contrast, requires extrinsic signals from myelinating glia, therefore they do not form in glia-free culture conditions (Hedstrom and Rasband, 2006). Two studies, one using cultured retinal ganglion cells of the CNS that are myelinated by oligodendrocytes, and the second using cultured dorsal root ganglion cells of the PNS that are myelinated by Schwann

cells, showed that co-culturing with the appropriate glia was required to develop nodes of Ranvier (Kaplan et al., 1997; Ching et al., 1999).

Furthermore, at the initial segment, ankyrinG is the first molecule to cluster at the membrane, and is required for the accumulation of all other known components of the initial segment, including neurofascin-186. At nodes of Ranvier, neurofascin-186 is initially localized to nodes by an extrinsic glial signal, and neurofascin-186 is required for localization of ankyrinG to nodes, which then recruits the other components (Lambert et al., 1997; Hedstrom and Rasband, 2006).

The differences in nodal and initial segment development may reflect different roles played by proteins that are common to both domains, and shed further light on how these specialized domains contribute to modulation of neuronal function. For instance, neurofascin appears to be required for nodes of Ranvier formation, but not initial segment formation. At the initial segment, neurofascin may be required for directing the synaptic localization of GABAergic inputs onto the initial segment, which regulate neuronal excitability (Ango et al., 2004; Dzhashiashvili et al., 2007).

The initial segment and nodes of Ranvier also differ ultrastructurally. The fasciculated microtubules observed running through the initial segment cytoplasm are absent at nodes of Ranvier (Palay et al., 1968). This suggests that whatever functional role is played by the fasciculated microtubules at the initial segment is not shared with nodes of Ranvier.

The potential role of the initial segment in dendritic transport

Several aspects of the initial segment suggest it could be involved in blocking transport of dendritic transport vesicles. It is appropriately positioned in the proximal axon and forms the boundary between axonal and somatodendritic domains. Additionally it has unique microtubule tracks and forms a membrane diffusion barrier that is important for polarity. Thus it is a reasonable hypothesis that the initial segment houses the mechanism that blocks the anterograde movement of vesicles containing dendritic proteins into the axon. This possibility, along with determination of when dendritic transport becomes selective during the development of neuronal polarity is explored in Chapter 2.

The transport of axonal proteins

The dimensions of the axon and the continuous need for newly synthesized axonal proteins and membrane material to support axonal function and growth is perhaps the most extreme challenge to intracellular trafficking in any cell type. It is critically important, for example, that synaptic proteins be supplied to synaptic sites to form new synapses, remodel synapses in response to activity, or replace degraded synaptic machinery. To fully understand how transport of axonal proteins is accomplished and regulated, we must identify the specific kinesins that are responsible for their transport.

Identifying kinesins that move axonal proteins

Various indirect strategies have been used to link the function of a kinesin to the transport of particular axonal proteins. These include biochemical fractionation

and immunoisolation studies to identify proteins and motors that co-purify (Okada et al., 1995); sciatic nerve ligation and immunostaining to see which proteins accumulate proximal to the axonal ligation site (Yonekawa et al., 1998); assessment of putative cargo-protein localization following interference of motor function through expression of dominant negative motor constructs (Rivera et al., 2007); RNAi knockdown (Ferreira et al., 1992); or in kinesin knock-out animals (Zhao et al., 2001). Recent advances in live-cell imaging make it possible to directly visualize *transport* of putative cargo proteins in conditions that modify or eliminate the activity of a specific kinesin. This direct ascertainment of the role of specific kinesins in the *movement* of putative cargo organelles will confirm or amend conclusions drawn from these earlier studies that linked the activity of a specific kinesin with the transport of putative cargo by less direct approaches.

The transport of axonal proteins by Kinesin-3 motor proteins

Two kinesins belonging to Kinesin-3 family of motor proteins, KIF1A and KIF1Bβ, have been implicated in the axonal transport of synaptic vesicle proteins (Okada et al., 1995; Yonekawa et al., 1998; Zhao et al., 2001; Zhou et al., 2001; Pack-Chung et al., 2007). Interestingly, KIF1A has also been shown to transport secretory granule proteins in the axon, whose biosynthesis and protein composition is thought to be strictly segregated from that of synaptic vesicle proteins (De Camilli and Jahn, 1990; Zahn et al., 2004; Pack-Chung et al., 2007; Barkus et al., 2008). The experiments described in Chapter 3 use two-color live-cell imaging of fluorescently tagged axonal proteins, including synaptic vesicle proteins, dense core granule proteins, plasma membrane proteins, and the motor

KIF1A to directly determine which proteins are transported in the same transport organelle, and with which of these moving vesicle populations KIF1A is associated.

In the following sections I will detail the important differences between synaptic vesicles and dense core granules, and then introduce the members of the Kinesin-3 family of motor proteins and the evidence that these motors are responsible for the transport of both synaptic vesicle proteins and dense core granule proteins.

Features of synaptic vesicles and large dense core granules

Neurons utilize two types of secretory organelles for regulated signaling, synaptic vesicles and large dense core granules. Both organelles undergo calcium-induced fusion with the plasma membrane to release their contents extracellularly; however, their biogenesis, size, localization, membrane protein composition, the way their exocytosis is regulated are all distinct (De Camilli and Jahn, 1990). Synaptic vesicles are uniformly sized, 40 nm-diameter clear-cored vesicles that cluster at presynaptic active zones and contain chemical neurotransmitters. Their membrane is densely populated with a highly characteristic set of membrane proteins involved in tethering at the presynaptic site, import of neurotransmitter molecules, and calcium-induced fusion with the presynaptic plasma membrane (Takamori et al., 2006; Burre and Volknandt, 2007). Dense core granules are larger than synaptic vesicles (70-200 nm) and have a dense proteinaceous core containing signaling molecules such neurotrophic factors, neuropeptides, and proteases. They localize to the

periphery of presynaptic sites, as well as the cell body and dendrites, and have their own distinct membrane protein composition (Winkler, 1997).

The biogenesis of synaptic vesicles and dense core granules

The biogenesis of synaptic vesicles and dense core granules has been studied in PC12 cells, a rat tumor cell line derived from chromaffin cells of the adrenal medulla (Bonanomi et al., 2006). PC12 cells are non-polarized and lack axons and dendrites, but they do synthesize synaptic-like-micro-vesicles (SLMVs) which are the diameter of synaptic vesicles, are clear cored, have synaptic vesicle membrane composition, store neurotransmitter, and group into clouds in the cell body, similar to the way synaptic vesicles cluster at presynaptic active zones (Thomas-Reetz and De Camilli, 1994). SLMVs may not, however, undergo regulated secretion, a fundamental property of bona fide synaptic vesicles (Faundez et al., 1997). None-the-less, PC12 cells have been used as model cells for studying the fundamentals of synaptic vesicle and dense core granule biogenesis.

In cells with regulated secretion, like neurons and endocrine cells, proteins depart the Golgi by two possible pathways, the constitutive pathway and the regulated pathway (Burgess and Kelly, 1987). Proteins of the constitutive pathway are added to the membrane continuously in an unregulated manner. Proteins of the regulated pathway are stored in the cytoplasm in dense core granules until they undergo calcium-induced regulated fusion.

To determine which trafficking route is taken by newly synthesized synaptic vesicle proteins during the *de novo* formation SLMVs in PC12 cells, pulse-chase labeling and biochemical fractionation were used to follow [^{35}S] sulfate-labeled synaptophysin through the biosynthetic pathway (Regnier-Vigouroux et al., 1991). This study showed that synaptophysin left the Golgi in the constitutive secretion pathway, and rapidly appeared on the plasma membrane. Synaptophysin then cycled between the plasma membrane and an early endosome compartment before it appeared in the mature SLMV population (Regnier-Vigouroux et al., 1991). This paradigm for the delivery of newly synthesized synaptic vesicle proteins form SLMVs has been extrapolated to synaptic vesicle formation in neurons, though it remains to be fully demonstrated that all synaptic vesicle proteins follow the same pathway to the mature synaptic vesicle (Bonanomi et al., 2006). Synaptic vesicles are filled with neurotransmitter locally at the synapse and can undergo multiple rounds of activity induced exocytosis, recycling, and reloading at the synapse (Valtorta et al., 1990).

Studies in PC12 cells suggest that the biogenesis of mature dense core granules differs considerably from that of synaptic vesicles. Electron microscopy studies showed that dense core granule proteins leave the Golgi by the regulated secretion pathway in a transport intermediate called the immature secretory granule (Orci et al., 1987). This was confirmed by a study using a cell-free system of homogenized PC12 cells, combined with pulse-chase labeling of protein markers of the regulated and constitutive pathways with [^{35}S] sulfate (Tooze and Huttner, 1990). The signaling peptides that are secreted by dense

core granules are synthesized in the Golgi. To ensure their departure from the Golgi in the immature secretory granule, signaling peptides aggregate with other dense core granule luminal and membrane components, including membrane proteins that serve as sorting receptors in the Golgi membrane (Cool et al., 1997). Thus, dense core granule components are 'sorted for entry' into discrete lipid domains that bud from the Golgi as immature secretory granules (Dikeakos and Reudelhuber, 2007). As the immature secretory granule is transported it undergoes a maturation process that involves the removal of non-dense core proteins that inadvertently departed the Golgi with the budding immature secretory granule (Kuliawat and Arvan, 1992) and further condensation of the dense core granule components resulting in the formation a mature dense core granule. Thus, dense core granules proteins are 'sorted by retention' in the immature secretory granule to form the mature dense core granule (Kuliawat and Arvan, 1994). Upon regulated fusion with the plasma membrane, signaling contents are released and dense core granule membranes are endocytosed, but cannot be refilled at the cell periphery with neuropeptides. To be reused, dense core granule membranes must be transported back to the Golgi (Hannah et al., 1999).

Debate exists about how segregated the constitutive and regulated pathways really are (Arvan and Castle, 1998). It has been suggested that the immature secretory granule represents a post-Golgi sorting station that also contains proteins of the constitutive secretory pathway and that these proteins are removed from the immature secretory vesicle into a 'constitutive like' secretion

pathway that buds from the immature secretory granule, rather than directly from the Golgi (von Zastrow and Castle, 1987; Arvan and Castle, 1992, 1998). In neurons, synaptic vesicles are synthesized in much larger quantities than dense core granules, while neuroendocrine cells synthesize a greater amount of dense core material than SLMVs. The difference in the amounts that synaptic vesicle proteins and dense core granule proteins are synthesized could affect how these proteins are sorted in neurons compared to neuroendocrine cells. The experiments described in Chapter three illustrate the usefulness of live-cell imaging studies in determining if dense core granule proteins and synaptic vesicle proteins are strictly segregated into distinct trafficking pathways upon Golgi departure in neurons, or if they can be detected in the same transport intermediate at some time during their voyage to mature dense core granules and mature synaptic vesicle proteins.

Transport of synaptic vesicle proteins and dense core granule proteins in the axon by KIF1A

Despite the differences in synaptic vesicles and dense core granules, the same kinesin, KIF1A, has been implicated in the axonal transport of synaptic vesicle proteins and dense core granule proteins (Okada et al., 1995; Yonekawa et al., 1998; Zahn et al., 2004; Pack-Chung et al., 2007; Barkus et al., 2008). KIF1A is expressed specifically in neurons, (Aizawa et al., 1992). Concurrent with the cloning of KIF1A in mouse, an additional member of the Kinesin-3 family was identified, KIF1Bβ, which may play redundant role in transport of synaptic vesicle proteins in neurons (discussed below) (Nangaku et al., 1994; Zhao et al., 2001).

However, where and when these motors are involved in their transport has not been resolved. For instance, KIF1A and KIF1Bβ could be required for the initial Golgi-derived transport of both types of proteins. Alternatively, they could participate in other steps during their transport. In the case of synaptic vesicle proteins, KIF1A or KIF1Bβ might mediate their transport as they cycle between the plasma membrane and the early endosome during synaptic vesicle biogenesis. Similarly, dense core granule proteins might be transported by KIF1A or KIF1Bβ when they reside in mature dense core granules but not immature secretory granules.

Transport of synaptic vesicle proteins in non-vertebrates by KIF1A homologs

The study of *C. elegans* with mutations in the uncoordinated behavior genes (*unc*) led to the identification of unc-104, a kinesin motor, the homolog of which was later identified as KIF1A in vertebrates (Otsuka et al., 1991; Aizawa et al., 1992) and classified as the founding member of the Kinesin-3 family (Miki et al., 2005). *Unc-104* mutant worms have a paralytic phenotype due to simultaneous contractions of dorsal and ventral muscles (Hall and Hedgecock, 1991). The axons of these worms were shown to have fewer presynaptic boutons, and those that were present contained smaller presynaptic active zones with fewer clustered synaptic vesicles. In addition, small clear vesicles similar in size to synaptic vesicles were accumulated in mutant neuronal cell bodies, suggesting a defect in transport of synaptic vesicles from the cell body to axonal presynaptic sites (Hall and Hedgecock, 1991). Consistent with this interpretation,

immunostaining showed that *unc-104* mutant worms had less synaptotagmin at synapses than wild type worms and that expression of GFP-tagged unc-104 rescued the paralyzed phenotype of *unc-104* worms (Zhou et al., 2001) These data provide strong evidence that unc-104 is required for axonal transport of synaptic vesicle proteins in *C. elegans*.

In a forward genetic screen in *Drosophila* for synaptic defects in the eye identified the gene named, *immaculate connections* (*imac*, for its phenotype of failure to form synaptic connections) which was found to encode the fly homolog of unc-104 and vertebrate KIF1A (Pack-Chung et al., 2007). In *imac* mutant flies synaptic proteins (synaptotagmin, AP180, and endophilin), and dense core granule proteins (discussed below) were both absent at synapses in the axon. Instead they were accumulated in the cell body. *Imac* flies showed normal axon outgrowth, normal mitochondria distribution, and normal distribution of axonal membrane proteins such as syntaxin and Fasciclin II suggesting that the loss of imac had specifically effected targeting of synaptic and dense core granules to synapses (Pack-Chung et al., 2007).

Transport of synaptic vesicle proteins in vertebrates by KIF1A and KIF1Bβ

The first evidence corroborating the notion that KIF1A transports synaptic vesicle precursors in mammals, as its homologs do in *C. elegans* and *Drosophila*, was provided by biochemical studies of organelles immunoisolated from rat cauda equina, a bundle of axons that exits the base of the spinal cord. The cauda equina lacks cell bodies and synapses, providing a source to obtain relatively

pure fraction of axonal transport organelles. Immunoisolation of organelles using beads coated with KIF1A antibody specifically pulled out three synaptic vesicle proteins: synaptophysin, synaptotagmin and rab3a, but not a 4th synaptic vesicle protein SV2. Plasma membrane proteins were also absent from organelles immunoisolated with KIF1A antibody. These results suggested that KIF1A is associated with a specific class of axonal transport organelles that contains a subset of synaptic vesicle proteins, including synaptophysin, synaptotagmin, and rab3a, but not SV2. KIF1A is not associated with transport vesicles containing axonal plasma membrane proteins (Okada et al., 1995).

KIF1A-knockout mice provided further evidence that KIF1A is required for the transport of synaptic vesicle proteins (Yonekawa et al., 1998). Homozygous KIF1A mutant mice die 24hrs after birth, and show significant ataxia and central nervous system neurodegeneration. Synaptic proteins were expressed at normal levels in brains of newborn animals, but immunostaining showed reduced amount of synaptophysin and SV2 at synapses in spinal anterior horn regions. Electron microscopy of these areas revealed that mutant animals had 35% fewer nerve terminals and 40% fewer synaptic vesicles at terminals. In addition, clusters of small clear vesicles were accumulated in neuronal cell bodies of mutant but not wild-type animals. These results provide evidence that lack of KIF1A results in impaired transport of vesicles containing synaptic vesicle proteins from the cell body to the axon. However, contrary to the previous study, which suggested that SV2 was not transported by KIF1A, SV2 localization at synapses was also reduced in KIF1A$^{-/-}$ mice (Yonekawa et al., 1998).

KIF1Bβ, the closely related family member of KIF1A, shares an almost identical motor domain and 61% homology in the tail with KIF1A (Nangaku et al., 1994; Zhao et al., 2001) and may also transport synaptic vesicle proteins to synapses (Zhao et al., 2001). Like KIF1A, KIF1Bβ co-fractionates with synaptic vesicle and not plasma membrane proteins. KIF1B knockout mice died 30 minutes after birth from severe neurological defects. Cultured hippocampal neurons from embryonic knockout mice died within 5 days of placement in culture. The viability of cultured neurons was rescued by expression of KIF1Bβ. Heterozygote $KIF1B^{+/-}$ mice survived but developed impaired locomotion during the first year. At two-months of age, the level of synaptic proteins in sciatic nerves of $KIF1B^{+/-}$ mice was reduced by ~50%, and when ligated, fewer synaptic proteins accumulated on the proximal side of the ligature, suggesting a reduction in anterograde transport of synaptic vesicle proteins in $KIF1B^{+/-}$ mice (Zhao et al., 2001).

If KIF1A and KIF1Bβ play redundant roles in transport of synaptic vesicle proteins, why don't they compensate for each other in knock-out animals? One explanation is that though each motor can transport the same cargos, they are not expressed highly enough to fully compensate for each other. Second, while they share some redundancy in cargo transport, each motor may bind additional types of cargo that the other cannot. This is particularly likely for KIF1Bβ, which is expressed in a variety of tissues other than brain, where it likely binds and transports other cargos (Zhao et al., 2001). Finally, KIF1A is expressed later during development than KIF1Bβ, thus KIF1A is not present to compensate for

loss of KIF1Bβ early during development (Yonekawa et al., 1998; Zhao et al., 2001).

A direct link has been found between KIF1Bβ and an inherited peripheral neuropathy, Charcot-Marie-Tooth Disease Type 2a. Afflicted members of one family were found to have inherited a point mutation in the ATP-binding site of the KIF1Bβ motor domain (residue 98 converted from glutamine to leucine, KIF1Bβ-Q98L). The *in vitro* ATPase activity of recombinant KIF1Bβ-Q98L was reduced and when expressed in Vero cells (cell line derived from African green monkey epithelium) KIF1Bβ-Q98L clustered around the cell body while wild type KIF1Bβ accumulated at the plus-end of microtubules at the cell periphery. Thus, the loss-of function mutation in KIF1Bβ-Q98L appears to cause impaired axonal transport, which leads to axonal degeneration and loss of motor function (Zhao et al., 2001).

Transport of dense core granule proteins in non-vertebrates by KIF1A homologs

The homologs of KIF1A in *C. elegans* (unc-104) and *Drosophila* (imac) have been implicated in the axonal transport of dense core granule proteins (Zahn et al., 2004; Pack-Chung et al., 2007; Barkus et al., 2008). In Drosophila, the *imac* gene was identified in a screen for fly mutants with synaptic defects (Pack-Chung et al., 2007). In addition to reduced transport of synaptic proteins to synapses, the localization of GFP-tagged atrial natriuretic factor, a marker of dense core granules, was absent at synapses and mislocalized to the cell body (Pack-Chung et al., 2007).

The role of unc-104 in the transport of secretory granules has been investigated in *C. elegans* and *Drosophila* by comparing the live-cell transport of dense core granules *in vivo* in wild type and *unc-104* mutant animals (Zahn et al., 2004; Barkus et al., 2008). In both studies, mutant and wild type animals were genetically engineered to express GFP-tagged membrane proteins that label dense core granules. This approach is particularly powerful, because it enables numerous aspects of *transport* of candidate cargo to be analyzed in the mutant background, rather than just looking at protein localization. A change in protein localization could be the result of impaired transport; however other mechanisms could cause mislocalization, such as impaired exit from the Golgi or anchoring at target sites. By analyzing transport itself, many more detailed insights specific to transport can be gained, as illustrated by the following experiments.

In wild type *C. elegans*, analysis of the transport of dense core granules labeled with GFP-tagged IDA-1 (IDA::GFP), an ortholog of human phogrin and marker of dense core granules (Wasmeier and Hutton, 1996), showed a distribution of velocities that peaked at ~1, 1.5, and 2.5 µm/sec (Zahn et al., 2004). This 3-peaked velocity distribution profile suggested that dense core granules are moved by multiple kinesins, each with its own characteristic velocity. The same analysis of velocities in *unc-104* mutant worms, showed a distinct loss of only the fast-moving dense core granules; granules moving faster than 1.7 µm/sec were absent. There was also an accumulation of IDA::GFP fluorescence in the cell body, suggesting that these vesicles failed to move efficiently into the axon. The authors were also able to compare transport in axon-like to dendrite-like (the

polarity of neurons in *C. elegans* has not been fully determined) processes in the worms and found no affect on anterograde dense core granule transport in dendrites compared to axons, suggesting that a different kinesin is responsible for dense core granule transport in dendrites (Zahn et al., 2004).

To determine the role of imac in dense core granule transport in *Drosophila*, granules were labeled by transgenic expression of GFP-tagged atrial natriuretic factor (ANF::GFP), a marker of dense core granules (Rao et al., 2001), in wild type and *imac* flies (Barkus et al., 2008). Velocity of ANF::GFP labeled vesicles was reduced 40% in mutant flies, and they moved 30-70% shorter distances before stopping. Interestingly, retrograde transport of dense core granules was also reduced in mutant flies, suggesting that imac regulates retrograde dynein-mediated transport. In this same set of experiments the transport of transgenically expressed synaptotagmin::GFP was compared in wild type and mutant animals. Velocity of synaptotagmin labeled vesicles was also reduced, and they paused more often. Meanwhile, the transport of mitochondria was unaffected (Barkus et al., 2008). These experiments strongly implicate the homologs of KIF1A in the transport of dense core granule proteins in non-vertebrates. Evidence that KIF1A is required for the transport of dense core granule proteins in vertebrates is presented in Chapter 3.

Concluding remarks

These live-cell imaging studies demonstrate the many aspects of transport— the number of anterograde and retrograde-moving vesicles, their velocity, run-length, pause and reversal frequency, the differences in movement between

axon and dendrites, at different developmental stages and between different types of neurons—that can be analyzed by live-cell imaging studies. The studies presented in Chapters 2 and 3 utilize live-cell imaging to study the transport of dendritic and axonal proteins in cultured hippocampal neurons, and exemplify the strength and necessity of the live-cell imaging technique when studying dynamic cellular events like kinesin-based transport. An additional benefit of working with the hippocampal culture preparation, which is taken advantage of in Chapter 3, is the ability to study transport in neurons during development of neuronal polarity.

Chapter 2

Selective transport of dendritic membrane proteins arises independently of the axon initial segment and prior to axon specification

Jennifer D. Petersen, Stefanie Kaech, and Gary Banker
Jungers Center for Neurosciences Research, Department of Neurology, Oregon Health and Science University, Portland, Oregon 97239

Summary

In the proximal axon, the anterograde transport of vesicles containing dendritic proteins is selectively blocked, preventing their entry to the distal axon. A specialized domain of the proximal axon, called the initial segment, forms the boundary between axonal and somatodendritic neuronal compartments and is appropriately localized to regulate the entry of dendritic transport vesicles to the axon. To determine the relationship between the selective transport of dendritic vesicles and the initial segment in mature neurons, we used live-cell imaging of GFP-tagged dendritic vesicles and immunostaining of protein markers of the axonal initial segment in cultured hippocampal neurons and found that dendritic transport vesicles become blocked at the cell-body proximal edge of the initial segment. However, during development, the transport of dendritic vesicles into the axon was blocked in recently formed axons of stage 3 cells, before markers of the initial segment membrane specialization were detectable. To determine when selective dendritic transport arose during axon formation, we examined dendritic transport with respect to the early axonal marker, constitutively active Kinesin-1 (CA-Kinesin-1) which selectively and dynamically accumulates in a subset of stage 2 neurites prior to axon specification. Remarkably, the abundance of dendritic transport into stage 2 neurites anti-correlated with the accumulation of the axon-preferring CA-Kinesin-1: transport of dendritic vesicles was reduced in CA-Kinesin-1 positive neurites relative to neurites with no CA-Kinesin-1 accumulation. Furthermore, when dendritic transport was recorded before and after CA-Kinesin-1 accumulation alternated between stage 2 neurites, dendritic transport decreased in the neurites that acquired CA-Kinesin-1 accumulation, and increased in neurites that lost CA-Kinesin-1 accumulation. These results show that selective transport of dendritic transport vesicles arises before axon specification and is dynamically regulated.

Introduction

Neuronal function depends on the trafficking and localization of different sets of proteins to axonal and somatodendritic domains. Both axonal and dendritic proteins are synthesized in the cell body, thus both must be transported long distances to achieve a polarized distribution. This long-range transport is carried out by the kinesin super-family of motor proteins (Nakata and Hirokawa, 2007). In the case of dendritic proteins, kinesin-based transport is selective. By an unknown mechanism, the anterograde movement of transport vesicles containing dendritic proteins becomes selectively blocked somewhere in the proximal axon, thus preventing their advancement into the distal axon, while vesicles containing axonal proteins move into the axon without impediment (Burack et al., 2000; Silverman et al., 2001). The selectivity of dendritic transport is likely the primary mechanism by which dendritic protein localization is restricted to the somatodendritic domain (Burack et al., 2000).

Interestingly, the boundary between axonal and somatodendritic domains occurs in the vicinity of where the transport of dendritic vesicles becomes blocked, and is marked by a specialized structure called the axon initial segment (Hedstrom et al., 2008). The initial segment is characterized by a membrane cytoskeleton comprised of ankyrinG and βIV-spectrin (Yang et al., 2007), which anchors cell adhesion molecules in the initial segment membrane (Hedstrom et al., 2007), as well as the high density of voltage-dependent sodium channels responsible for action potential generation (Khaliq and Raman, 2006; Kole et al., 2008). Together these integral membrane proteins contribute to the maintenance of

neuronal polarity by creating a diffusion barrier, which prevents the intermixing of axonal and dendritic proteins in the membrane of the proximal axon (Winckler et al., 1999; Nakada et al., 2003; Boiko et al., 2007; Hedstrom et al., 2008; Song et al., 2009).

We used live-cell imaging and retrospective immunostaining for ankyrinG in cultured hippocampal neurons to look in more detail at the transport of dendritic vesicles in the proximal axon of mature neurons and determine the spatial relationship between where dendritic transport becomes blocked and the location of the initial segment. We also looked at dendritic transport in neurons before (stage 2) and after (stage 3) the development of polarity to determine when selective transport arose with respect to axon formation (Dotti et al., 1988).

We found that in mature neurons, dendritic transport vesicles become blocked at the cell body proximal edge of the initial segment. Live-cell recordings of transport in stage 3 cells showed that the movement of dendritic vesicles into the distal axon was blocked as soon as the axon was formed, before the initial segment membrane specialization was detectable. To determine when selective dendritic transport arose with respect to axon formation, we examined dendritic transport in relation to the localization of the axon-preferring Kinesin-1 motor domain (CA-Kinesin-1) (Nakata and Hirokawa, 2003), which dynamically accumulates in the growth cones of one or two stage 2 neurites prior to axon specification, revealing early biochemical changes in stage 2 neurites that precede axon formation (Jacobson et al., 2006). Remarkably, the amount of dendritic transport into stage 2 neurites with accumulation CA-Kinesin-1 motor

domain was selectively reduced. Furthermore, imaging of dendritic transport in the same cell over time showed that the reduction in dendritic vesicle transport dynamically changed in concert with translocation of the CA-Kinesin-1 between stage 2 neurites. These results show that transport of dendritic proteins is selectively regulated even prior to axon formation and the development of neuronal polarity.

Results

The morphology of the initial segment in cultured hippocampal neurons

To characterize the morphology of the initial segment in mature hippocampal neurons in culture, we immunostained 10-14 day old cultures (10-14DIV) for ankyrinG, an ankyrin isoform highly enriched in the initial segment membrane (Kordeli et al., 1995). Staining for ankyrinG labeled a well-defined region along the proximal portion of a neurite near its origin from the cell body (Fig. 1A), a pattern consistent with ankyrinG staining of the axonal initial segment seen in nervous tissue (Kordeli et al., 1995; Zhang and Bennett, 1998; Zhou et al., 1998). In most cells, only a single neurite was labeled, suggesting that this was likely to be the axon. The identity of the ankyrinG-stained processes was confirmed by co-staining with antibodies against MAP2 (Fig. 1B), a marker of the dendritic cytoskeleton. The ankyrinG-stained neurites were invariably MAP2-negative, demonstrating that they were axons. Faint granular staining for ankyrinG was also present in the cell body, as noted in previous studies (Zhang and Bennett, 1998).

Staining for ankyrinG provided a view of the proximal axon and its origin from the cell body, which is otherwise difficult to observe because of the dense network of neurites that forms in mature cultures (see Fig. 6E and F). We noted several variations in the origin of the axon. In the great majority of cases (94%, n=217 10-20DIV) the axon arose directly from the cell body and the initial segment began a few micrometers beyond its origin (Fig. 1A-C). In the remaining 6% of cells, the axon emerged from a dendrite, rather than directly from the cell body (Fig. 1D-F). In such cases, the initial segment began somewhat farther from the cell body. Occasionally (about 7% of cells when the axon emerged from the cell body), the axon branched near the cell body, producing a bifurcated initial segment, with ankyrinG staining extending along both branches (Fig. 1G).

An initial segment pattern of ankyrinG enrichment was present in the proximal region of more than one process in 27% of mature neurons (n=288 cells, 10-14DIV) (Fig. 1H). Absence of MAP2 staining in the multiple ankyrinG stained processes confirmed their identity as axons (not shown). Often, one of the multiply stained initial segments was dimmer and thinner than the other (arrow in 1H).

The length of the initial segment and its position relative to the cell body were quantified based on ankyrinG staining. Both were found to be highly consistent between cells from which the axon emerged directly from the cell body. The initial segment was on average 6 µm from the cell body (6.1 ± 3.4 µm) and its average length was 21.6 ± 5.6 µm (n=67, 10-12DIV).

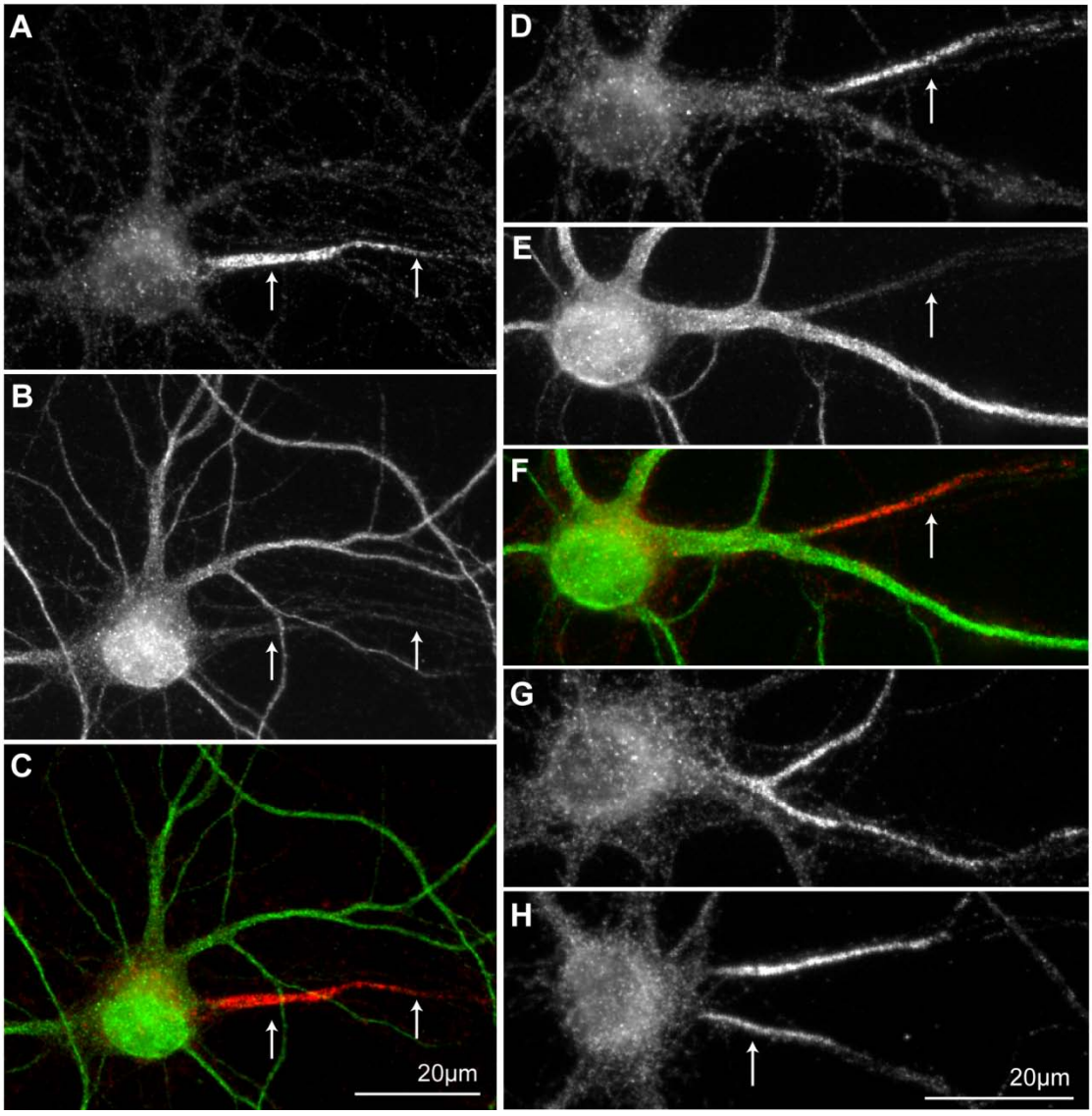

Figure 1. Initial segment morphologies in cultured hippocampal neurons.

(A) A mature neuron stained for ankyrinG showed enrichment of staining within a defined region at the base of the axon, which typically emerged directly from the cell body. (B) MAP2 staining of the cell in A shows an absence of MAP2 in the ankyrinG-positive neurite, and confirms its identity as the axon. (C) Color-overlay of cell shown in A and B (ankyrinG: red; MAP2: green). (D) Staining for ankyrinG revealed instances when the axon emerged from a proximal dendrite rather than the cell body, in which case ankyrinG enrichment is located adjacent to the dendrite. (E) Absence of MAP2 in the dendrite-derived axon shown in D confirms its identity as the axon. (F) Color-overlay of cell shown in D and E (ankyrinG: red; MAP2: green). (G) AnkyrinG staining extended

along both branches of axons that branched within the region of ankyrinG staining. (H) 25% of cells showed an initial segment pattern of staining for ankyrinG present in more than one neuronal process, indicating multiple-axon cells. Commonly, one of the axons was thinner and stained more dimly for ankyrinG (indicated by arrow). All neurons, 10-14DIV.

Sodium channels and βIV-spectrin colocalize with ankyrinG at the initial segment

At the initial segment, ankyrinG is required for the clustering of voltage dependent sodium channels (isoform $Na_v1.6$) in the axolemma (Zhou et al., 1998) and linking them to βIV-spectrin (Berghs et al., 2000). Thus, these three proteins would be expected to colocalize. To test this, neurons were double-stained for both ankyrinG and βIV-spectrin or βIV-spectrin and sodium channels (using a pan-sodium channel antibody, see methods). Examples of double-stained cells are shown in Figure 2. In most cells, ankyrinG staining began abruptly at the proximal end of the initial segment, but declined gradually at the distal end (Fig. 2A). The pattern of βIV-spectrin staining strongly matched that of ankyrinG, even co-localizing in the discontinuous patches of ankyrinG staining that are frequently observed at the distal end of the initial segment (arrows in Fig. 2B). Linescans along the proximal axon of double-stained images showed a nearly identical staining pattern, and correlation analysis (which compares the intensity of each pixel in images in each channel) revealed an exceptionally high degree of colocalization ($r = 0.90 \pm 0.04$, n=51, 10DIV, see Fig. 2C). A similar analysis of cells doubly stained for βIV-spectrin and sodium channels (Fig. 2D and E) also revealed a high degree of colocalization, but sodium channel staining

often remained slightly elevated past the region labeled for βIV-spectrin, which may account for the lower correlation coefficient ($r = 0.78 \pm 0.10$, n=51 10DIV, see Fig. 2F).

The initial segment is a specialized cytoskeletal domain

We were also interested in the localization of cytoskeletal markers within the initial segment, especially those that are enriched in axons or dendrites. To compare the location of the marker of dendritic microtubules with markers of the initial segment membrane specialization, we double stained cells for ankyrinG and MAP2, a marker of the dendritic microtubules. Staining for MAP2 was low in the cell body and proximal axon, compared to dendrites. Staining for MAP2 in the proximal axon, dropped off precipitously where ankyrinG staining began (Fig. 3A and B), thus, microtubules in the initial segment do not have dendritic properties.

We next examined markers of axonal microtubules, and their spatial relationship to the initial segment. Axonal microtubules are enriched for the tubulin posttranslational modifications acetylation and polyglutamylation (Fukushima et al., 2009). Immunostaining for these modifications was low in the proximal axon. Staining intensity began to increase 20 µm from the cell body, and continued to rise well beyond the initial segment (Fig.3 C-F). The antibody Tau1 labels a dephosphorylated form of the microtubule associated protein, tau (dephosphorylated at serine 199/202), that is abundant in the axon (Shahani and Brandt, 2002). Tau1 showed a similar spatial pattern to that of acetylation and polyglutamylation. Tau1 enrichment on axonal microtubules began at the distal

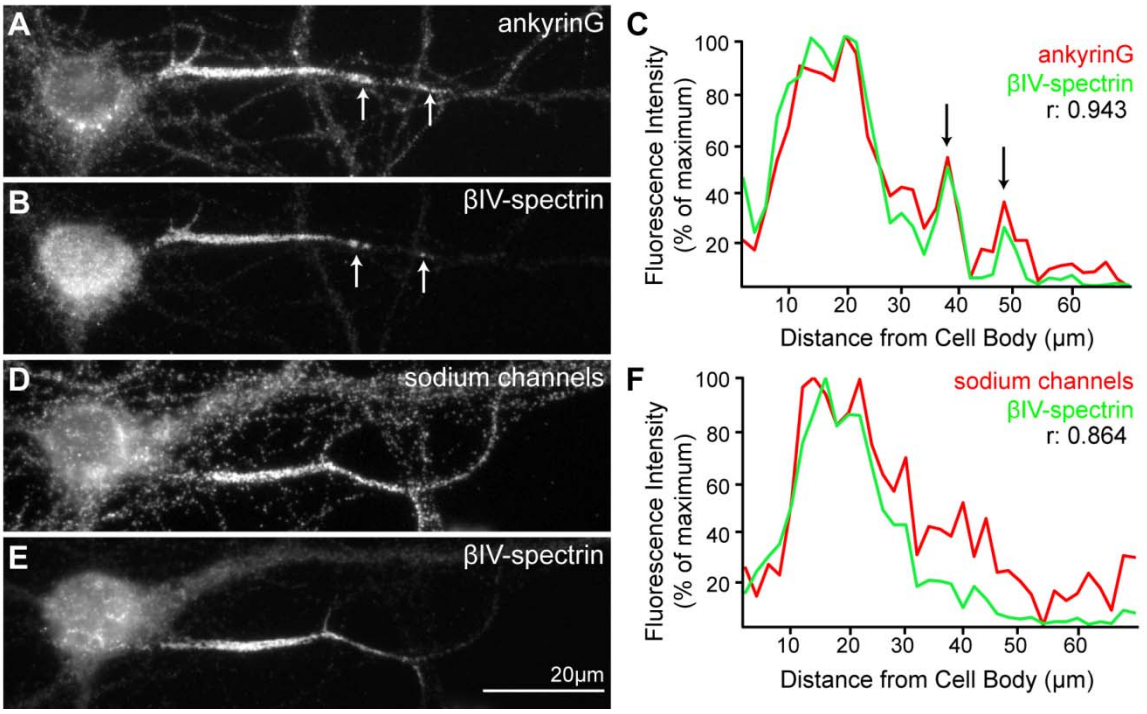

Figure 2. Initial segment proteins colocalize at initial segment membrane in double-stained neurons.

A mature neuron double-stained for ankyrinG (A) and βIV-spectrin (B) shows overlapping patterns of enrichment at the initial segment. Arrows indicate colocalization of the proteins in discontinuous patches of staining present adjacent to the distal edge of the initial segment. (C) A linescan showing staining intensity along the proximal axon of this cell shows that the staining intensity for ankyrinG and βIV-spectrin per micron is closely matched; arrows indicate peaks in the linescan that correspond to discontinuous patches of staining adjacent to the distal edge of the initial segment. The correlation value of ankyrinG and βIV-spectrin staining intensity per micron in this cell is 0.943. A neuron double stained for sodium channels (D) and βIV-spectrin (E) shows an overlapping pattern of enrichment at the initial segment. (F) The linescan corresponding to this cell shows that enrichment for sodium channels extends slightly beyond the distal end of the βIV-spectrin resulting in a slightly lower, but still highly colocalized correlation value of 0.864. Both cells 10DIV.

end of the initial segment (not depicted) and continued to rise along the axon in a proximo-distal gradient. A composite linescan, which quantifies the spatial relationship of ankyrinG and these cytoskeletal markers, indicates that the microtubules in the initial segment are not enriched in either markers of dendritic or axonal microtubules, and thus may constitute a unique cytoskeletal domain (Fig. 3G).

The transport of dendritic vesicles at the base of the axon

It was previously shown that vesicles containing GFP-tagged dendritic membrane proteins are transported into dendrites in large numbers, but few if any are transported along the axon (Burack et al., 2000; Silverman et al., 2001). By imaging the transport of dendritic vesicles near the point of origin of the axon, we aimed to determine where the dendritic vesicles become blocked, and how this site relates spatially to the axon initial segment. To address this question, we introduced a marker of dendritic transport vesicles, GFP-tagged transferrin receptor (TfR-GFP), into dissociated hippocampal neurons by electroporation at the time of plating. After a week in culture, the intracellular transport of TfR-GFP labeled vesicles was captured by live-imaging, then these cultures were fixed and immunostained for ankyrinG and the imaged cells were relocated.

As shown in Figure 4, cells expressing TfR-GFP showed bright GFP fluorescence throughout the cell body and dendrites, but minimal labeling beyond the first few micrometers of the axon (arrows Figure 4C and E), consistent with previous reports. Time-lapse recordings showed that numerous vesicles and short tubulovesicles underwent long-range bidirectional movement in the

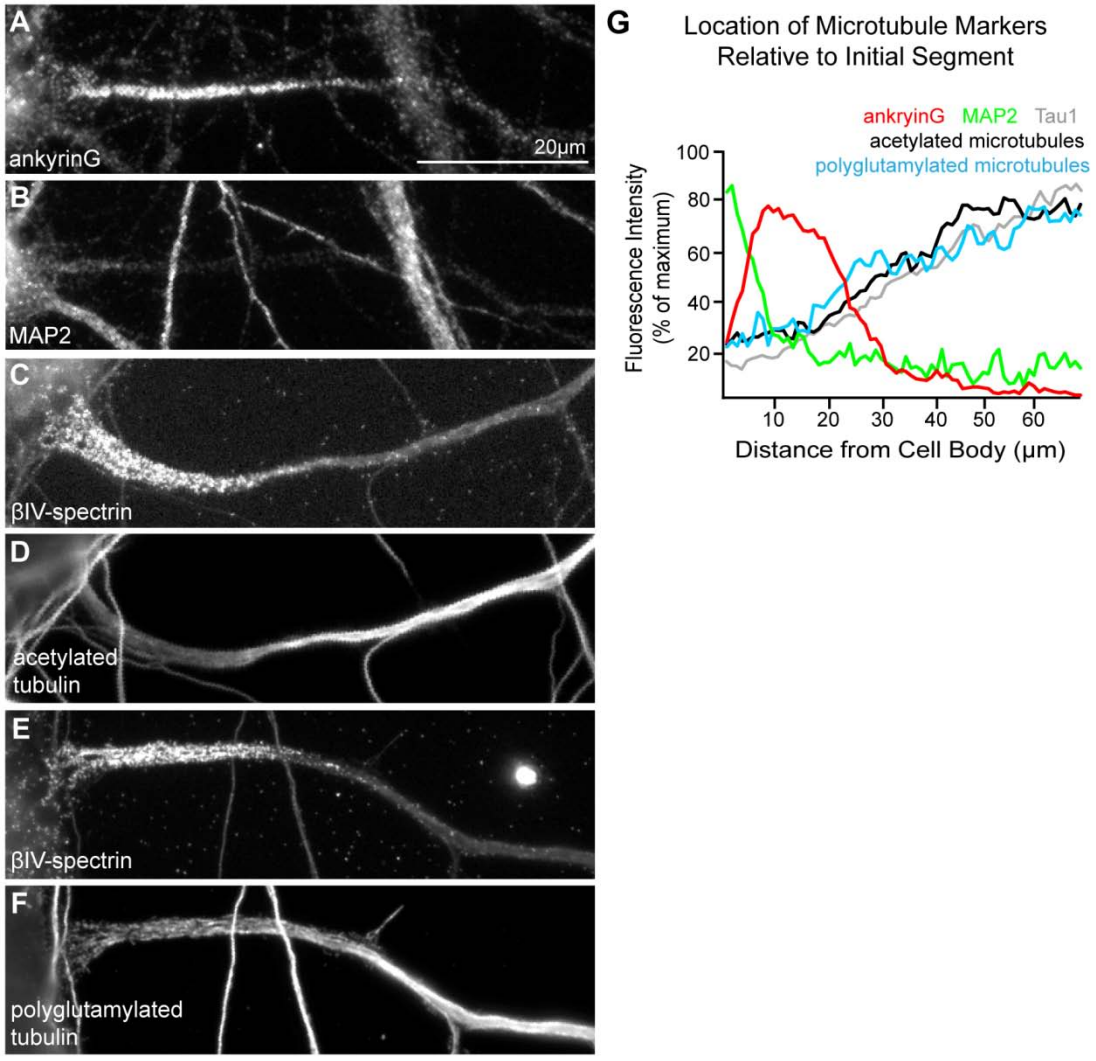

Figure 3. The initial segment is a unique cytoskeletal domain.

Neurons double-stained for ankyrinG (A) and MAP2 (B); βIV-spectrin (C) and acetylated microtubules (D); βIV-spectrin (E) and polyglutamylated microtubules (F); and Tau1 (not depicted) were used to construct a composite line-scan (G) showing the average location of enrichment for each protein along the proximal 70 µm of the axon. Staining of ankyrinG (n=12 cells) peaks between 5-25 µm from the cell body. MAP2 staining (n=12 cells) drops precipitously within the first 10 µm of the axon. Staining for polyglutamylated (n=8 cells) and acetylated microtubules (n=9 cells), and Tau1 (n=17 cells) start to become enriched 20 µm from the cell body, and their enrichment continues well beyond the initial segment.

dendrites (Movies 1 and 2). On average, these vesicles moved at an anterograde rate of 0.72 ± 0.35 µm/sec, with excursion lengths averaging 4.9 ± 2.9 µm (n=289 transport events in 1658 µm of dendrites from 12 cells). Vesicles labeled with TfR also moved bidirectionally in the axon, but only in the proximal few micrometers. Kymographs illustrate TfR transport in the sections of axon and dendrite shown in Figure 4C and 4E. Numerous positively and negatively sloping lines (indicating anterograde and retrograde transport events, respectively) are present in the dendrite kymographs. In contrast, the axon kymographs show little anterograde transport of TfR-GFP beyond the first few microns of the axon. There are also fewer stationary TfR-labeled puncta in the axons (indicated by horizontal lines on the kymograph). Enlarged views of the proximal portions of the axon kymographs show the behaviors of three vesicles that enter the base of the axon (Fig. 4 G and H). Each stopped within ~7 µm of entering the axon and two appeared to undergo exocytosis, whereas the third returned to the cell body. We quantified the number of anterograde events as function of distance from the cell body in the axons of 14 cells and found that within 15 µm of the cell body, the number of anterograde vesicles had dropped by 85%, compared to the number that entered the axon, thus dendritic transport becomes blocked ~10-15 µm from the cell body (0.59 ± 0.83 events/5 µm/min between 0 and10 µm from cell body; 0.08 ± 0.33 events/5 µm/min at 15-40 µm from cell body). In some cells one or two dimly labeled vesicles were detected in the distal axon. These vesicles, which moved predominantly in the retrograde direction, may represent a different organelle population than the more brightly

labeled vesicles found in dendrites and the proximal axon. In the case of cells that had two axons and two initial segments, dendritic vesicles were excluded from both axons (Movie 3).

To determine where the anterograde moving TfR-labeled vesicles that entered the base of axon became blocked with respect to the location of ankyrinG for individual cells, we fixed and stained cells for ankyrinG after live-cell imaging. In 7 cells it was possible to unambiguously follow individual organelles over long periods of time (30 seconds to 3 minutes) and determine their fate. In all, we tracked 8 organelles. Of these, 4 fused with the plasma membrane, and 4 reversed direction back toward the cell body after pausing for several seconds. The position at which these vesicles stopped is shown diagrammatically in Figure 5, which also displays the position of ankyrinG staining for the same cell. The position where anterograde transport stopped varied considerably from cell to cell (ranging from 3 to 10 µm from the cell body), but in nearly every case this point corresponded within ± 1-2 µm of the proximal boundary of ankyrinG staining. These observations imply that the unique features of the initial segment include specializations of both the plasma membrane and of the underlying cytoplasm and that the two specializations are in register with one another.

The Development of the Initial Segment

To learn more about the relationship between the initial segment membrane specialization and the mechanism that prevents vesicles containing dendritic proteins from entering the axon, we compared the time-course of their development in our culture system. To determine when the initial segment arises

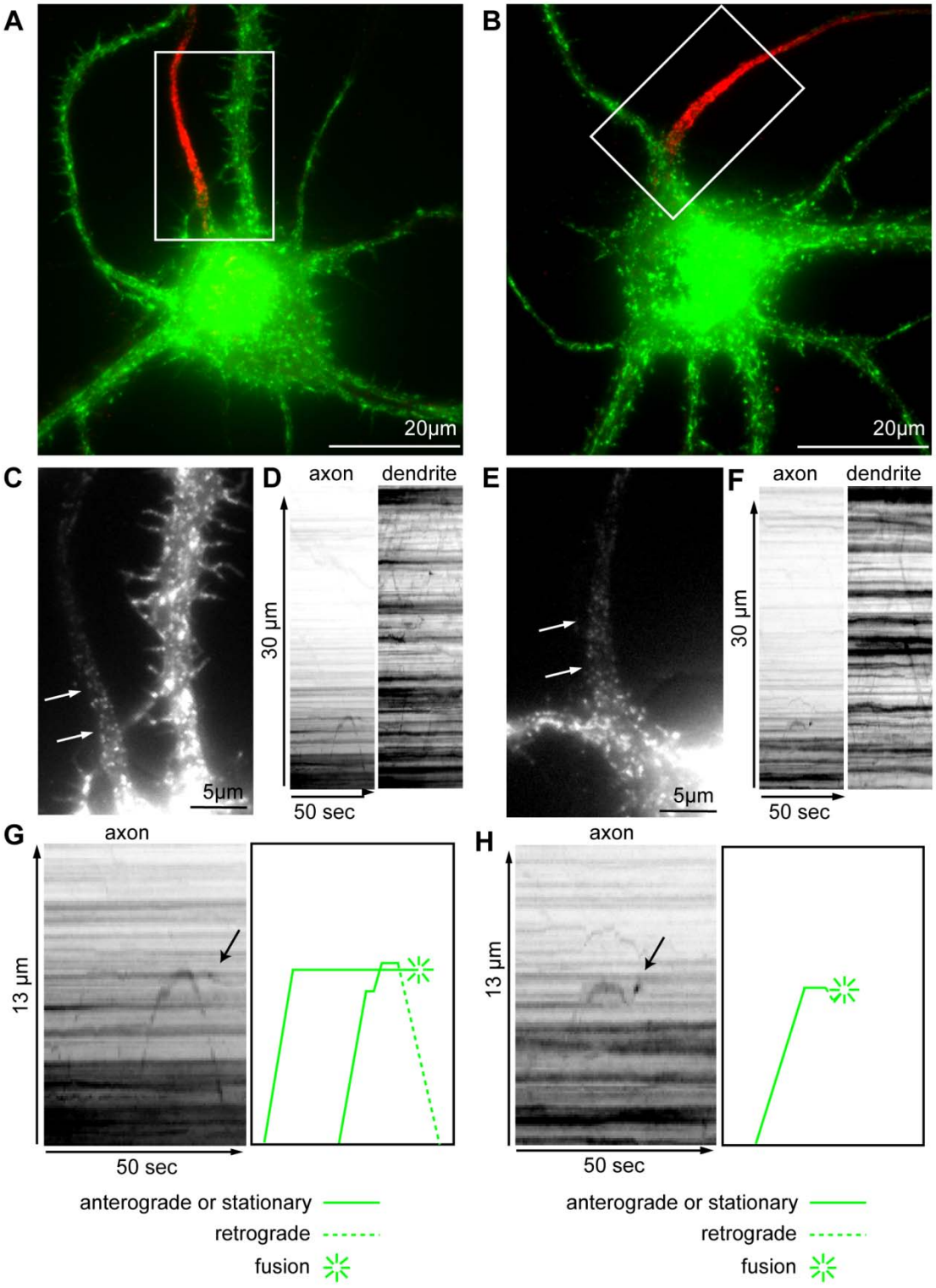

Figure 4. The transport of dendritic vesicles in mature neurons is blocked in the proximal axon.

Figure 4. The transport of dendritic vesicles in mature neurons is blocked in the proximal axon.

(A-B) Fluorescence images show that TfR-GFP (green) is localized to punctate structures in the cell body, dendrites and proximal axon. Immunostain for ankyrinG (red), conducted after live-cell imaging, confirms the identity of the axon. (C and E) Individual frames from the time-lapse recordings of the boxed areas in A and B show numerous TfR-GFP labeled structures in dendrites, but TfR-GFP label in the proximal axon disappears within a few microns from the cell body (Supplemental movie 1 and 2). (D and F) Kymographs from the sections of axons and dendrites in C and E, oriented with time in the x-axis and distance from the cell body in the y-axis, such that anterograde-directed movements of vesicles appear as positively sloping lines, and retrograde-directed movements appear as negatively sloping lines (contrast on kymographs has been inverted so labeled structures appear as black). Kymographs show numerous diagonal lines indicating bidirectional transport of TfR-GFP labeled vesicles in the dendrites, while mobile vesicles in the axons are virtually absent. There is also abundant stationary TfR-labeling in the dendrites, indicated by horizontal lines on the kymographs, which are greatly reduced in the axon kymographs. (G) An enlarged view of the proximal region of the axon kymograph shown in D. Two TfR- labeled vesicles entered the axon. Both move 7 µm and then stalled. One fused with the plasma membrane, and the other reversed out of the axon. These transport events are illustrated in a cartoon representation to the right. (H) An enlarged view of the axon kymograph shown in F. One vesicle that entered the axon paused after 6 µm and then fused with the plasma membrane. This transport event is illustrated in a cartoon representation to the right. Arrows on the kymographs in G and H indicate the sites of vesicle fusion, which appear in kymograph as a black dot.

---

during development, we immunostained cultures for ankyrinG, βIV-spectrin, and voltage-dependent sodium channels at times ranging from 2 to 20 days in culture. Results are shown in Figure 6. Consistent with previous evidence that ankyrinG is required for localization of other initial segment proteins (Zhou et al.,

1998; Jenkins and Bennett, 2001; Hedstrom et al., 2007; Yang et al., 2007; Hedstrom et al., 2008), staining for βIV-spectrin or sodium channels was never detected in the absence of ankyrinG staining. At 2DIV, 18% of cells had dim, but detectable enrichment of staining for ankyrinG. By 6DIV, 100% of cells had staining for ankyrinG, and staining was more intense. Staining with ankyrinG continued to intensify until 12DIV. The time course of development of βIV-spectrin and voltage-dependent sodium channels was very similar to that of ankyrinG, and is summarized in Figures 6G and 6H. Beyond 12 days, the intensity of staining with each of these markers declined. These data indicate that the initial segment arises during the first week in culture and its maturation continues throughout the second week, similar to other reports (Boiko et al., 2007; Hedstrom et al., 2007; Yang et al., 2007; Sanchez-Ponce et al., 2008).

These experiments also provide information concerning the development of cells with multiple initial segments (Figure 7). The number of such cells increased significantly, from ~ 6% at 4DIV to ~30% by 12DIV. Often, one initial segment was thicker and stained more intensely than the other (Fig. 1H). This difference might indicate that the thinner, less intensely stained initial segment developed more recently.

The selectivity of transport at stage 3 of development

To determine when the transport of dendritic vesicles into the axon becomes blocked, we introduced TfR-GFP by electroporation and imaged transport at stage 3 of development (1DIV), soon after the axon formed. An example of the transport of dendritic vesicles in a stage 3 cell is shown in Figure 8 and Movie 4.

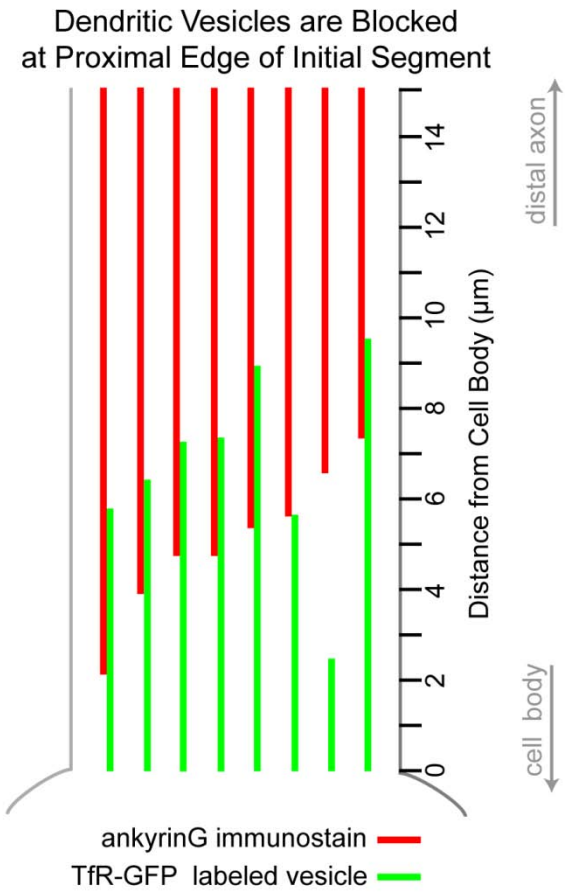

Figure 5. Dendritic vesicles are blocked at proximal edge of initial segment.
A diagram relating the location along the proximal axon that transport of vesicles labeled with TfR-GFP stopped relative to the location of ankyrinG immunostain in that cell. On average, vesicles moved 1.7 ± 2.6 µm into the region of ankyrinG staining before stopping (fate of 8 transport events tracked in 7 cells).

In this cell, numerous TfR-GFP labeled vesicles enter each of the 5 minor neurites, travel to their tips, and then reverse back to the cell body. The kymograph corresponding to the time-lapse recording of the cell shown in Figure 8B illustrates the abundant anterograde transport of TfR-labeled vesicles along the entire length of the minor neurites, which at this stage of development are 30 µm or less in length (Fig 8 C, D). Several vesicles entered the axon, but reversed direction, fused with the plasma membrane, or disappeared from view within 25 µm from the cell body. The TfR-GFP fluorescence that was present in the distal axon was predominantly stationary or occasionally moved retrograde to

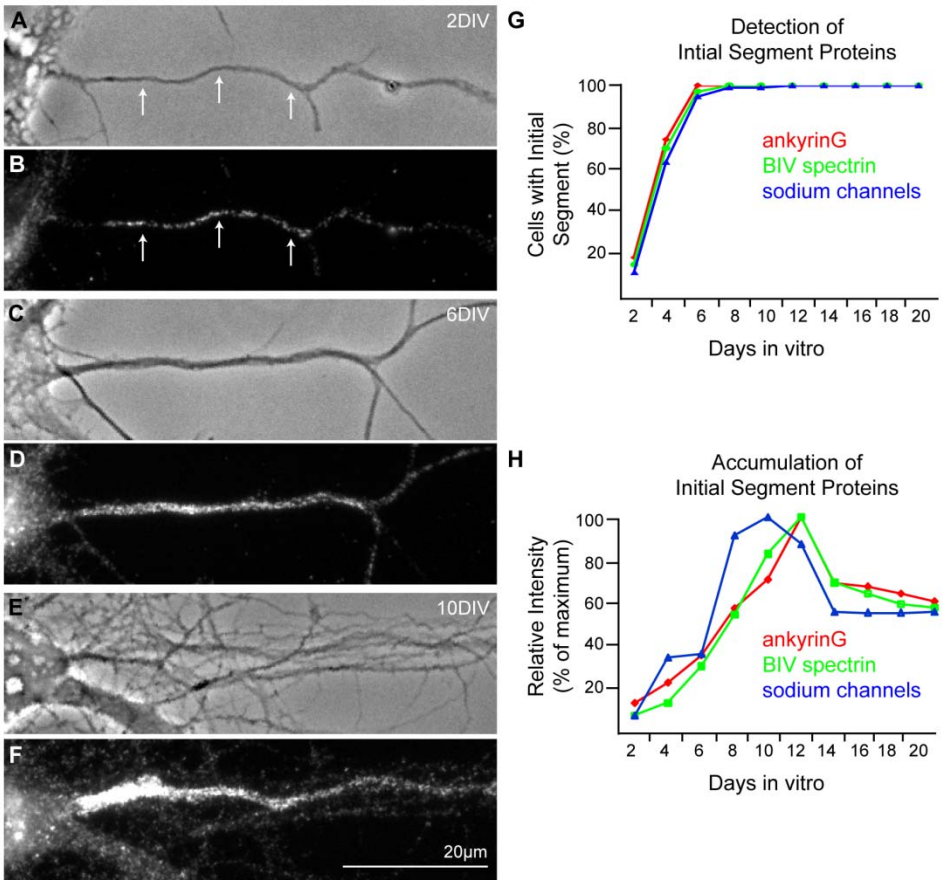

Figure 6. The initial segment develops during the first 2 weeks in culture.

Cultured neurons stained for ankyrinG at 2DIV (A,B), 6DIV (C,D), and 10DIV (E,F) are shown with phase image above and corresponding fluorescence image below. (A,B) At 2DIV 18% of neurons had very dim initial segment staining for ankyrinG, indicated by arrows. (C,D) By 6DIV, ankyrinG was detectable in 100% of cells, and staining was more intense. (E,F) AnkyrinG staining continued to intensify until 12DIV. (G) Quantification of the proportion of neurons with detectable enrichment for ankyrinG, βIV-spectrin and sodium channels during development. (H) Quantification of staining intensity for ankyrinG, βIV-spectrin and sodium channels in the cell body proximal 50 µm of the axon during development. (Data are based on analysis of 700-1500 cells from 3-6 experiments). All fluorescence images collected with identical illumination conditions and images were scaled identically.

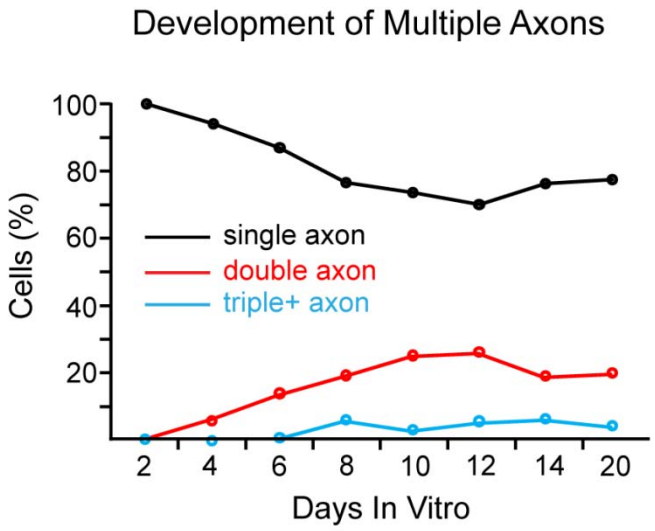

Figure 7. The proportion of cells with multiple axons increased during development in cultured hippocampal neurons. AnkyrinG staining was used to quantify the number of cells with multiple axons during the first 20 days in culture. There was a concomitant decrease in the proportion of cells with a single axon and increase in multiple-axon cells during development, indicating that neurons initially specify a single axon, but can develop secondary axons during the first two weeks in culture.

---

the cell body. This may represent TfR that was present in the neurite plasma membrane before it became the axon.

We analyzed kymographs of 8 stage 3 neurons expressing TfR-GFP and compared the number of anterograde transport events in the minor neurites and nascent axon as a function of distance from the cell body (Fig. 8F). The number of anterograde events throughout the length of the minor neurites averaged 5.5 ± 0.9 events/5 µm/minute. Forty percent fewer vesicles entered the base of the axon than minor neurites. Their numbers further declined by 85% within 30 µm from the cell body. Beyond 30 µm there were virtually no anterograde events in

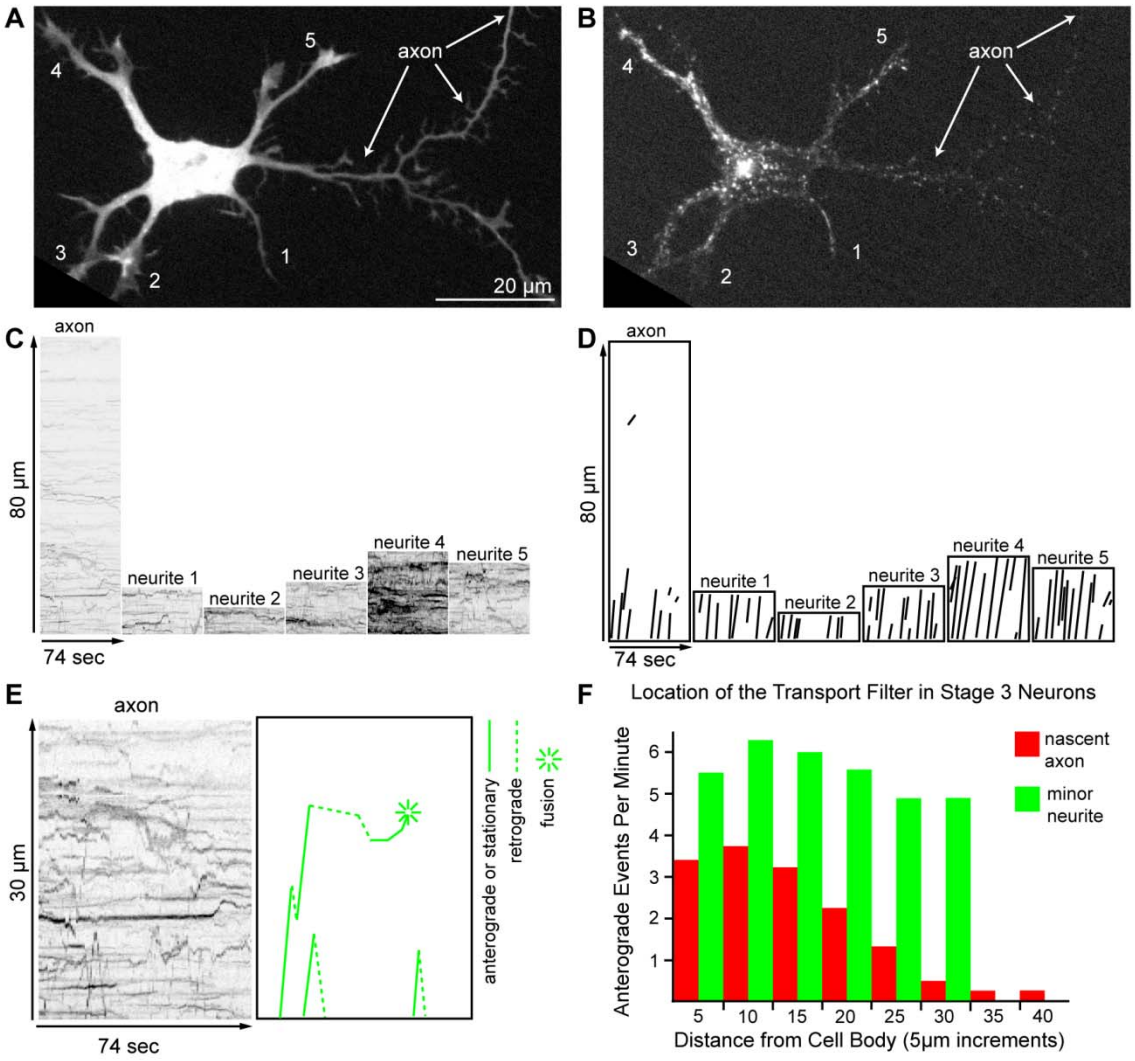

Figure 8. Selective transport of dendritic vesicles is present in stage 3 neurons.

(A) Fluorescence image of a stage 3 neuron (1DIV), co-expressing soluble mRFP to visualize cell morphology and (B) TfR-GFP. TfR-GFP labels puncta present throughout the cell body and minor neurites. Faint TfR-GFP-labeling is also detectable in the nascent axon and is indicated by arrows. Neurites are numbered to correspond to the kymographs below. (C) Kymographs generated from the time-lapse recording of the cell shown in A-B. Many TfR-labeled puncta are mobile vesicles traveling bidirectionally the entire length of the minor neurites. Anterograde-directed TfR-GFP labeled vesicles were present only in the proximal axon. (D) Illustration of anterograde transport events present in kymograph shown in C shows abundant anterograde events in neurites. In comparison, transport of TfR-labeled vesicles into the distal axon is absent. (E) An

enlarged view of the cell-body proximal 30 µm of the axon kymograph shown in C shows that several TfR-labeled vesicles enter the proximal axon, but either reverse direction, fuse with the plasma membrane, or disappear from view. Three clear examples of vesicles whose fates could be unambiguously followed are shown in the cartoon to the right. Two vesicles advance ~15 µm into the axon, and then quickly reverse direction without pausing. A third vesicle advances ~ 20 µm into the axon, before eventually fusing with the plasma membrane. (F) The number of anterograde transport events per 5 µm increment in the first 40 µm of the axon was quantified and compared to that in neurites (which were 30 µm or shorter at stage 3) for 8 cells. The number of anterograde events in the axon dropped between 20-30 µm from the cell body.

---

the axon, except for a few short range movements of dimly labeled puncta (n=8 cells, 8 axons, 31 neurites, and 10 minutes of total combined recording).

These results indicate that the selective transport of vesicles containing dendritic proteins is already established in stage 3 neurons, shortly after the axon first arises. In mature neurons, this block of dendritic transport vesicles occurs in the cell-body-proximal edge of the initial segment, ~10 µm from the cell body. In stage 3 cells, dendritic vesicles become blocked 20-30 µm from the cell body. Comparing these findings with the results of immunostaining for initial segment membrane markers indicates that the development of selective dendritic transport precedes formation of the membrane specialization because selective transport was observed in all stage 3 cells, whereas less than 20% of stage 3 cells stained for membrane markers of the initial segment.

The selective transport of vesicles containing dendritic proteins was detected prior to axon specification

Constitutively active forms of Kinesin-1 (also known as conventional kinesin), the motor protein that mediates the anterograde transport of vesicles containing axonal plasma membrane proteins (Ferreira et al., 1992; Nakata and Hirokawa, 2003), selectively accumulate at the tips of axons but not dendrites (Nakata and Hirokawa, 2003). The ability of Kinesin-1 to distinguish among different neurites begins before morphological polarization, as Kinesin-1 accumulates in only one or a small subset of neurites in stage 2 hippocampal neurons (Jacobson et al., 2006) . These results indicate that Kinesin-1 recognizes differences in the microtubule cytoskeleton in different stage 2 neurites and raises the question of whether vesicles containing dendritic membrane proteins might also be transported selectively into a subset of stage 2 neurites. To address this question, we co-electroporated hippocampal neurons with a marker for dendritic vesicles together with truncated, constitutively active Kinesin-1 (CA-Kinesin-1) tagged at its C-terminus with tdTomato. Vesicle transport was imaged in stage 2 neurons that had accumulated CA-Kinesin-1 in a subset of neurites. In this set of experiments, the membrane associated small GTPase rab11b, which mediates the transport of recycling TfR (Schlierf et al., 2000), was chosen as a marker for dendritic vesicles because it does not accumulate in the plasma membrane, thus enhancing the detection of transport vesicles. Like vesicles labeled with TfR, rab11b tagged N-terminally with GFP (GFP-rab11b) labeled vesicles that were selectively excluded from the axon at stage 3 and stage 4 of development (data not shown).

A representative cell from these experiments is shown in Figure 9 and Movie 5. In this cell, CA-Kinesin-1 accumulated at the tips of two of the cell's 4 neurites (neurite 1a and neurite 2). Kymographs illustrating the transport of rab11b-labeled vesicles in this cell show that there were far more anterograde movements in neurites that lacked than CA-Kinesin-1 (neurites 1b, 3, and 4) than in those where the motor construct accumulated (neurites 1a and 2) (Fig. 9 C-D). This is what would be expected if dendritic vesicles were preferentially excluded from those stage 2 neurites that supported the translocation of the axon-preferring kinesins. The behavior of rab11b-labeled vesicles in neurites 1a and 1b is of particular interest because both neurites originated as branches from a common segment; CA-Kinesin-1 accumulated only at the tip of branch 1a. There was abundant transport of rab11b vesicles in the common segment proximal to the branch point and along branch 1b, but there were only a few short movements of rab11b vesicles along branch 1a suggesting that the modifications that inhibit dendritic transport and enhance CA-Kinesin-1 transport originate at the branch point that leads to neurite 1a.

In all, we analyzed the transport of rab11b vesicles in 10 stage 2 cells (Fig. 10). The number of anterograde transport events in neurites with little or no accumulation of CA-Kinesin-1 (≤ 20% of total CA-Kinesin-1 fluorescence in distal half of neurite; 33 out of 45 neurites) averaged 1.15 ± 0.68 events/µm/min. In contrast, there were 50% fewer anterograde movements of dendritic vesicles in neurites that accumulated CA-Kinesin-1 (≥ 20% CA-Kinesin-1, 0.59 ± 0.34 events/µm/min; T-test, $p < 0.001$; 12/45 neurites) (Fig. 10A). The summed

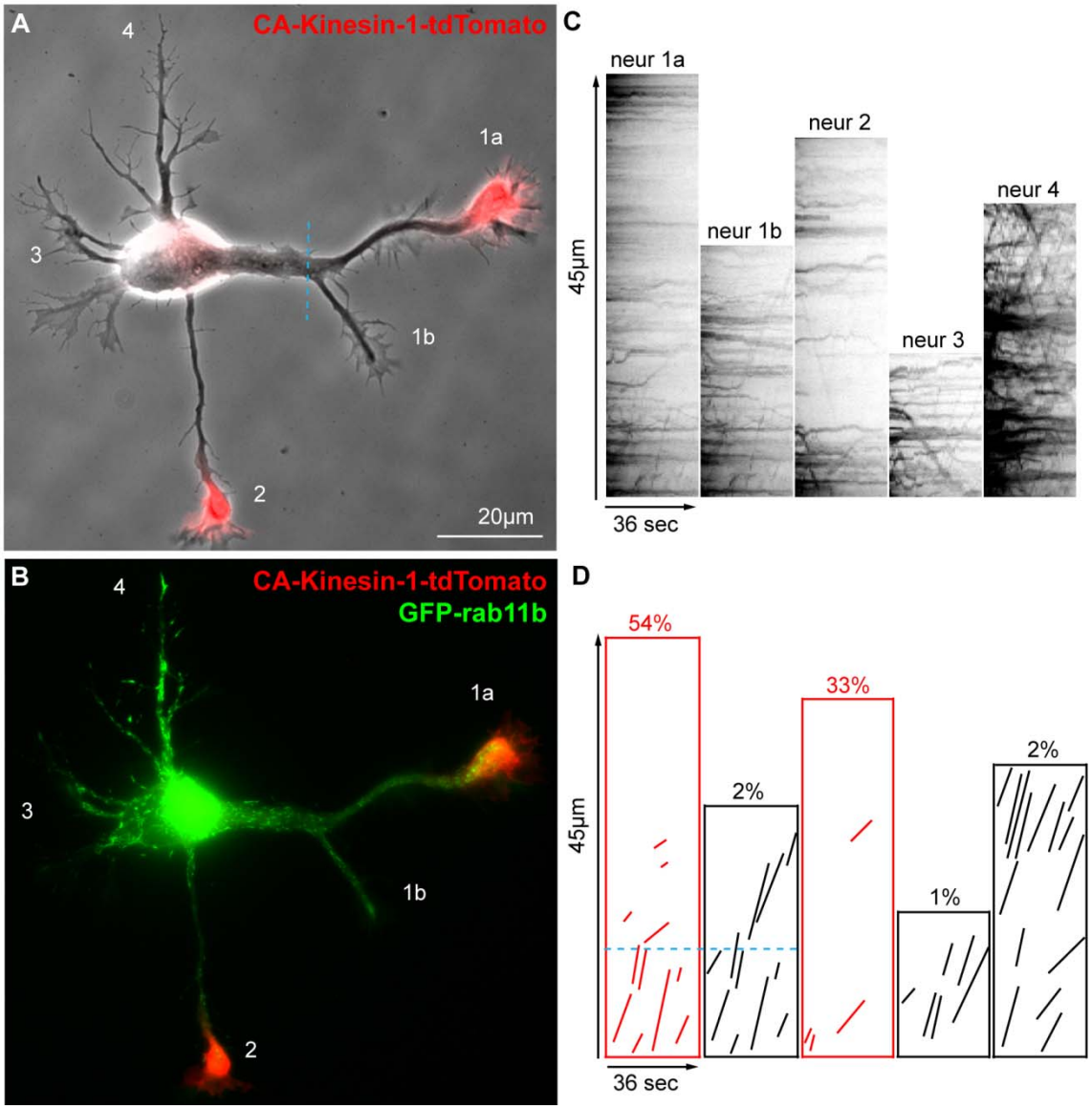

Figure 9. Selective transport of dendritic vesicles was detected stage 2 of development.

(A) A stage 2 cell expressing CA-Kinesin-1-tdTomato is shown in phase with fluorescence overlay to show location of CA-Kinesin-1 accumulation. Neurites are numbered to correspond with kymograph. A dashed blue line indicates the bifurcation point that separates neurites 1a and 1b. (B) Fluorescence image of the same cell shown in A, which co-expressed GFP-rab11b. A time-lapse recording was conducted to detect a correlation between dendritic transport and CA-Kinesin-1 accumulation. (C) The kymograph corresponding the live-cell recording of the cell shown in A and B. (D)

Illustration of anterograde transport events present in kymograph shown in C. The % accumulation of CA-Kinesin-1 in each neurite is listed above each kymograph. A reduction in anterograde transport events in neurite 1a beyond the bifurcation point that separates neurites 1a, 1b, and in neurite 3 compared to the other neurites is evident.

---

excursion length of dendritic vesicles (sum of anterograde excursion lengths per neurite/ length of neurite/ min) was also significantly reduced in neurites that accumulated CA-Kinesin-1, from an average of 3.4 ±1.8 μm to 1.4 ± 1.3 μm ($p < 0.001$, Fig. 10B). Vesicles that underwent long excursions (> 4 μm) were virtually absent in neurites that accumulated CA-Kinesin-1. The average velocity of vesicle transport was marginally lower in CA-Kinesin-1 positive neurites (1.71 ± 0.54 μm/ sec in neurites with ≤20% CA-Kinesin-1 accumulation; 1.18 ± 0.6 μm / sec in neurites with ≥20% CA-Kinesin-1 accumulation).

The number of rab11b-labeled anterograde events per 5 μm interval moving away from the cell body was calculated for neurites with greater than and less than 20% of CA-Kinesin-1 fluorescence accumulation (Fig. 10C). On average, 40% fewer rab11b-labeled vesicles entered the first 10 μm of stage 2 neurites with CA-Kinesin-1 accumulation. Along the length of stage 2 neurites with CA-Kinesin-1 accumulation, the number of anterograde events reduced gradually by 60%, compared to the number of dendritic vesicles that entered the axon.

To confirm that stage 2 neurites with high levels of CA-Kinesin-1 accumulation could support vesicular transport and the reduction in transport was specific to dendritic transport vesicles, we co-electroporated neurons with GAP-43, a

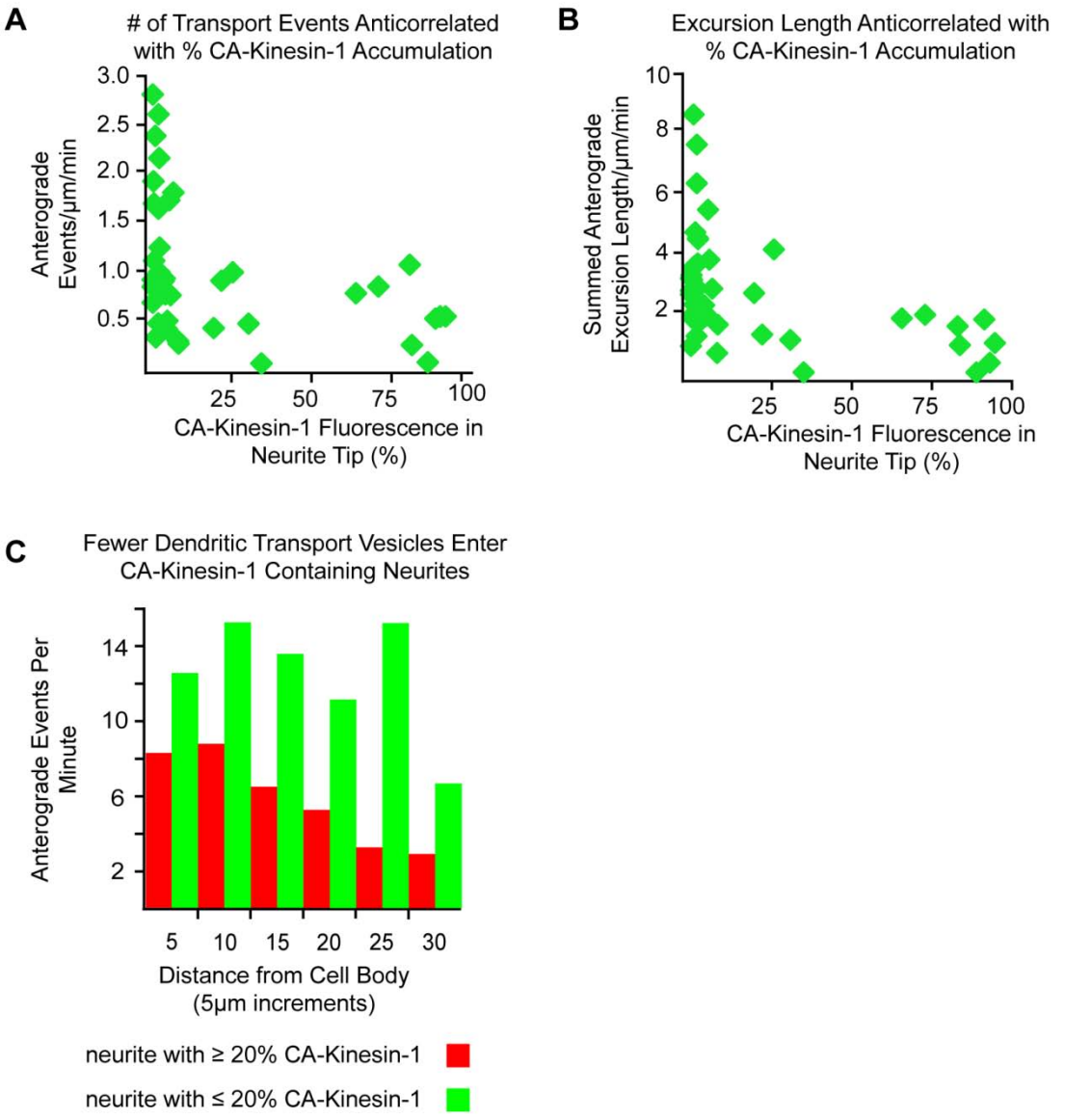

Figure 10. Dendritic transport was reduced in stage 2 neurites with CA-Kinesin-1 accumulation.

(A) Quantification of the number of dendritic transport events in stage 2 neurites relative to neurites CA-Kinesin-1 accumulation. Neurites with ≥20% of fluorescence signal for CA-Kinesin-1 localized in the distal half of the neurite consistently have a low number of dendritic transport events. (B) Summed excursion length of the dendritic transport events is low in neurites with ≥ 20% of fluorescence signal for CA-Kinesin-1 localized in the distal half. (C) The number of dendritic vesicles that enter neurites with ≥ 20% CA-Kinesin-1 accumulation is reduced by 40%, and their numbers gradually reduce with distance from the cell body. (n=10 cells, 43 neurites)

Kinesin-1 cargo (Ferreira et al., 1992; Nakata and Hirokawa, 2003), and imaged transport at 1DIV. GAP-43 labeled long tubulovesicular transport organelles that transported without hindrance into stage 2 neurites with accumulated CA-kinesin-1 (data not shown).

One of the most striking features of CA-Kinesin-1 accumulation in stage 2 cells is that it can be very dynamic, with the accumulation of constitutively active Kinesin-1 motors alternating between neurites within a matter of minutes (Jacobson et al., 2006). This indicates that the molecular signals that direct the transport of Kinesin-1 must also be dynamic. The strong inverse relationship between dendritic vesicle transport and the accumulation of CA-Kinesin-1 described above implies that the preferential transport of dendritic vesicles into a subset of stage 2 neurites is also likely to be dynamic. To investigate this question directly, we recorded the transport of rab11b-GFP vesicles in the same neuron at different times, to determine whether the amount of transport in different neurites changed over time and whether these changes were related to changes in the accumulation of CA-Kinesin-1.

An example is shown in Figure 11 and Movie 6. At the beginning of this recording, CA-Kinesin-1 was concentrated at the tips of two branches of neurite 1 (Fig. 11A). After 189 minutes, CA-Kinesin-1 had become concentrated in neurite 3 and was no longer detectable in neurite 1 (Fig. 11C). Illustrations from kymographs made by tracing anterograde lines on the original kymographs (not depicted) show the anterograde vesicle traffic in this cell at the corresponding times. The number of anterograde transport events of rab11b-labeled vesicles

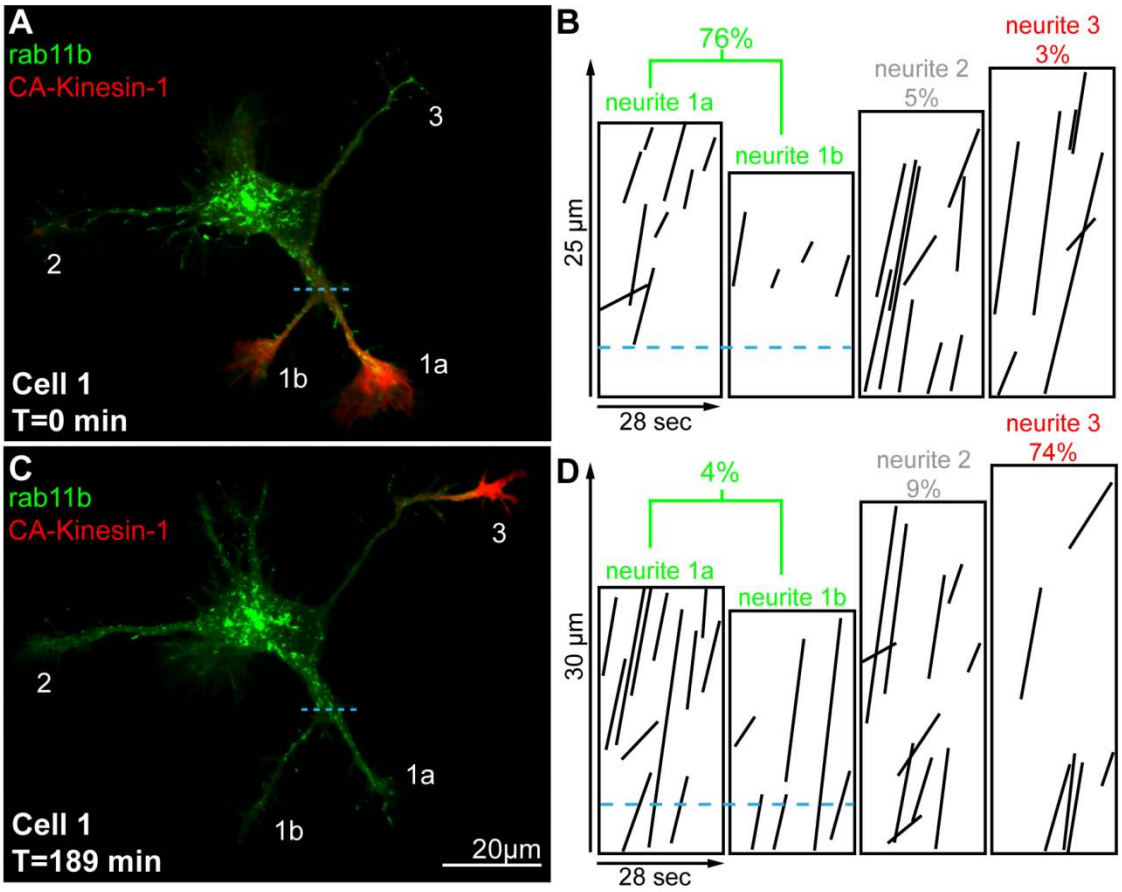

Figure 11. **Selective transport of dendritic vesicles is dynamically anti-correlated with CA-Kinesin-1 translocation at stage 2.**

(A, C) Fluorescence overlay images of a stage 2 cell co-expressing the dendritic protein, rab11b-GFP (green) and CA-Kinesin-1-tdTomato (red) recorded 189 minutes apart, after CA-Kinesin-1 translocated from neurite 1a/b to neurite 3. Transport of rab11b-labeled vesicles was recorded at each time point. (B and D) Illustration of the kymographs that correspond to the two live-cell recordings of the cell shown in A and C show anterograde transport events of rab11b-labeled vesicles in each neurite at the first and second time points. The % of CA-Kinesin-1 accumulated in the tip of each stage 2 neurite is listed above each kymograph and coded red for neurite that gained CA-Kinesin-1 accumulation, green for a neurite that lost motor accumulation, and gray for a neurite in which motor accumulation did not increase above or decrease below 20%. Dendritic transport in neurite1a/b increased at the second time point, after CA-Kinesin-1

accumulation dropped by 72%. Dendritic transport in neurite 3 decreased at the second time-point, after CA-Kinesin-1 accumulation increased by 71%.

---

increased markedly in the neurite that lost CA-Kinesin-1 (neurite1a and 1b). Transport of rab11b-labeled vesicles decreased substantially in neurite 3, in which CA-Kinesin-1 accumulated. The length of neurite 1a and 1b increased after loss of CA-Kinesin-1 accumulation, showing that accumulation of CA-Kinesin-1 is not correlated with neurite elongation, as previously demonstrated (Jacobson et al., 2006). In recordings from three different stage 2 cells (spanning intervals from 66 to 189 minutes) we identified 3 neurites in which CA-Kinesin-1 became accumulated and 2 neurites in which an accumulation of CA-Kinesin-1 was lost. In the three neurites that gained CA-Kinesin-1, transport decreased by 46%, 29%, and 82%, relative to the first time point, based on summed excursion length. Conversely, in the two neurites that lost CA-Kinesin-1, transport increased to 216% and 302% of transport at the first time point. These results show that transport of vesicles containing dendritic proteins is dynamically regulated during stage 2 of development, and that changes in the amount of dendritic transport are inversely related with the accumulation of CA-Kinesin-1.

Discussion

Two components of selective dendritic transport that arise early during development

Live-cell imaging revealed key aspects of the selective transport of dendritic transport during development of neuronal polarity. In mature neurons, the

anterograde movement of dendritic vesicles was completely blocked at a site along the proximal axon that aligned with the cell body-proximal edge of the initial segment membrane specialization. This block of dendritic transport was already present in the proximal region of newly formed stage 3 axons that lack a detectable initial segment membrane specialization. Quantification of dendritic transport in stage 3 neurons further revealed that dendritic transport vesicles had a lower probability of entering the axon compared to minor neurites. Finally, reduced dendritic transport was also detected in neurites of stage 2 neurons prior to axon specification, and was dynamically regulated. These observations allow us to identify two spatially distinct mechanisms that prevent dendritic transport vesicles from reaching the distal axon. The first is the transport filter, which describes the selective block of anterograde-directed dendritic vesicles that occurs at a defined location in the proximal axon. The second is selective entry, which refers to the reduced preference dendritic vesicles show for entering the axon compared to dendrites and must be localized to the cell body or area immediately preceding the opening to the axon.

The transport filter and its relationship to the axon initial segment

The transport filter was detected in stage 3 axons; most dendritic vesicles were blocked within 25 µm from the cell body. Therefore the molecular machinery that inhibits the transport of dendritic vesicles into the axon arises before the initial segment membrane specialization during development. However, as the initial segment develops, the transport filter shifts closer to the cell body and the two become precisely aligned at the cell body-proximal edge of the initial segment,

located 10-15 µm from the cell body. Indeed, it makes functional sense that dendritic proteins are not transported intracellularly beyond the area of the initial segment diffusion barrier where they could be inserted in the axonal membrane. This suggests a functional and physical link exists between the two entities in mature neurons. In support of this idea, a recent report showed that dismantling the initial segment membrane specialization in mature neurons by RNAi-mediated knockdown of ankyrinG caused the axon to gradually acquire a MAP2-positive microtubule cytoskeleton and dendritic membrane proteins and postsynaptic specializations appeared in formerly axonal plasma membrane (Hedstrom et al., 2008). It seems likely that dendritic proteins would be transported along the converted MAP2-positive microtubules, thus disassembly of the initial segment membrane specialization in mature neurons may disrupt the transport filter, but this remains to be tested. There was also reduced dendritic transport in stage 2 neurites, however when transport was quantified as a function of distance from the cell body, there was a gradual decline in the number of transport events rather than the steeper decline as seen in stage 3 and mature neurons suggesting that there is not a well established transport filter in stage 2 neurites. However, due to the short length of stage 2 neurites (less than 30 µm), it may be difficult to detect.

The potential role of specialized microtubules in transport filter function

Modifications to the microtubules in the axon could contribute the selective transport of dendritic vesicles. Two posttranslational modifications of microtubules, acetylation and polyglutamylation, are enriched in the axon of

mature neurons and have been shown to enhance Kinesin-1 translocation (Larcher et al., 1996; Reed et al., 2006; Fukushima et al., 2009). It is possible that these modifications affect the translocation of the kinesin moving dendritic transport vesicles. However, our staining of these modifications showed that their enrichment begins at the distal end of the initial segment, while the transport filter is located at the proximal edge of the initial segment, and selective entry even more proximally. Thus acetylation- and polyglutamylation-enriched axonal microtubules do not appear to be properly localized to account for the transport filter or selective entry in mature cells.

Still, in mature neurons there are multiple lines of evidence that show microtubule tracks in the initial segment are structurally and biochemically different from those in the dendrites or the axon, differences that could regulate kinesin transport of dendritic vesicles through this region. First, electron microscopy studies have shown that the microtubules in the initial segment are uniquely bundled (Palay et al., 1968; Peters et al., 1968). Second, exogenously expressed KIF5B rigor mutant preferentially binds to microtubules of the initial segment in cultured neurons (Nakata and Hirokawa, 2003), as does the microtubule plus-end binding protein EB1 (Tirnauer and Bierer, 2000) when expressed at high levels. Third, endogenous phosphorylated IKappaBα localizes to initial segment microtubules (Schultz et al., 2006). Finally, our staining shows that microtubules in the initial segment lack markers for both dendritic and axonal microtubules, such as MAP2, Tau1, and polyglutamylated and acetylated microtubules. While the bases of these structural and biochemical singularities

of the initial segment microtubules is unknown, the fact that initial segment microtubules are different supports the idea that differences in the microtubule tracks are at least in part, the basis of the dendritic transport filter.

The potential role of kinesin regulation in transport filter function

Alternatively, or in addition to microtubule modifications, dendritic transport could be blocked by direct regulation of the kinesin carrying the dendritic vesicle. Phosphorylation of Kinesin-1 has been shown to regulate its microtubule binding (Morfini et al., 2006), and cargo binding (Morfini et al., 2002; Pigino et al., 2009). Through similar means of regulation by phosphorylation, the transport filter could result from selective inactivation of the motor carrying dendritic cargo or its dissociation from the dendritic transport vesicle. Identification of the kinesin responsible for the transport of dendritic vesicles will be critical to elucidating the mechanism of the transport filter. Another possibility is that the dendritic cargo, rather than the motor, is recognized as it enters the axon. The presence of the dendritic transport vesicle could trigger a signaling event that causes its dissociation from the kinesin, or activation of a dynein causing its reversal out of the axon.

An alternative mechanism of selective dendritic transport was recently proposed (Song et al., 2009). The authors describe an ankyrinG- and actin-dependent cytoplasmic filter at the initial segment which imparts a viscous drag on kinesin-cargo vesicle complexes as they enter the axon and blocks the diffusion of soluble proteins into the axon. They suggest that selective transport is achieved because kinesins transporting axonal cargo have a higher efficacy and can

provide the force required to pull their cargo through the flexible actin meshwork of the cytoplasmic filter. In contrast, motors transporting dendritic cargos would lack sufficient power to traverse the cytoplasmic filter and therefore could not move beyond the initial segment. The cytoplasmic filter arose after 5DIV in conjunction with the enrichment of ankyrinG and actin in the initial segment (Song et al., 2009).

Our results contrast with those of Song et al. First, the timecourse at which the transport filter arose differed between studies. They detected a block of dendritic transport into the axon that arose between 3-5 DIV and depended on ankyrinG accumulation, while we detected the transport filter as soon as an axon formed at 1DIV, before ankyrinG accumulation. There was also a significant difference in the transport rates of dendritic vesicles between studies. This discrepancy may be explained by the different methods by which vesicular transport was imaged. We imaged transport at a rate of 2 frames per second and detected a majority of dendritic vesicles moving at 1-2 µm/sec. Song et al. imaged the transport of vesicles that moved into a 15 µm-long photobleached area of the proximal axon at 1 frame every 5 seconds and detected vesicles moving an average of 0.4 µm/sec. Due to the slower rate of imaging used in their study, it is possible that faster moving vesicles were not detected. Finally, our findings differ with respect to the location of the transport filter. They reported that the block to dendritic transport took place 50-60 µm from the cell body at the distal end of the initial segment. We showed that the transport of dendritic vesicles is blocked at the cell body proximal edge of the initial segment. Explanations for these

inconsistencies are not immediately evident but will be clarified with further investigation.

Selective entry of dendritic vesicles into the axon

Selective entry, the second component of selective transport, was detected at all stages of development. In mature neurons, fewer dendritic transport vesicles entered the axon than dendrites; however it was not clear if this was a selective transport phenomenon, or a practical result of the reduced diameter and fewer microtubule tracks in the axon compared to dendrites. This question could be addressed in stage 3 neurons because the neurites and stage 3 axon are of equivalent diameter, have the same density of microtubule tracks (Deitch and Banker, 1993), and are uniformly oriented plus-end-out (Heidemann et al., 1981; Stepanova et al., 2003). In stage 3 cells, selective entry was evident in the finding that on average 40% fewer dendritic vesicles entered the first 10 µm of the nascent axon than neighboring neurites. Intriguingly, the same 40% reduction was observed for dendritic vesicles entering stage 2 neurites that had accumulated CA-Kinesin-1. These data suggest that the mechanism that accounts for selective entry of dendritic vesicles is present at stage 2 of development, and is rapidly modified prior to axon specification.

The mechanism of selective entry

The dynamic changes in dendritic transport during stage 2 of development shows that the molecular cue driving selective transport at this stage is rapidly modifiable. The temporal link between the frequency of dendritic transport and the accumulation of CA-Kinesin-1 suggests they are reacting to the same or

related molecular cue(s) and the Kinesin-1 motor domain and endogenous dendritic motor have opposite preference for that cue. Because the motor domain provides a read-out of differences in microtubules, we think the cue is associated with the microtubule. Posttranslational modifications of tubulin, such as acetylation, can occur rapidly and have been shown to increase Kinesin-1 velocity (Reed et al., 2006). A weak correlation between increased acetylation levels along microtubules of stage 2 neurites with Kinesin-1 accumulation has been detected (C.F. Huang, personal communication). Thus, it is possible that these modifications are involved in selective entry during stage 2 of development, although they do not seem to be at maturity.

The mechanism regulating selective entry of vesicles to the axon must be localized to the cell body. Interestingly it was recently demonstrated that a special population of polyglutamylated microtubules extends from the *trans* Golgi to the plasma membrane for “fast-track” delivery of newly synthesized polarized proteins to the cell surface of MDCK cells, another polarized cell type (Spiliotis et al., 2008). If some of the microtubule tracks leading to the axon are optimized for transport of axonal vesicles, then this could result in a reduction in the number of eligible tracks for dendritic vesicles, and cause fewer dendritic vesicles we to enter the axon.

This model would predict that more axonal vesicles enter the axon compared to dendrites. In support of this model, Nakata and Hirokawa showed that newly synthesized axonal proteins are transported directly into the axon with a 3.8-fold bias over dendrites in 60% of cultured hippocampal neurons (Nakata and

Hirokawa, 2003). Similarly, Burack et al. observed twice as many anterograde-directed vesicles in the first 25 µm of the axon compared to dendrites of mature neurons, suggesting that vesicles containing axonal proteins are preferentially transported into the axon (Burack et al., 2000).

Selective transport and the development of polarity

Our findings, coupled with results from the former study that showed selective accumulation of the kinesin-1 motor domain in the stage 2 neurite destined to become the axon (Jacobson et al., 2006), strengthen the notion that selective transport of both axonal and dendritic proteins arises prior to axon specification, and might be a required element of the cell-intrinsic developmental program that results in specification of a single axon. Several putative Kinesin-1 cargos have been identified whose preferential accumulation in a stage 2 neurite could promote axon specification (Arimura and Kaibuchi, 2007). Perhaps the simultaneous exclusion of dendritic cargos from these neurites facilitates axon specification. For instance, it can be imagined that reduced entry of dendritic cargo-containing vesicles is required to increase the concentration of axon-promoting factors in a stage 2 neurite, or that molecules localized to dendritic transport vesicles could compete with axon specification, and thus need to be kept out of a stage 2 neurite for it to become the axon. Alternatively, the reduced transport of dendritic vesicles plays no functional role in axon specification and is merely a side effect of the molecular specializations that enhance transport axonal transport vesicles. In any event, the findings that transport of dendritic vesicles is selectively at stage 2 and stage 3 (Silverman et al., 2001) of

development disprove the bulk flow hypothesis proposed by Bradke and Dotti, which posits that axon specification is accompanied by the bulk transport of vesicles containing axonal and dendritic proteins into the stage 2 neurite destined to become the axon, and the axon of stage 3 neurons (Bradke and Dotti, 1997).

In conclusion, we have shown that selective transport of vesicles containing dendritic proteins consists of at least two components: 1) the transport filter in the proximal axon that aligns with the initial segment in mature neurons but arises prior to the initial segment during development and 2) the selective entry of dendritic vesicles which arises prior to axon specification, the mechanism of which must be localized to the cell body. While selective entry contributes the reduction of dendritic vesicles that reach the distal axon, the absolute block of anterograde transport by the transport filter likely plays the main role in preventing dendritic transport vesicles from advancing into the axon of mature neurons.

Methods

Cell Culture and transfection

Dissociated primary hippocampal cultures from day-18 rat embryos were electroporated (Amaxa, cat. no. VPG-1003) immediately prior to plating with cDNAs encoding the following proteins: TfR tagged C-terminally with GFP in pJPA expression vector (J. Adelman, Vollum Institute) (4µg), or chicken β-actin expression vector (Niwa et al., 1991); rab11b tagged N-terminally in chicken β-actin expression vector (1µg); Kinesin-1 (KIF5c isoform) truncated at amino acid

560 tagged C-terminally with tdTomato (Shaner et al., 2004); mRFP for soluble fill in chicken β-actin expression vector. 500K neurons were plated per 60 mm culture dish as described previously (Kaech and Banker, 2006). Briefly, neurons plated on poly-L-lysine coated coverslips and co-cultured over an astroglial feeder monolayer were maintained in serum-free N2 medium (Bottenstein and Sato, 1979).

Immunostaining and antibodies

Neurons were immunostained as follows: cells were fixed in 4% paraformaldehyde in PBS containing 4% sucrose, rinsed briefly in PBS, and then permeabilized in 0.25% TritonX-100 (Sigma T8787) for 5 minutes. Coverslips were then rinsed briefly in PBS, blocked using 1% fish gelatin (Sigma G7765) in PBS, and incubated in primary antibody for 1 hour, blocked again in 1% fish gelatin and then incubated in secondary antibodies for 30 minutes and rinsed briefly in PBS. Coverslips were rinsed in water briefly before mounting in Elvanol mounting medium. All steps were conducted at room temperature.

The following primary antibodies were diluted in 1% fish gelatin/PBS for use: mouse α AnkyrinG 1:50 (Santa Cruz Biotechnology, sc-12719); chicken α βIV-spectrin 1:300 (generously provided by Dr. M. Komada, Department of Biological Sciences, Tokyo Institute of Technology); mouse α pan-sodium channel 1:200 (Sigma S8809, clone K58/35); rabbit α MAP2 1:1000 (Chemicon International AB5622); mouse α acetylated alpha tubulin 1:10,000 (6-11B-1, Sigma T6793); mouse α polyglutamylated α/β (clone B3, IgM, Sigma T9822); mouse α Tau1 1:1000 (Chemicon International MAB 3420). All secondary antibodies were

obtained from Jackson ImmunoResearch Laboratories Inc. (West Grove, PA) and used at the following dilutions in 1% fish gelatin/PBS: biotin-SP-donkey α mouse 1:600 (used to amplify ankyrinG staining, cat. no. 715-065-150), FITC-donkey α chicken 1:500 (cat. no. 703-095-155); Cy3-donkey α mouse 1:600 (cat. no. 715-165-151); FITC-donkey α rabbit 1:200 (cat. no. 111-165-003) and Cy3-streptavidin 1:10,000 (cat. no. 016-160-084).

Neurons from three separate culture preparations were fixed at the following time points following plating: 2 days *in vitro* (2DIV), 4DIV, 6DIV, 8DIV, 10DIV, 12DIV, 14DIV, and 20DIV. Two cover slips from each time point were double stained for either ankyrinG and βIV-spectrin, or voltage-dependent sodium channels and βIV-spectrin. Images were collected on a Leica DRMXA widefield microscope with either a 60x/1.32 oil or 40x 1.25/oil objective lens. Images of at least twenty cells from different areas of the two cover slips were collected for each staining pair at each time point; cells to be imaged were selected randomly by phase contrast, and then the fluorescence image was collected to avoid bias. Data analysis was conducted separately for each culture to detect any variability in development between cultures. No significant variation was detected, so data from the three experiments was pooled.

The dimensions of the initial segment during development, including the overall length and distance from the cell body, were measured using images of cells stained for ankyrinG, because it had the brightest signal early in development. To begin, a 1 μm-thick and 50 μm-long line was traced down the center of each axon originating at the edge of the cell body and extending 50 μm away from the

cell body. A line this length and width was adequate to encompass the entire length of the initial segment and width of the axon at all stages of development. The edge of cell body was defined as a point centered between the tapering sides of the emerging axon (axon hillock) that is congruous with curvature of the cell body on either side of axon hillock. The linescan tool of Metamorph was used to generate a graph plotting the average intensity of the fluorescence at each pixel along the 50 µm line. The initial segment was defined as the continuous region of ankyrinG stain in the proximal axon that was at least 2.5 times above background, which was defined as the average intensity of staining in the axon 50-90 µm from the cell body, beyond the initial segment. Proximal to the cell body, ankyrinG staining increased abruptly, thus the cell body proximal edge of the initial segment was easy to define. Staining for ankyrinG at the distal end of the initial segment was granular and often diminished more gradually resulting in a peaky line scan as staining tapered off. The end of the initial segment was determined by viewing the line scan and image of each cell simultaneously, and a somewhat subjective determination was made; generally, the end of the initial segment was reached when intensity of staining between peaks began to reach background intensity, and to the eye, the end of the continuous region of intensified staining was reached. Discontinuous patches of staining for ankyrinG present beyond the distal end of the initial segment were not considered part of the initial segment's length. Initial segment dimension measurements were collected for at least 10 cells from each time point from each experiment.

The accumulation of ankyrinG, βIV-spectrin, and voltage dependent sodium channels at the initial segment during development (2DIV-20DIV) was quantified based on enrichment of staining for these proteins in the proximal axon. Background was defined for each individual image as the average pixel intensity in a line drawn along the axon 50-90 µm from the cell body, beyond the initial segment. This background value was subtracted from each image, and then the integrated intensity in the 50 µm-long region encompassing the proximal axon was measured using Metamorph. 10-20 cells from each time point, from each of the three experiments were pooled and averaged to obtain the average intensity of staining for each protein at each time point. Detection of enrichment of initial segment proteins in the proximal axon was obvious at later time points, but at 2-4DIV, was very dim, and judged by eye as being enriched.

Correlation coefficients of colocalization (how closely the intensity of fluorescence for one protein at a given pixel predicted the intensity of fluorescence for the other protein at that pixel) were obtained for ankyrinG and βIV-spectrin or βIV-spectrin and voltage dependent sodium channels in 12DIV double-stained cells. Line-scans values of staining intensity in the first 50 µm of double stained cells were entered into Excel, and the correl function of Excel was applied to generate the correlation coefficient for each cell. Results for 50 cells from 3 experiments were averaged for each staining pair.

Imaging of vesicle transport

Coverslips with attached neurons were loaded into sealed heating chamber (Warner Instruments, Hamden, CT) in phenol-red-free imaging medium (Hank's

balanced salt solution buffered to pH 7.4 with 10mM Hepes and supplemented with 0.6% glucose). Transport in mature neurons (7-9DIV) was recorded on a Leica DM-RXA widefield microscope using a Leica 63x Plan Apo, 1.32 N.A. objective lens. 600msec exposures were streamed continuously for 30 seconds or longer, and captured on a CCD camera (Princeton Instruments). Transport at stage 2 and stage 3 (1DIV) was recorded using a Nikon Spinning disc confocal microscope equipped with a 60x Plan Apo, 1.45 N.A. Nikon objective lens heated to 37 degrees. Images were recorded using a Hamamatsu Orca ER CCD camera.

Image Analysis

Metamorph was used to generate kymographs from time-lapse recordings. After manually drawing a line down the center of the axon moving away from the cell body (anterograde), the software scans each pixel perpendicular to the line, and records the location of the brightest pixel at each point along that line at each frame in the movie. Thus as a labeled vesicle moves further along the axon in the anterograde direction during the course of the recording, a positively sloping line is created on the kymograph. Conversely, a labeled vesicle moving in the direction of the cell body (retrograde) appears as a negatively sloping line. Stationary puncta are represented by straight lines across the kymograph. To measure velocity and excursion length, lines (called regions) were traced on the anterograde and retrograde events on the kymograph and the coordinates of these regions were transferred to an excel spreadsheet which calculated the number, velocity, excursion length of transport events. The number of

anterograde events per 5 µm increment moving away from the cell body in stage 2 and stage 3 cells was counted manually by overlaying a 5 µm-increment template on each cell's kymograph and counting the number of transport events that were present in each increment. Transport events that spanned multiple 5 µm increments were counted in each increment they crossed.

Chapter 3

Newly synthesized synaptic vesicle proteins, dense core granule proteins, and axonal plasma membrane proteins are transported along the axon in a common tubule

Jennifer D. Petersen, Stefanie Kaech, and Gary Banker
Jungers Center for Neuroscience Research, Department of Neurology, Oregon Health and Science University, Portland, Oregon

Summary

The efficient transport of proteins involved in neuronal signaling, such as protein components of synaptic vesicles and dense core granules, is essential to neuronal function and survival. Evidence suggests that synaptic vesicle proteins depart the Golgi in synaptic vesicle precursor organelles for transport into the axon, while dense core granule proteins depart the Golgi in immature secretory granules. KIF1A, a kinesin belonging to the Kinesin-3 family of motor proteins, has been implicated in the axonal transport of both synaptic vesicle and dense core granule proteins. However, two other kinesins, KIF1Bβ and Kinesin-1, may also be involved in the transport of synaptic vesicle precursors. To determine if KIF1A associates with components in the regulated secretory pathway, we expressed fluorescently-tagged versions of various synaptic vesicle and dense core granule proteins, together with KIF1A, to characterize the Golgi-derived transport vesicle populations they labeled. Next, two-color imaging was conducted to confirm the co-localization of proteins in the same transport vesicle, and with which transport vesicle populations KIF1A associated. Results show that synaptic vesicle proteins, dense core granule proteins and other types of axonal proteins, including plasma membrane proteins, depart the Golgi in the same tubulovesicular transport organelles. KIF1A does not associate with these organelles. After longer expression times, when axonal proteins had reached their destinations in the axon, KIF1A did associate with moving vesicles containing dense core granule proteins. These results suggest that axonal proteins are transported into the axon in a common transport tubule from which more specialized vesicle populations arise by sorting or retention. KIF1A may be involved in the transport of mature dense core granules and other organelles that arise from the Golgi-derived common transport tubule.

Introduction

Neurons utilize two types of membrane-bound organelles for regulated extracellular signaling—synaptic vesicles, which release neurotransmitter at presynaptic active zones during synaptic transmission, and dense core granules, which release peptides, hormones, and trophic factors that promote cell survival (De Camilli and Jahn, 1990). Because synaptic and trophic signaling is essential to neuronal function, the kinesins mediating the axonal transport of dense core granule proteins and synaptic vesicle proteins has been the subject of much investigation. However, the way in which these proteins are transported—specifically, the transport vesicle populations in which they travel and the kinesins that are responsible for their transport—remains unclear.

Synaptic vesicle membrane proteins and dense core granule components are synthesized in the cell body and depart the *trans* Golgi network (TGN) in membrane-bound vesicular organelles that are trafficked into the axon by kinesin-based transport (Nakata et al., 1998; Ahmari et al., 2000; Kaether et al., 2000; Rudolf et al., 2001). Neuroendocrine cell lines, such as PC12 cells, have been used to study the biosynthesis of synaptic-like-micro-vesicles (SLMVs) as a model for synaptic vesicle biosynthesis (Thomas-Reetz and De Camilli, 1994). These studies show that synaptic vesicle proteins depart the TGN via the constitutive pathway in precursor vesicles, not as mature synaptic vesicles (Tsukita and Ishikawa, 1980; Regnier-Vigouroux et al., 1991). The precursors fuse with endosomal compartments or the plasma membrane, and through multiple rounds of endo- and exocytosis, mature synaptic vesicles are formed

and filled with neurotransmitter locally at the synapse (Hannah et al., 1999; Bonanomi et al., 2006).

In contrast, dense core granule proteins are sorted into the regulated pathway, and depart the TGN in immature secretory granules (ISGs) which also contain some proteins of the constitutive pathway that inadvertently left the TGN in the ISG (Arvan et al., 1991). Maturation of ISGs involves the selective removal of non-dense core proteins from the ISG by sorting into the 'constitutive-like' pathway, while dense core granule components are retained in the ISG (Kuliawat and Arvan, 1992). Unlike synaptic vesicle proteins, which can undergo multiple rounds of activity-induced release and be recycled locally at the synapse (Valtorta et al., 1990), dense core granule proteins must be transported back to the TGN for reuse (Arvan and Castle, 1998; Kim et al., 2006)

Despite the differences in biogenesis and ultimate localization to distinct organelles, various studies suggest that the same kinesin, called KIF1A, transports both synaptic vesicle precursors and dense core granule proteins in axons. KIF1A is a member of the Kinesin-3 family; it has a C-terminal pleckstrin homology (PH) domain that participates in cargo binding (Okada et al., 1995; Klopfenstein and Vale, 2004). Indeed, numerous studies implicate KIF1A motor activity in the transport of synaptic vesicle precursors to synaptic sites (Hall and Hedgecock, 1991; Otsuka et al., 1991; Okada et al., 1995; Yonekawa et al., 1998; Klopfenstein and Vale, 2004; Pack-Chung et al., 2007).

However, it remains unclear whether KIF1A transports all synaptic vesicle proteins and if other kinesins also transport synaptic vesicle proteins. A biochemical fractionation and immunoisolation study indicated that two synaptic vesicle proteins, synaptophysin and synaptotagmin, but not a third, SV2, are transported together in a vesicle population that is moved by KIF1A (Okada et al., 1995). This study suggests that different sets of synaptic vesicle proteins are transported in subclasses of synaptic vesicle precursors, and that KIF1A is required for transport of synaptic vesicle precursors that contain synaptotagmin and synaptophysin, but not SV2. However, the study of KIF1A-knockout mice revealed that transport of SV2 to synapses was impaired as well as synaptophysin and synaptotagmin, suggesting that SV2 transport requires KIF1A (Yonekawa et al., 1998).

A closely related Kinesin-3 family member, KIF1Bβ, has also been linked to the transport of synaptic vesicle precursors (Zhao et al., 2001), as have members of a second family of kinesins, Kinesin-1 (Leopold et al., 1992; Sato-Yoshitake et al., 1992; Miller et al., 2005; Sakamoto et al., 2005). Additionally, Kinesin-1 family members (also known as conventional kinesin and KIF5) have been implicated in the transport of a third class of axonal transport vesicles, those containing axonal plasma membrane proteins (Ferreira et al., 1992; Kaether et al., 2000; Nakata and Hirokawa, 2003), which are believed to be distinct from synaptic vesicle precursors (Kaether et al., 2000).

There is also compelling evidence that KIF1A transports dense core granules in *C. elegans* and *Drosophila* (Zahn et al., 2004; Pack-Chung et al., 2007; Barkus et

al., 2008). In vivo imaging showed impaired transport of GFP-tagged dense core granules in animals carrying mutations in *unc-104*, the gene encoding the invertebrate ortholog of KIF1A (Zahn et al., 2004; Barkus et al., 2008). The role of KIF1A in dense core granule transport in mammalian neurons remains to be investigated.

These varying reports raise interesting questions about the regulation of trafficking of synaptic vesicle precursor proteins and dense core granule components into the axon—and axonal proteins in general. Are different sets of synaptic proteins sorted into separate vesicle populations for transport to the axon? Does the transport of each vesicle population require a different kinesin, or do multiple kinesins play redundant roles in their transport? For instance, do KIF1A, KIF1Bβ, and Kinesin-1 family members all transport synaptic vesicle protein precursors? And finally, are different kinesins required at different stages of transport (i.e. from cell body to axon versus local movements within the axon)? Biochemical fractionation or immunofluorescence colocalization studies in fixed cells provide indirect evidence with regards to which proteins reside in the same transport vesicle, and by which motor they are moved. However, visualization of transport by live-cell imaging allows discernment between co-localization on stationary structures versus colocalization on *moving* organelles, providing a more direct approach to answering these questions.

To determine which proteins are transported together in the same vesicle, and with which of these vesicle populations KIF1A associates, we used single-color, live-cell imaging to assess the appearance and transport characteristics of

moving vesicles labeled by expressed, fluorescently tagged KIF1A in cultured hippocampal neurons. We then expressed fluorescently tagged putative KIF1A cargo proteins, and recorded transport to see if they were associated with vesicles that had the same morphology as vesicles labeled by KIF1A and if they moved at the same velocity and excursion length as vesicles labeled by KIF1A. For comparison, we also characterized transport of NgCAM, the chicken homolog of human L1, an axonal plasma membrane protein of the Ig family of cell adhesion molecules (Hortsch, 1996). NgCAM is not associated with synapses and most likely is transported in vesicles that contain other axonal plasma membrane proteins and are moved by Kinesin-1 (Kaether et al., 2000; Nakata and Hirokawa, 2003). All live-cell imaging was carried out within 8 hours of transfection with Lipofectamine 2000, with the aim of imaging newly synthesized proteins associated with Golgi-derived transport carriers. Once we identified vesicle populations that appeared to have the same morphology (spherical v. tubulovesicular) and parameters of transport (velocity and excursion length), we co-expressed these proteins tagged with either GFP or a red fluorescent tag (mRFP or mCherry) and conducted two-color imaging to confirm the co-labeling of the same moving transport vesicles.

Using this approach, we demonstrate that early after expression, when labeled transport vesicles consist mainly of newly synthesized Golgi-derived carriers, all the proteins destined for the axon, including synaptic vesicle proteins, dense core granule proteins, and axonal plasma membrane proteins, are transported in a common tubular carrier. KIF1A was not associated with these tubular carriers.

This finding suggests that sorting into distinct transport vesicles occurs only after transport into the axon in a common transport carrier has occurred. In support of this model, KIF1A was found to be associated with moving carriers containing BDNF in the distal axon when imaged at later time points, when perhaps, mature dense core granules had arisen from the common transport tubule.

Results

Live-cell imaging distinguishes KIF1A-labeled vesicles from vesicles carrying axonal membrane proteins

To begin, we imaged KIF1A tagged N-terminally with GFP (GFP-KIF1A) and found that in the axon, GFP-KIF1A predominantly labeled spherical vesicles or small tubules (Figure 1A-B and Movie 1). Kymograph analysis was used to quantify velocity and excursion length of anterograde-directed KIF1A-labeled vesicles. The kymograph corresponding to the axon shown in Figure 1A is shown in Figure 1C. The kymograph shows that many KIF1A labeled vesicles moved continuously for the entire duration of the recording. A few KIF1A-labeled vesicles moved more slowly and stopped and started with greater frequency. There was also a small proportion of KIF1A labeled puncta that were stationary. On average KIF1A-labeled vesicles moved with an anterograde velocity of 1.6 ± 0.8 µm/sec. The average excursion length of KIF1A-labeled vesicles was 12 ± 10 µm.

As a control experiment to demonstrate that we could discriminate transport vesicle populations that were different from those labeled by GFP-KIF1A, we expressed NgCAM-GFP, an axonal plasma membrane protein that is transported

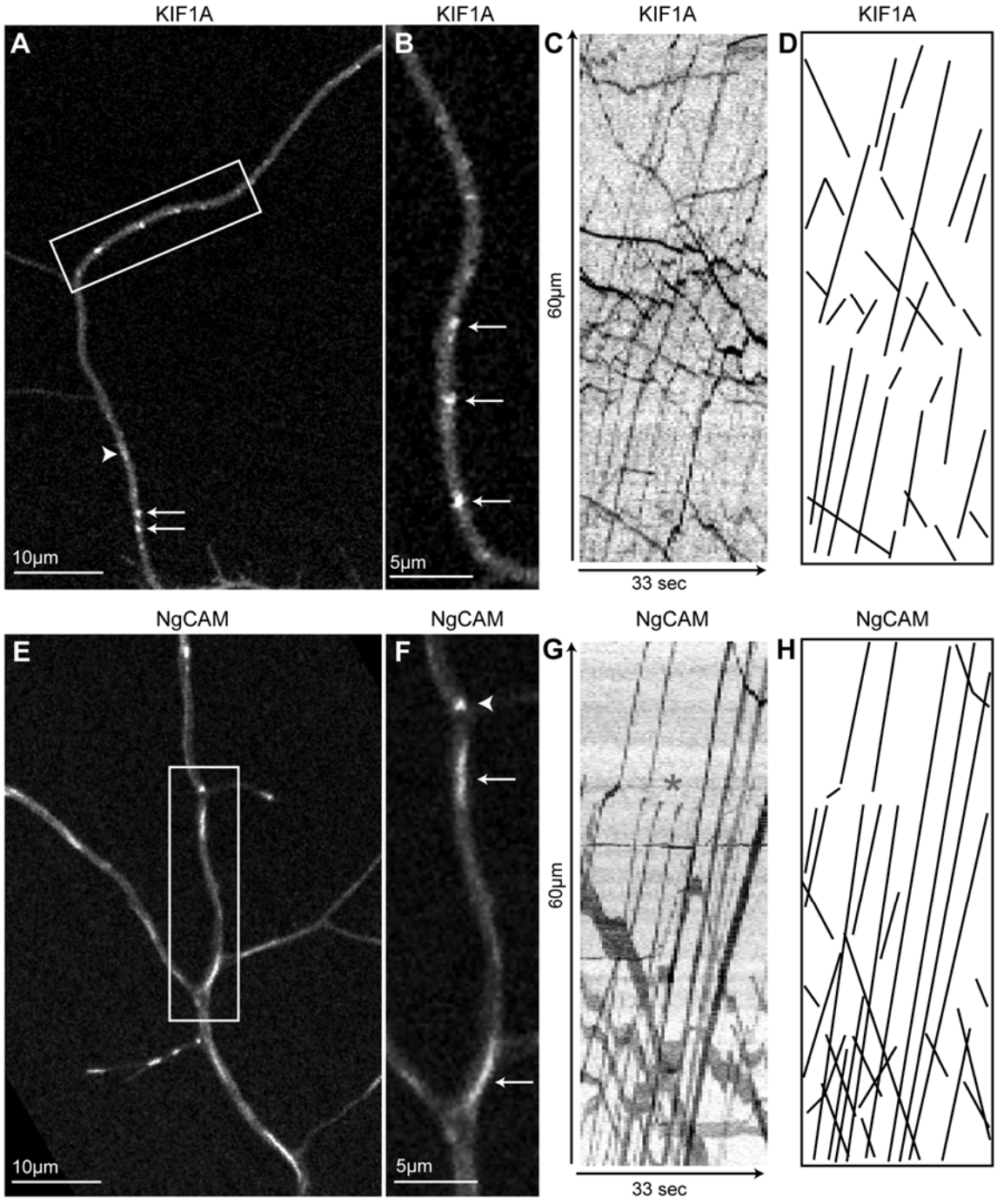

Figure 1. Transport vesicles labeled by KIF1A and NgCAM.

Figure 1. Transport vesicles labeled by KIF1A and NgCAM.

(A) Fluorescence image showing a section of axon from a neuron expressing GFP-KIF1A. Mobile GFP-KIF1A-labeled vesicles were predominantly spherical, indicated by arrows, or occasionally small tubules, indicated by arrowhead. All images are oriented with anterograde direction toward top of image. (B) Enlarged view of boxed area shown in A. Spherical KIF1A-labeled vesicles are indicated by arrows. Soluble GFP-KIF1A labeled motors not bound to vesicles create diffuse background fluorescence. (C) Kymograph corresponding to the live-cell recording of axon shown in A, oriented with time in the x-axis, and distance from the cell body in the y-axis. Contrast is inverted such that bright fluorescence in image appears dark in kymograph. KIF1A-labeled vesicles moving anterograde are represented by positively sloping lines, while lines with a negative slope correspond to retrograde transport events. Fluorescent puncta that remained stationary during recording appear as straight lines across kymograph. Several KIF1A-labeled vesicles move anterograde without stopping for the duration of recording. Others stop after moving shorter distances. (D) Illustration of the anterograde and retrograde events present in the kymograph shown in C. (E) Fluorescence image of a section of axon from a mature neuron expressing NgCAM-GFP. (F) Enlarged view of boxed area shown in E. Mobile NgCAM-GFP-labeled vesicles were predominantly tubulovesicular, indicated by arrows, or occasionally spherical, indicated by arrowhead. (G) Kymograph corresponding to live-cell recording of axon shown in E. Most NgCAM-labeled vesicles move the entire duration of the recording. The three anterograde moving vesicles marked by red asterisk disappear because they turned down a different branch of axon. (H) Illustration showing the anterograde and retrograde events present in the kymograph shown in G.

---

in vesicles likely to be moved by Kinesin-1, which has been shown to transport other axonal plasma membrane proteins (Kaether et al., 2000; Nakata and Hirokawa, 2003). NgCAM labeled some small spherical vesicles, but the majority of labeled structures were long tubulovesicular transport vesicles (called tubules henceforth), usually 2-4 μm in length, that were clearly morphologically

distinguishable from the KIF1A-labeled vesicles (Figure 1 E and F, Movie 2). NgCAM-labeled vesicles moved at an average rate of 2.5 ± 1.1 µm/sec, which is significantly faster than KIF1A-labeled vesicles. Additionally, the average excursion length of NgCAM-labeled vesicles was 19 ± 14 µm—markedly longer excursion lengths than KIF1A-labeled vesicles. These results suggest that KIF1A does not transport vesicles containing plasma membrane proteins, consistent with previous reports (Okada et al., 1995).

Transport of synaptic vesicle proteins was similar to that of NgCAM

We next expressed the synaptic vesicle proteins synaptotagmin and synaptophysin to see if the mobile organelles they labeled resembled KIF1A-labeled vesicles and if they moved at the same rate and excursion length as KIF1A. The shape and appearance of synaptotagmin-labeled structures was reminiscent of KIF1A-labeled vesicles; a mixture of vesicles that were spherical in appearance, with some tubular carriers (Figure 2 A-B, Movie 3). Unexpectedly, synaptotagmin-labeled vesicles moved at a velocity of 2.3 ± 1.0 µm/sec, which is a much faster rate than KIF1A-labeled vesicles. They also moved with longer excursion lengths, averaging 17 ± 12 µm (Figure 2 C-D). Expression of synaptophysin tagged with GFP (synaptophysin-GFP) yielded similar results as synaptotagmin. Synaptophysin-GFP labeled a combination of spherical and tubular vesicles that moved at an average velocity of 2.6 ± 1.3 µm/sec, with an average excursion length of 15 ± 11 µm (Figure 2 E-H and Movie 4). Interestingly, the synaptic vesicle proteins labeled structures that moved at rates and excursion lengths that matched those of vesicles labeled by NgCAM.

To confirm that the GFP-tag on the synaptic proteins did not interfere with trafficking to presynaptic sites, we expressed these proteins for 48 hours and then immunostained endogenous synapsin 1a, a marker of presynaptic sites. The GFP-tagged synaptic proteins were appropriately localized at synaptic sites (data not shown).

Transport of dense core granule proteins was similar to that of NgCAM

KIF1A motor activity has also been linked to the axonal transport of dense core granule proteins (Zahn et al., 2004; Pack-Chung et al., 2007; Barkus et al., 2008). To visualize transport of dense core granule proteins we expressed BDNF tagged with mRFP (BDNF-mRFP). Lochner et al. have shown that BDNF-mRFP colocalized with endogenous markers of dense core granules at longer times of expression, showing that the fluorescently tagged BDNF was correctly targeted to dense core granules (J. Lochner, personal communication). BDNF-mRFP labeled a mixed population of both spherical and tubulovesicular carriers that looked similar to the vesicles labeled by KIF1A (Figure 2 I-J and Movie 5). However, BDNF-labeled vesicles moved at an anterograde rate and excursion length that was almost exactly the same as NgCAM, but significantly different from KIF1A-labeled vesicles. The average velocity of BDNF-labeled vesicles was 2.5 ± 1.1 µm/sec, and the average excursion length was 16 ± 12 µm.

Figure 3 compares the anterograde rate and excursion length profiles for vesicles labeled by KIF1A with those labeled by NgCAM, synaptotagmin, synaptophysin, and BDNF. Average velocities and excursion lengths for each population of

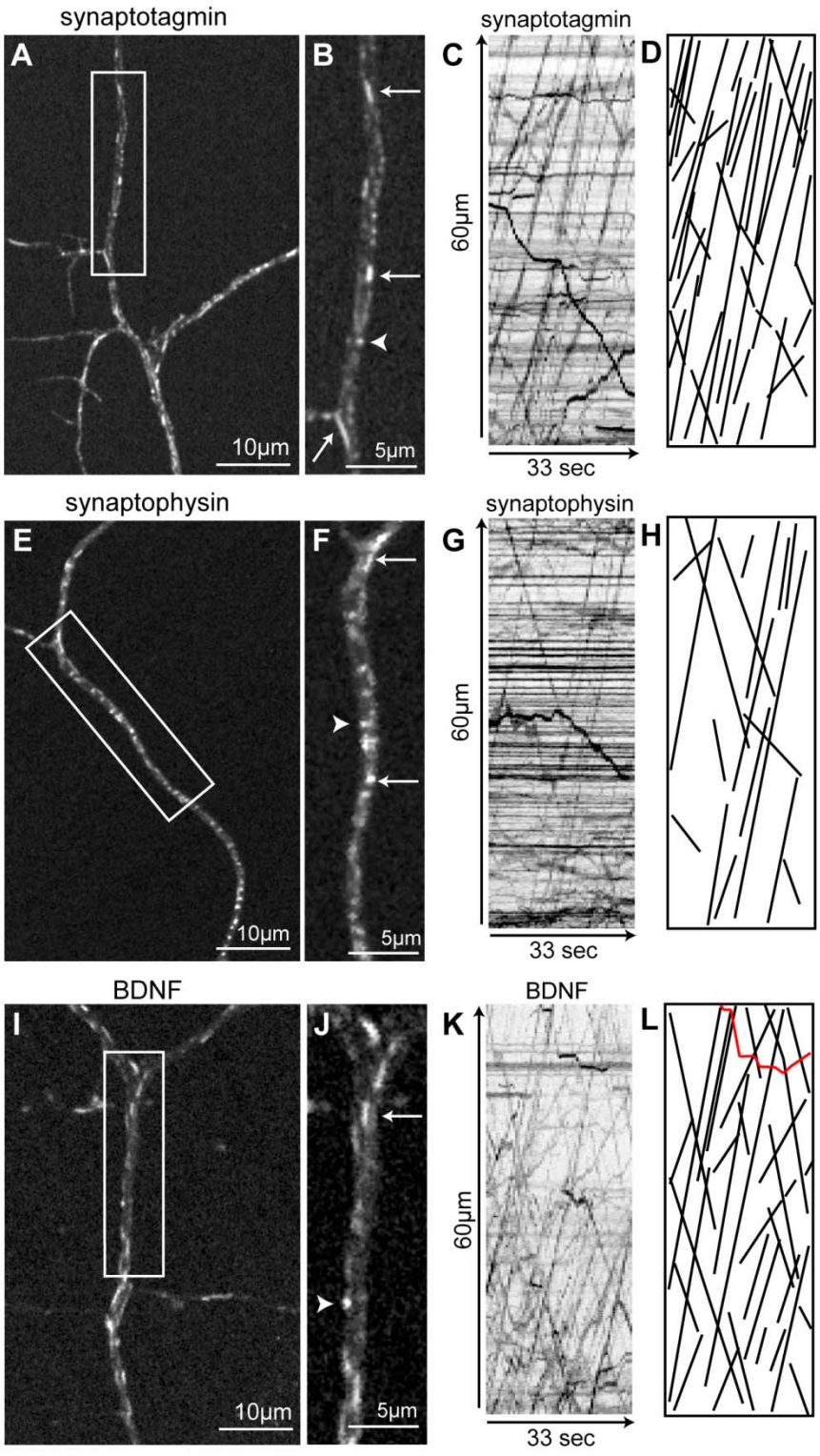

Figure 2. Transport vesicles labeled by synaptic vesicle and dense core granule proteins.

Figure 2. Transport vesicles labeled by synaptic vesicle and dense core granule proteins.

(A) Fluorescence image showing a section of axon from a neuron expressing synaptotagmin-GFP. All images are oriented with anterograde direction toward top of image. Synaptotagmin labeled a mixture of spherical and tubular vesicles. Numerous small stationary puncta were also labeled. (B) Enlarged view of boxed area in A shows morphology of mobile synaptotagmin labeled vesicles and tubules, indicated by arrows. Immobile puncta indicated by arrowhead. (C) Kymograph corresponding to live-cell recording of axon shown in A. Many synaptotagmin-labeled vesicles move anterograde the entire duration of the movie. The numerous small stationary labeled puncta are evident by the many horizontal lines on the kymograph. (D) Illustration showing the anterograde and retrograde events present in kymograph shown in C. (E) Fluorescence image showing a section of axon from a neuron expressing synaptophysin-GFP. Synaptophysin labeled a combination of spherical and tubular vesicles. Numerous small stationary puncta were also labeled. (F) Enlarged view of boxed area in E shows morphology of mobile synaptophysin labeled vesicles and tubules, indicated by arrows. Immobile synaptophysin puncta indicated by arrowhead. (G) Kymograph corresponding live-cell recording of axon shown in E. Many synaptophysin labeled vesicles move anterograde throughout the recording. Numerous stationary synaptophysin-labeled puncta are evident in the many horizontal lines on the kymograph. (H) Illustration showing the anterograde and retrograde events in kymograph shown in H. (I) Fluorescence image showing a section of axon from neuron expressing BDNF-mRFP, which labeled a combination spherical and tubular moving vesicles. (J) Enlarged view of boxed area in I shows morphology of mobile BDNF-labeled vesicles. Tubular vesicle indicated by arrow; brightly labeled spherical vesicle indicated by arrowhead. (K) Kymograph corresponding live-cell recording of axon shown in I. Brightly labeled spherical vesicles tended to pause frequently during movement, and often change direction. (L) Illustration of anterograde and retrograde events in the kymograph shown in K. The path taken by a brightly labeled spherical BDNF-labeled vesicle that stopped and started frequently is highlighted in red.

labeled transport vesicles are summarized in Table 1. Vesicles labeled by KIF1A moved with a significantly slower velocity and excursion length than vesicles labeled by NgCAM, synaptotagmin, synaptophysin and BDNF.

Synaptic vesicle proteins transport with NgCAM in tubules

Because NgCAM, synaptic vesicle proteins, and BDNF all labeled vesicles that moved with similar velocities and excursion lengths, we tested their colocalization in the same moving carrier by two-color imaging. We co-expressed NgCAM tagged with mCherry (NgCAM-mCherry) and synaptotagmin-GFP and recorded transport sequentially in both colors. Corresponding frames of the two-color movies are shown in Figure 4 A-C**.** Based on the still images, NgCAM- and synaptotagmin-labeled structures appear to have dissimilar morphologies; NgCAM labeled long tubules; synaptotagmin labeled spherical vesicles and smaller tubules. However, the kymographs corresponding to these two-color recordings show that the majority of anterograde and retrograde moving vesicles are common to both kymographs, indicating that NgCAM and synaptotagmin label the same moving organelles (Figure 4 D). The kymograph for

Table 1. Velocity and Excursion Length of Axonal Transport Vesicles

Labeled vesicle population	#vesicles/#cells	velocity[a]	excursion length[b]
KIF1A	244/6	1.58 ± 0.77	11.92 ± 9.56
NgCAM	450/8	2.54 ±1.05*	19.21 ±14.21*
synaptotagmin	489/7	2.34 ±1.02*	16.66 ± 11.94*
synaptophysin	167/3	2.58 ± 1.29*	14.59 ± 11.18**
BDNF	349/7	2.47 ± 1.05*	16.24 ± 11.45*

[a]µm/sec ± SD
[b]µm ± SD
*different from KIF1A p<0.001 Student's t-Test
**different from KIF1A p<0.01 Student's t-Test

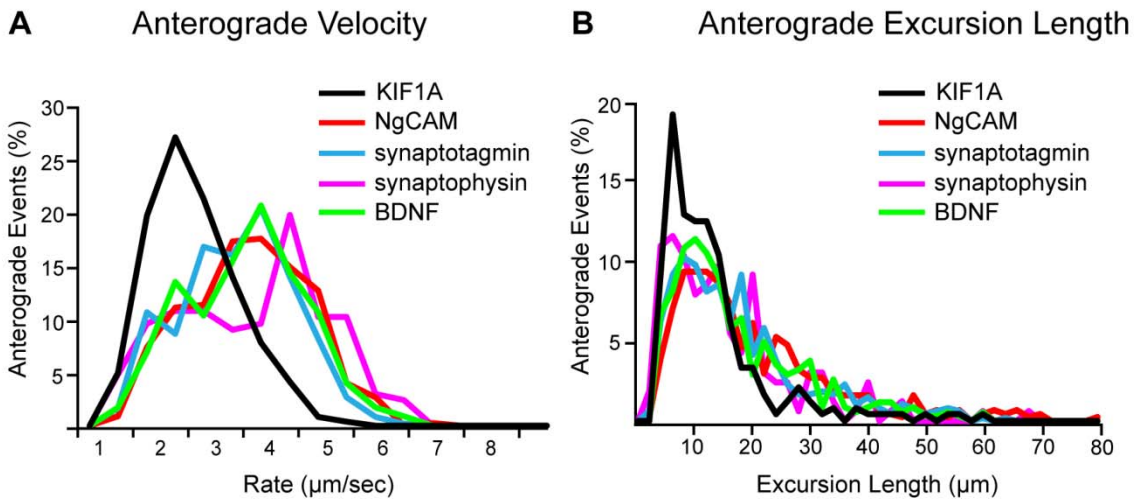

Figure 3. Distribution of velocities and anterograde excursion lengths of labeled vesicle populations. Distribution of anterograde velocities (A) and anterograde excursion lengths (B) for each labeled vesicle population.

---

synaptotagmin-GFP shows numerous stationary puncta that are not present in the NgCAM-mCherry kymograph.

When the movies were overlaid and viewed in two colors (NgCAM:red, synaptotagmin:green), it became evident that despite their different morphologies, both labels were associated with the same tubule and moved together (Figure 4C, and Movie 6). Remarkably, the two-color movies showed that the synaptotagmin-GFP was often localized to a puncta at the trailing end of moving NgCAM-labeled tubules. The synaptotagmin dot at the trailing end of an NgCAM-labeled tubule was not an artifact of sequential imaging. Tubules that paused for several frames maintained an overall tubular shape with a stationary dot of synaptotagmin at the trailing end (Figure 4F and Movie 6).

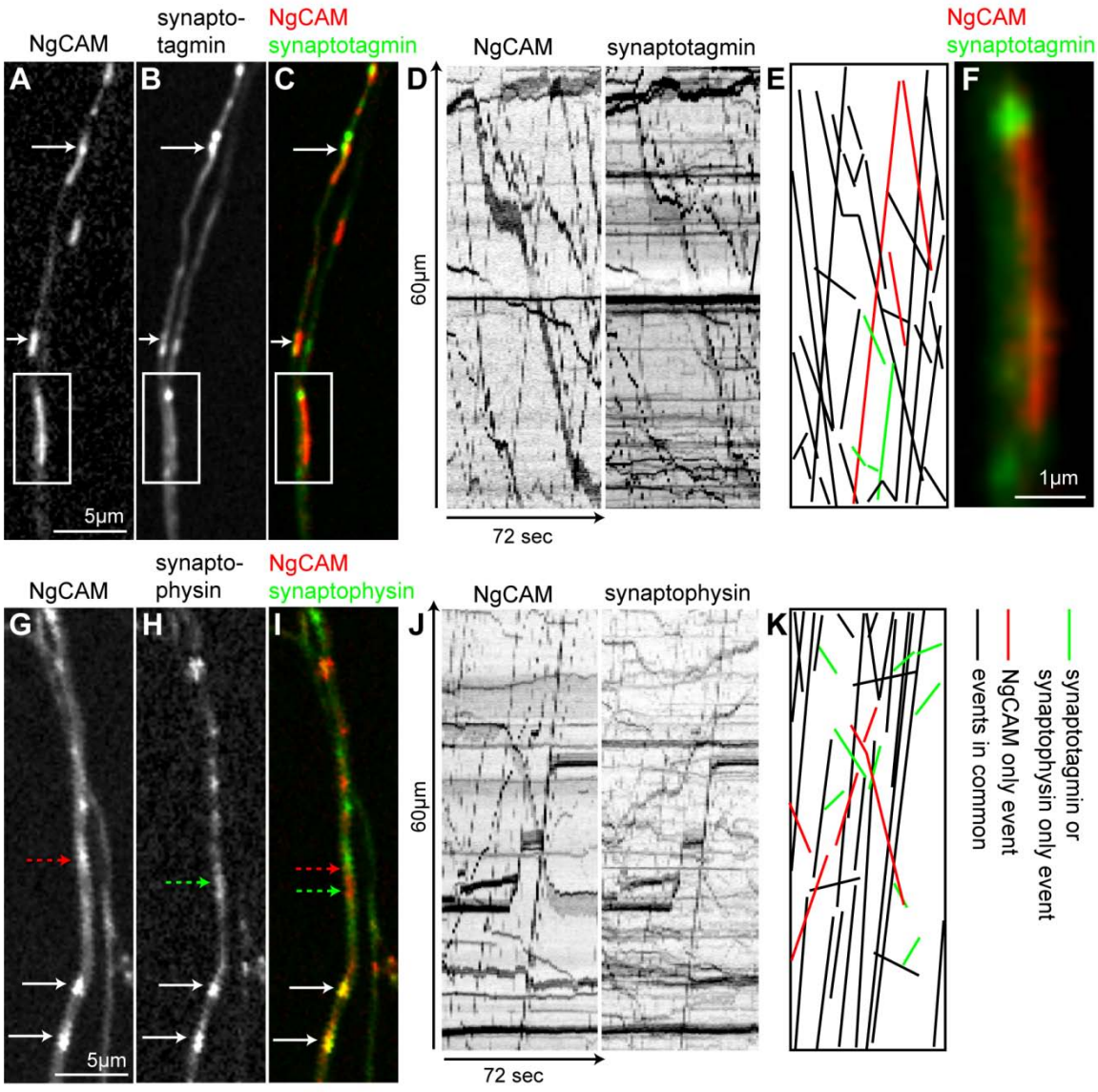

Figure 4. Synaptic vesicle proteins co-localized with NgCAM in transport tubules.

Fluorescence image of a section of axon from a cell co-expressing NgCAM-mCherry (A) and synaptotagmin-GFP (B), shown in color overlay in (C). All images are oriented with anterograde direction oriented toward top of image. Arrows indicate labeled vesicles that are labeled for both NgCAM and synaptotagmin. (D) Kymographs corresponding to live-cell, two-color recording of axon shown in A-C. Many of the anterograde and retrograde transport events are common to both kymographs. Kymograph corresponding to recording of synaptotagmin shows numerous stationary puncta that are not co-labeled by NgCAM. (E) Illustration showing the transport events that are common to both

kymographs (black lines), events present in the NgCAM kymograph only (red lines), and events present in the synaptotagmin kymograph only (green lines). (F) Enlarged view of boxed area in C, showing a paused transport tubule labeled for NgCAM (red) with an associated synaptotagmin (green) label in dot at the trailing end. (G) Fluorescence image of a section of axon from a cell co-expressing NgCAM-mCherry and (H) synaptophysin-GFP, shown in overlay in (I). White arrows indicate paused vesicles labeled for both NgCAM and synaptophysin. Green and red dashed arrows point to a fast moving vesicle that appears half red and half green in color-overlay which is an artifact of sequential imaging (red frame captured before green). (J) The kymographs corresponding to live-cell, two-color recording of the axon shown in G-I showing many anterograde and retrograde events common to both kymographs. (K) Illustration showing the transport events that are common to both kymographs (black lines), events present in the NgCAM kymograph only (red lines), and events present in the synaptophysin kymograph only (green lines).

Similar results were obtained when NgCAM-mCherry and synaptophysin-GFP were co-expressed (Figure 4 and Movie 7). The majority of moving structures were labeled for both NgCAM and synaptophysin. Unlike synaptotagmin, compartmentalization of synaptophysin label within the NgCAM tubule was not observed. These data suggest that plasma membrane proteins, such as NgCAM, and synaptic vesicle proteins are transported together in a common post-Golgi transport tubule.

To test the possibility that expressed NgCAM, which contains multiple protein interaction domains (Hortsch, 1996), interacted with and caused missorting of synaptic vesicle proteins, we labeled the tubular carriers with a construct consisting of the signal sequence of neuropeptide Y followed by mCherry (ssNPY-mCherry). Once synthesized, the short signal sequence is cleaved,

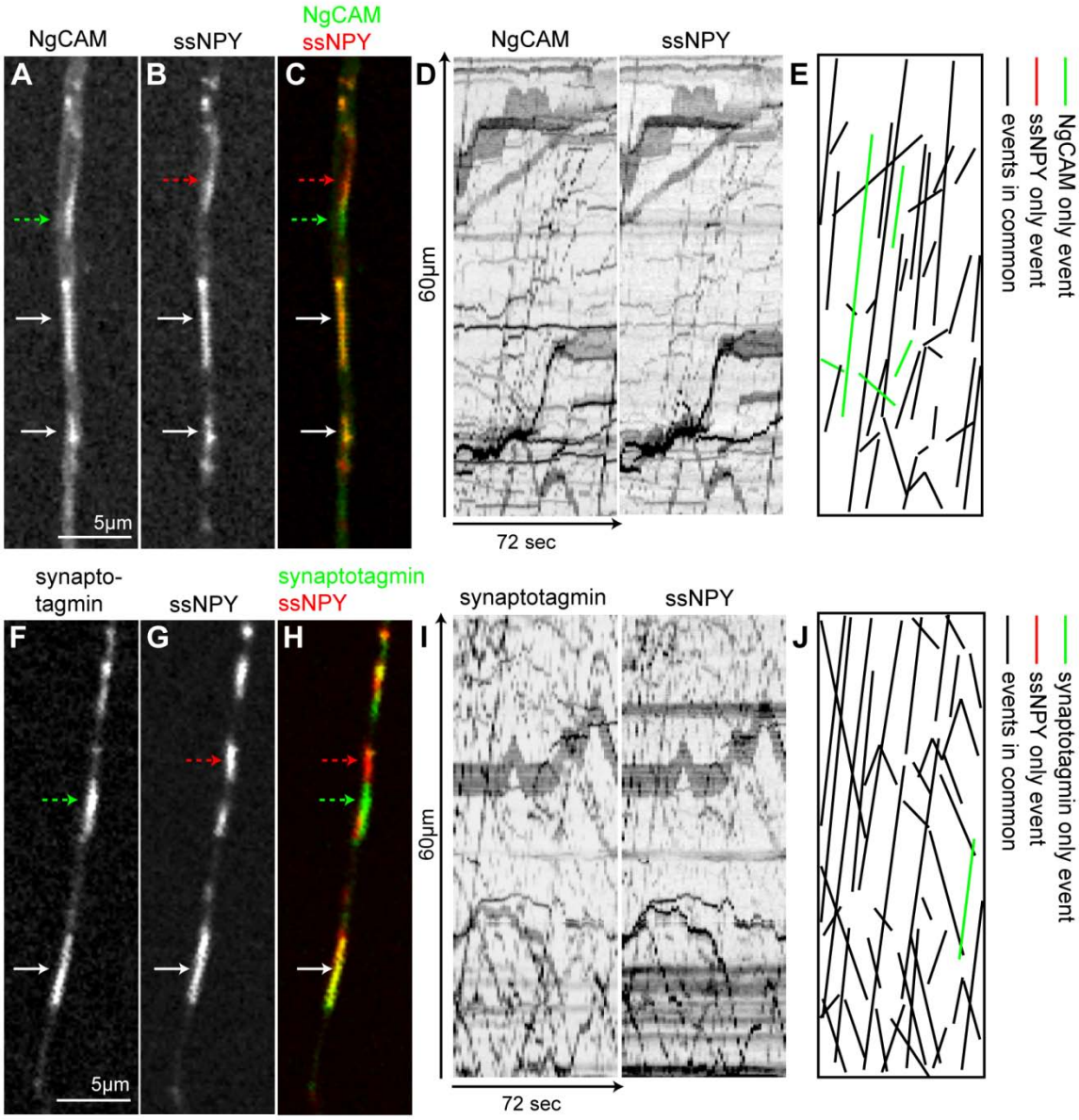

Figure 5. Synaptotagmin co-localized with soluble marker of NgCAM transport tubules.

Fluorescence image of a section of axon from a cell co-expressing NgCAM-GFP (A) and ssNPY-mCherry (B), shown in overlay in (C). All images are oriented with anterograde direction toward top of image. White arrows indicate vesicles labeled by both proteins. Red and green dashed arrows point to fast moving vesicle that appears red at the leading end, and green at the trailing end, an artifact of sequential imaging (red image captured before green). (D) Kymographs corresponding to the two-color recording of the

section of axon in A-C showing that nearly all transport events are common to both kymographs. (E) Illustration showing transport events common to both kymographs (black lines) and those labeled for NgCAM only (green lines). No transport events were detected that labeled for ssNPY only. (F) Fluorescence image of a section of axon from a cell co-expressing synaptotagmin-GFP and ssNPY-mCherry (G), shown in overlay in (H). White arrows indicate vesicle labeled for both synaptotagmin and ssNPY. Green and red dashed arrows indicate a fast moving vesicle that appears half red and half green due to sequential imaging. (I) Kymographs corresponding to two-color recording of axon shown in F-H show almost all transport events in common to both kymographs. (J) Illustration showing transport events common to both kymographs (black lines) and those labeled for synaptotagmin only (green lines). No transport events were detected that labeled for ssNPY only.

---

leaving mCherry as an inert soluble marker of Golgi-derived vesicles. We first confirmed that ssNPY-mCherry co-labeled vesicles that contained NgCAM-GFP (Figure 5 A-E and Movie 8). We then co-expressed ssNPY-mCherry and recorded their transport. As when expressed with NgCAM, synaptotagmin co-labeled the same vesicles as ssNPY (Figure 5 F-J and Movie 9). These results suggest that the co-localization of synaptic vesicle proteins in the transport tubule that also contains the plasma membrane protein NgCAM is not caused by missorting.

A previous study found that a plasma-membrane protein, amyloid precursor protein, tagged with YFP (APP-YFP), labeled tubulovesicular carriers in the axon that were not labeled with co-expressed synaptophysin-CFP after 24 hours of expression (Kaether et al., 2000). We tested whether or not APP-YFP labeled the tubular vesicles labeled by ssNPY-mCherry (which also labeled for synaptophysin) early after transfection. We found that 5 hours after transfection,

APP-YFP colocalized with ssNPY-mCherry on moving vesicles (Figure 6 A-E and Movie 10). This result implies that APP and synaptophysin are present in the same tubule early after transfection. Why our results differ from those obtained by Kaether et al. is addressed in the discussion.

Dense core granule proteins transport with NgCAM in tubules

Next, we set out to determine if BDNF-mRFP1 and NgCAM were in the same or different transport vesicle populations. We co-expressed BDNF-mRFP1 and NgCAM-GFP and recorded transport. Corresponding still images from a two-color recording are shown in Figure 7A-B. Overlap of BDNF and NgCAM label can be seen on the tubular structures, but some brightly labeled spherical structures were labeled with BDNF only (dashed arrow in Fig. 7B). The corresponding kymographs show that the double-labeled tubular structures were fast-moving vesicles (Figure 7D and Movie 11). The spherical structures that labeled only with BDNF sometimes moved short distances (5-10µm), but then stopped. These data suggest that BDNF is transported in the same tubule as NgCAM and the synaptic vesicle proteins.

We next wondered if the over-expression of BDNF caused missorting. Perhaps over-expression of BDNF, a soluble protein, saturated the BDNF-sorting machinery causing passive uptake into the NgCAM/ssNPY-labeled tubule population. To test this possibility, we chose phogrin, a membrane protein specific to dense core granules, as an alternative to BDNF (Wasmeier and Hutton, 1996). After confirming that phogrin-GFP and BNDF labeled the same transport vesicles (not depicted) we co-expressed ssNPY-mCherry with phogrin-

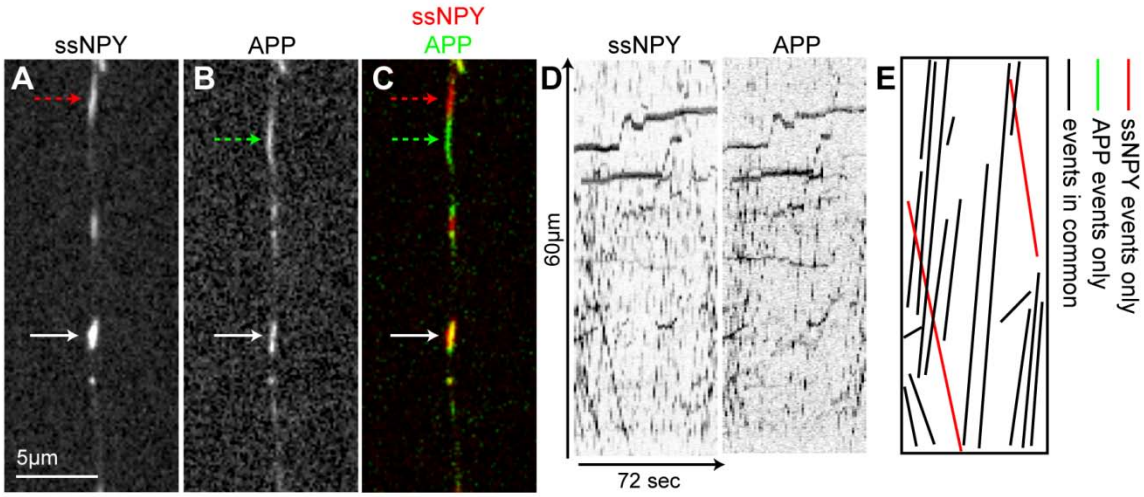

Figure 6. APP colocalized in common transport tubule.

Fluorescence image of section of axon from a neuron co-expressing ssNPY-mCherry (A) and APP-YFP (B), shown in overlay in (C). All images are oriented with anterograde direction toward top of image. White arrow indicates vesicle labeled for both ssNPY and APP. Green and red dashed arrows indicate a fast moving vesicle that appears half red and half green due to sequential imaging. (D) Kymographs corresponding to two-color recording of axon shown in A-C showing that most transport events are common to both kymographs. (E) Illustration of kymograph showing transport events common to both kymographs (black lines), labeled for APP only (green lines), or labeled for ssNPY only (red lines).

GFP. Still images corresponding to the same frame of the two-color movie are shown in Figure 7 F-G. Structures labeled with phogrin-GFP appeared more punctate than the tubules labeled with ssNPY. However, the kymographs corresponding to this recording showed extensive overlap of anterograde and retrograde transport (Figure 7I and Supplemental Movie 12). The color-overlay showed that ssNPY-labeled tubules had multiple phogrin labeled subdomains that appeared as dots (Figure 7H and J). Thus, like synaptotagmin (Fig. 4 C and

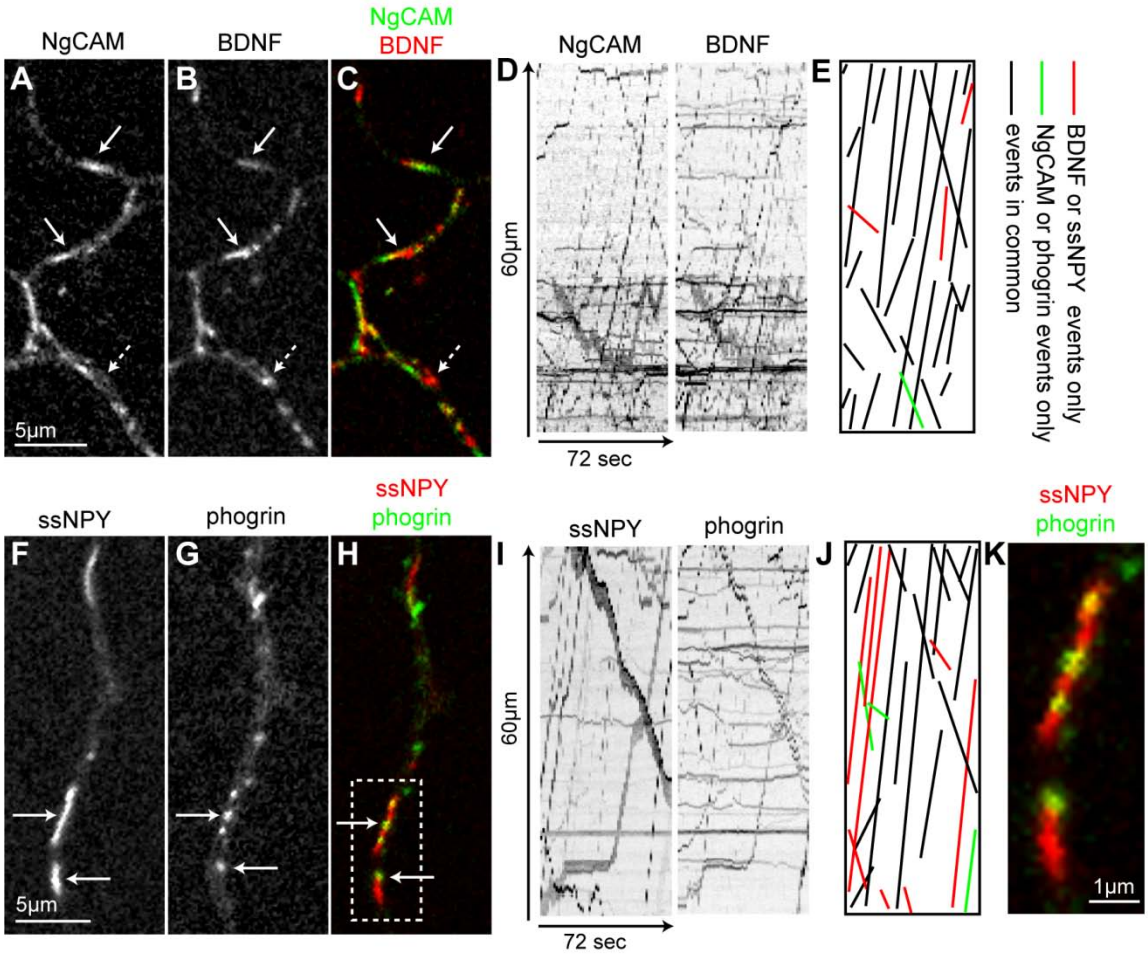

Figure 7. Dense core granule markers co-localize with NgCAM in transport tubules.

Fluorescence images of section of axon from a neuron co-expressing NgCAM-GFP (A) and BDNF-mRFP1 (B), shown in overlay in (C). All images are oriented with anterograde direction toward top of image. White arrows indicate vesicles labeled for both NgCAM and BDNF. Dashed arrow indicates bright spherical vesicle labeled for BDNF only. (D) Kymographs corresponding to two-color recording of axon shown in A-C. Most of the transport events are present on both kymographs. (E) Illustration showing transport events common to both kymographs (black lines), events that occur in the NgCAM kymograph only (green lines), and events that occur in the BDNF kymograph only (red lines). (F) Fluorescence image of section of axon from cell co-expressing ssNPY-mCherry and phogrin-GFP (G), shown in overlay in (H). Arrows indicate vesicles labeled for both proteins, however phogrin label is present in dots within the tubules labeled for

ssNPY. (I) Kymographs corresponding to two-color recording of axon shown in F-H show many transport events common to both kymographs. Lines on the kymograph corresponding to the two vesicles boxed in H, show three thin lines retrograde lines in the phogrin kymograph correspond to the brightly labeled thick black retrograde line in the ssNPY kymograph. Likewise, the shorter anterograde moving vesicle contains two phogrin dots (see Supplemental Movie 12) and appears as two parallel lines on the phogrin kymograph and a thicker solid line on the ssNPY kymograph. (J) Illustration of kymographs showing transport events common to both kymographs (black lines), labeled for phogrin only (green lines), or labeled for ssNPY only (red lines). (K) Enlarged view of boxed area in H shows ssNPY-labeled tubule (red) with associated phogrin-labeled subdomains (green).

F), phogrin is associated with subdomains of tubules moving in both anterograde and retrograde directions. These data provide further evidence that dense core granule proteins are transported in the tubule that contains plasma membrane proteins and synaptic vesicle proteins.

Steady state association of KIF1A with vesicles containing dense core granule proteins

The finding that synaptic vesicle proteins, dense core granule proteins, and axonal plasma membrane proteins were transported in a common transport tubule that moved at a considerable faster velocity and longer excursion length than the vesicles moved by KIF1A was surprising for two reasons. First, KIF1A is thought to transport both synaptic vesicle proteins and dense core granule proteins (Okada et al., 1995; Yonekawa et al., 1998; Zahn et al., 2004; Pack-Chung et al., 2007; Barkus et al., 2008). Second, synaptic vesicle proteins and dense core granule proteins are thought to leave the Golgi by distinct pathways (the constitutive and regulated, respectively) thus they should not be in the same

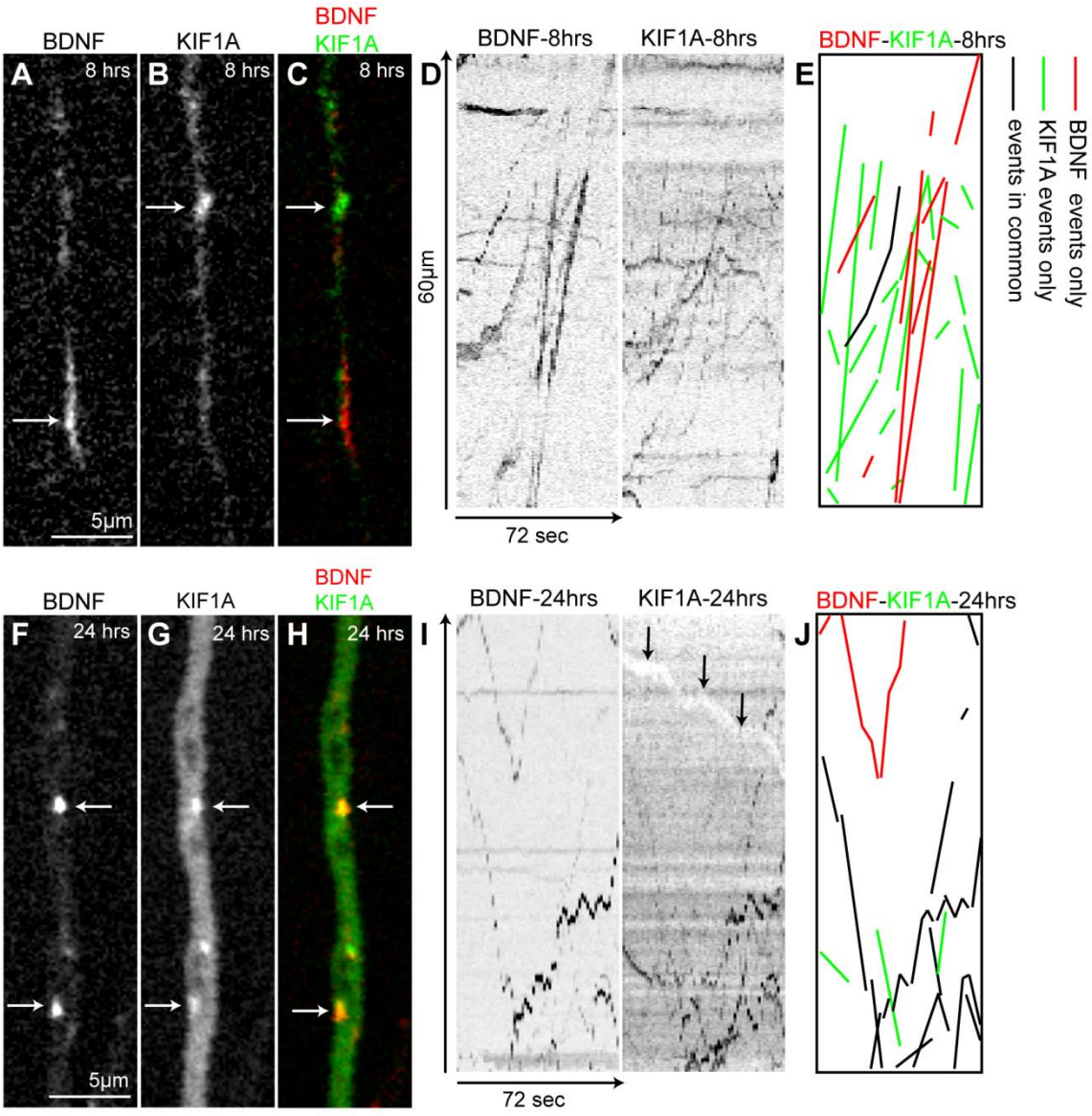

Figure 8. KIF1A and BDNF colocalize on moving vesicles at steady state.

Fluorescence images of axon from a neuron co-expressing (A) BDNF-mRFP1 and (B) KIF1A-GFP for 8 hours, shown in overlay in (C). All images are oriented with anterograde direction toward top of image. Arrows point to a tubule labeled singly for BDNF in A, and a spherical vesicle labeled singly for KIF1A in B, that do not co-localize in C. (D) Kymographs corresponding to the two-color recording of the axon shown in A-C shows few transport events in common between the kymographs. (E) Illustration of kymographs showing transport events common to both kymographs (black lines), labeled for KIF1A only (green lines), or labeled for BDNF only (red lines). (F)

Fluorescence images of axon from a cell co-expressing BDNF-mRFP1 and GFP-KIF1A (G) for 24 hours, shown in overlay in (H). Arrows indicate spherical vesicles labeled by both proteins. (I) Kymographs corresponding to the two-color recording of the axon from F-H shows several transport events in common between kymographs. Black arrows on the KIF1A kymograph indicate a non-labeled vesicle moving through and displacing the soluble GFP fluorescence created by non-vesicle bound GFP-KIF1A. (J) Illustration of kymographs showing transport events common to both kymographs (black lines), labeled for KIF1A only (green lines), or labeled for BDNF only (red lines).

---

transport organelle (De Camilli and Jahn, 1990; Tooze and Huttner, 1990; Regnier-Vigouroux et al., 1991).

One possible explanation is that these proteins leave the Golgi in a common tubule, but subsequently are sorted to different organelles. To examine this possibility we transfected hippocampal neurons with GFP-KIF1A and BDNF-mRFP1 and compared labeling after 8 hours of transfection, to image predominantly newly synthesized Golgi-derived transport vesicles, and at 24 hours after transfection, when proteins had reached a steady state distribution. At 8 hours, there was virtually no co-labeling of vesicles with BDNF and KIF1A (Figure 8 A-E and Movie 13). However, after 24 hours of expression, there was considerably more co-localization. KIF1A co-localized with the bright spherical BDNF-labeled structures that moved short distances **(**Figure 8 F-J and Movie 14). These resembled the spherical vesicles brightly labeled with BDNF but not co-labeled with NgCAM (Figure 7 A-C). These results suggest that KIF1A associates with and may be required for the transport of mature dense core granules that arise from the common transport tubule.

Discussion

Using single and two-color live-cell imaging of fluorescently tagged proteins, we have shown that newly synthesized axonal proteins—be they synaptic vesicle proteins, plasma membrane proteins, or dense core granule proteins—exit the Golgi in a common tubule and are transported together into axons. KIF1A-labeled vesicles moved at a slower average velocity and had a shorter excursion length than fast moving tubules. When the transport of a dense core granule protein, BDNF, was recorded at a later time-point, two-color imaging showed that KIF1A and BDNF co-labeled spherical organelles in the axon. Thus the common tubule does not appear to be transported by KIF1A, but some of the vesicle populations derived from it may be.

Although unexpected, the idea that proteins destined for different sub-compartments within the axon are transported in a common tubule from the Golgi to the axon is not entirely new. Nakata et al. proposed this idea in their 1998 study that was the first to use GFP-tagged protein chimeras to visualize axonal transport in living neurons (Nakata et al., 1998). They found that GFP-tagged versions of three types of axonal proteins—lipid associated plasma membrane proteins (GAP-43 and SNAP-25), an integral plasma membrane protein (TrkA), and a synaptic vesicle protein (synaptophysin)—all labeled a population of elongated tubular carriers that underwent fast long-range movement in the axon. While tubular carriers were most abundant, they also observed brightly labeled globular structures that were stationary or moved short distances and then stopped. TGN38, a resident protein of the trans Golgi network escapes the Golgi

in Golgi-derived carriers. TGN38 also labeled fast, far moving elongated tubules, but not the less mobile globular carriers, suggesting that the tubular carriers were Golgi-derived vesicles containing newly synthesized membrane proteins. Supporting this interpretation, they found that the tubules were never labeled by extracellularly applied Texas red-dextran and FM1-43, while the smaller brightly labeled globular vesicles were, distinguishing them as endocytic vesicles. Since the tubular vesicles labeled by all the axonal proteins had the same dimensions and moved at the same velocity, Nakata et al. posited that these diverse types of axonal proteins were labeling the same vesicle population, and depart the Golgi in a bulk transport container for transport into the axon (Nakata et al., 1998). The results presented here confirm this hypothesis using two-color imaging.

In contrast to this view, Kaether et al. 2000 concluded that APP and synaptophysin are transported in the axon in separate vesicles. Kaether and colleagues found that APP-YFP labeled fast-moving tubular carriers, while synaptophysin-GFP labeled vesicles were less tubular, moved at a slower rate and moved with shorter excursion lengths than APP. These results suggested that APP and synaptophysin did not label the same transport carriers. They then performed two-color imaging of APP-YFP and synaptophysin-CFP, and observed that most of the structures labeled for APP and synaptophysin were not co-labeled (Kaether et al., 2000).

The apparent discrepancy between our and Kaether et al.'s data could be explained by the time-window during which transport was imaged. Because we imaged early after transfection, most of the labeled vesicles we observed were

likely to be Golgi-derived and to contain newly synthesized APP and synaptophysin that had yet to reach the plasma membrane. The vesicles labeled in the Kaether study (after 24 hours of expression) were likely a mixed population of Golgi-derived vesicles and endosomes. Indeed, they showed that many of the synaptophysin-labeled structures co-labeled with extracellularly applied Rhodamine-dextran, suggesting these structures were endosomes. Thus it may be that axonal proteins of all types are transported initially in a common bulk carrier and become sorted into distinct organelle populations once they have reached distal axon locations.

Evidence that transport tubules are not artifacts of over-expression

We wondered if the elongated tubules labeled by over-expressing axonal proteins were physiologically relevant or artifactual. Perhaps over-expression of these proteins put the cell's protein synthesis machinery in overdrive, and with excessive protein exiting the Golgi, tubules were formed that were much larger than what would exist under normal conditions. Early electron microscopy studies argue against this possibility. Tubulovesicular profiles up to 3 μm in length were shown in longitudinal thin-sections of axons, where no protein was over-expressed (Tsukita and Ishikawa, 1980; Lindsey and Ellisman, 1985). Also, in our studies and those of others, tubular carriers were visible in neurons with very low expression levels, not just the high expressing cells (Nakata et al., 1998; Kaether et al., 2000; Nakata and Hirokawa, 2003; Sabo et al., 2006).

Evidence that more specialized vesicle populations are derived from the common tubule

Multiple reports describe seeing the tubules fragment as they moved in neurons (Nakata et al., 1998; Sabo et al., 2006) or deposit some of their contents at specific sites, such as synaptic sites, as they moved along the axon (Sabo et al., 2006). We too observed instances where it appeared a tubule fragmented or paused and interacted with stationary puncta, perhaps depositing some of its contents; however we feel that imaging at faster frame rates (more than 2 frames per second) will be necessary to definitively identify such dynamic events.

The presence of subdomains within common tubules raises the possibility that the tubules may consist of sub-compartments connected like cars of a train rather than a continuous membrane bound tubule. However, Nakata observed that tubules in distal regions of the axon were shorter than those in proximal regions, suggesting that they had lost some of their contents en route. Importantly, these carriers were also dimmer. If the shortening of the tubule was due to loss of independent units (train cars) then the overall fluorescence would maintain intensity. The fact that the tubes became dimmer and shorter suggests that they are a non-partitioned tubule from which membrane and proteins had been removed.

Two correlative electron microscopy (EM) studies have examined the ultrastructure of transport tubules in axons labeled by GFP-tagged axonal proteins (Nakata et al., 1998; Ahmari et al., 2000). Both studies imaged live cells to identify moving tubules, then fixed and prepared the sample for thin section

EM. In one study, the GFP-tagged tubule was found to be a continuous membrane-bound tubule (Nakata et al., 1998). However, a second study found that the GFP-labeled tubule seen at the light-level corresponded to clusters of pleiomorphic organelles, including dense core vesicles and tubulovesicular structures, which were immunopositive for synaptic vesicle and plasma membrane proteins (Ahmari et al., 2000). More ultrastructural studies will be required to better characterize the axonal transport tubule and determine if it is a continuous compartment or has additional substructure.

Dense core granule proteins and the common transport tubule

The identification of transporting tubules that contained newly synthesized synaptic vesicle proteins and dense core granule proteins contradicts numerous studies that indicate that these proteins depart the Golgi in segregated pathways, namely, constitutive and regulated, respectively (Tooze and Huttner, 1990; Regnier-Vigouroux et al., 1991). However, many of the studies that led to this model used endocrine or neuroendocrine cell lines, and not neurons. Relative to neuroendocrine cells, neurons synthesize more synaptic vesicles and fewer dense core granules, thus it is possible that the Golgi sorting of these proteins differs in neurons. Interestingly, it has been proposed that the immature secretory granule is in effect a post-Golgi sorting station from which proteins are extracted by sorting and budding (von Zastrow and Castle, 1987; Arvan and Castle, 1998). Our data strongly support the Arvan and Castle model, that many, if not all, types of axonal proteins depart the Golgi in a common transport tubule (which may be equivalent to the immature secretory granule) for mass transit to

the axon). Distinct vesicle populations could arise from the common tubular carrier via two routes: (1) Sorting for entry: non-secretory granule proteins are sorted into vesicles that bud from the common carrier while it is moving or paused in the axon. (2) Sorting by retention: non-dense core granule proteins are removed from the common transport tubule while dense core granule proteins are retained, thus the common transport tubule matures into a dense core granule (Arvan and Castle, 1998).

Importantly, this could mean that for some classes of proteins, final delivery to the appropriate subcellular domain (i.e. the synapse, dense core granule, or plasma membrane) could involve a series of transport intermediates: the common tubule, vesicles that bud from the common tubule, or vesicles cycling between the plasma membrane and early endosome—each of which could be moved by a different kinesin. This may explain why Kinesin-1 as well as KIF1A and KIF1Bβ have been implicated in the transport synaptic vesicle proteins.

Previous studies suggest that the Kinesin-1 family of motors transport tubular organelles containing various axonal plasma membrane proteins in the axon (Kaether et al., 2000; Nakata and Hirokawa, 2003), thus, Kinesin-1 family motors may transport synaptic vesicle proteins and dense core granule proteins while they are in the Golgi-derived common tubule. KIF1A's role in transporting synaptic vesicle or dense core granule proteins may begin when these proteins are present in vesicle populations downstream from the Golgi-derived tubule (i.e. mature dense core granules or synaptic vesicle proteins cycling between endosomes and the plasma membrane). Our observation, that KIF1A

colocalized on spherical vesicles containing BDNF at steady state expression, but not with the predominantly Golgi-derived tubules labeled early after expression, support this model.

Methods

Cell Culture and Transfection

500K neurons were plated per 60mm culture dish as described previously (Kaech and Banker, 2006). Briefly, neurons plated on poly-L-lysine coated coverslips and co-cultured over an astroglial feeder monolayer were maintained in serum-free N2 medium (Bottenstein and Sato, 1979). Dissociated primary hippocampal cultures from day-18 rat embryos were transfected with Lipofectamine 2000 (Invitrogen Cat. No. 11668-027 with cDNAs encoding the following proteins: N-terminally or internally-tagged KIF1A in peGFP vector; NgCAM tagged C-terminally with GFP in the JPA7 expression vector (J. Adelman, Vollum Institute) or tagged with mCherry in JPA5 expression vector (J. Adelman, Vollum Institute); synaptotagmin tagged C-terminally with GFP in the Clontech vector; synaptophysin in the chicken β-actin expression vector (Niwa et al., 1991); BDNF tagged C-terminally with mRFP1 in the chicken β-actin vector; phogrin tagged C-terminally with GFP in the Clontech vector; ssNPY tagged C-terminally with mCherry (start methionine for mCherry removed) in chicken β-actin vector; APP tagged C-terminally with YFP in the pCDNA3 vector; SV2 tagged C-terminally with GFP in the Clontech vector; CSP1 tagged N-terminally with GFP in the Clontech vector.

Immunostaining

Eight-day-old cells were transfected with synaptic protein constructs encoding synaptophysin, synaptotagmin, SV2 and CSP1. Two days later, the cells were immunostained for synapsin 1a using rabbit anti synapsin 1 and 2 (Synaptic Systems cat. no. 106-002) at 1:1500 dilution followed by Cy3 goat α rabbit at 1:1000 (Jackson ImmunoResearch Laboratories Inc., cat .no 111-165-003). Cells were fixed with 4% paraformaldehyde in PBS containing 4% sucrose, rinsed briefly in PBS, and then permeabilized in 0.25% TritonX-100 (Sigma T8787) for 5 minutes. Coverslips were rinsed briefly in PBS, blocked using 1% fish gelatin (Sigma G7765) in PBS, and incubated in primary antibody for 1 hour, blocked again in 1% fish gelatin and then incubated in secondary antibodies for 30 minutes and rinsed briefly in PBS. Coverslips were rinsed in water for several seconds before mounting in Elvanol mounting medium. All steps were conducted at room temperature.

Live-cell imaging

To record a population of mainly of Golgi-derived transport vesicles, all live-cell recordings were made within 8-hours of transfection. To observe transport of steady state vesicle populations, imaging was conducted 24-hours after transfection. Coverslips with attached neurons were loaded into a sealed heating chamber (Warner Instruments, Hamden, CT) in a medium consisting half of cell culture medium from the dish of coverslips and half phenol-red-free imaging medium (Hank's balanced salt solution buffered to pH 7.4 with 10mM Hepes and supplemented with 0.6% glucose). All single and dual-color movies were

recorded using a Nikon Spinning disc confocal microscope equipped with a 60x Nikon objective lens heated to 37 °C. 600 msec exposures were captured continuously for single color movie acquisition. Two-color recordings were captured sequentially with 600msec exposures for each color. Immunostained samples were viewed on a Leica DM-RXA widefield microscope using a Leica 63x Plan Apo, N.A. 1.32 objective lens and images captured on a CCD camera (Princeton Instruments).

Image Analysis

Metamorph was used to generate kymographs from time-lapse recordings. After manually drawing a line down the center of the axon moving away from the cell body (anterograde), the software scans each pixel perpendicular to the line and records the location of the brightest pixel at each frame in the movie. Thus as a labeled vesicle moves further along the axon in the anterograde direction during the course of the recording, a positively sloping line is created on the kymograph. Conversely, a labeled vesicle moving in the direction of the cell body (retrograde) appears as a negatively sloping line. The steepness of slope of the lines corresponds to the moving particle's anterograde or retrograde velocity. Stationary puncta are represented by straight lines across the kymograph. To test for colocalization, lines (called regions) were traced on the anterograde and retrograde events on the kymograph of a two-color pair, and then these regions were transferred to the kymograph corresponding to the other color to see if anterograde events in the partner kymograph had matching anterograde and retrograde lines.

Chapter 4

Discussion and future directions

Overview

The live-cell imaging experiments described in this thesis document several new findings relating to selective dendritic transport and the trafficking of axonal proteins, which provide insights as well as raise new questions about how transport is regulated in neurons. I will discuss some of these questions and possible experimental approaches by which they can be addressed.

Two components of selective transport: selective entry and the transport filter

The findings presented in Chapter 2 revealed two important aspects of selective dendritic transport in neurons that will assist future experimenters seeking to understand its mechanism. My work shows that selective transport of dendritic vesicles can be broken into two components: selective entry, which lowers the probability by 40% that dendritic vesicles will enter the axon compared to dendrites, and the transport filter, which prevents dendritic vesicles from advancing beyond the initial segment. The mechanistic bases of these two components must be spatially distinct—the selective entry of dendritic vesicles must be located in the cell body, while the transport filter is located in the base of the axon. Development of the two components may be different as well. Selective block of entry of dendritic vesicles to neurites containing the constitutively active Kinesin-1 motor domain was detected beginning at stage 2 of development. Whether the transport filter was present at stage 2 was difficult to resolve, because the neurites of stage 2 neurons are very short (30 µm). However, the transport filter was fully functional as soon as one of the stage 2

neurites elongated to become the axon, suggesting that the transport filter forms concurrently with axon formation at the latest. These findings will be important to the design and interpretation of future studies that seek to understand the molecular underpinnings of these two transport phenomena.

Are the transport filter and initial segment functionally distinct entities?

The alignment of the transport filter with the initial segment in mature neurons suggests a functional link between the two. A recent study showed that RNAi mediated knockdown of ankyrinG in mature cultured hippocampal neurons led to the disassembly of the initial segment and gradual conversion of the axon to a dendrite (Hedstrom et al., 2008). Microtubules in the former axon became MAP2 positive and dendritic proteins appeared in the formerly axonal plasma membrane, suggesting that the initial segment is required for the maintenance of neuronal polarity (Hedstrom et al., 2008). Interestingly, in a separate study neuronal polarity developed normally in cultured hippocampal neurons in which RNAi targeting ankyrinG was administered before the initial segment was formed (Hedstrom et al., 2007). In these neurons, a MAP2-negative axon arose despite the fact that an initial segment never developed.

Our live-cell imaging showed that the transport filter arose early during development, prior to the initial segment. This finding suggests that during early development the transport filter almost certainly functions independently of the initial segment membrane specialization, a postulate that should be tested by live-cell imaging of dendritic transport in neurons in which the formation of the

initial segment is prevented by RNAi. The early development of the transport filter suggests that it may be required for the development of neuronal polarity. Future experiments that succeed in disrupting the function of the transport filter can test this possibility. Whether or not the transport filter becomes functionally linked to the initial segment in mature neurons is an outstanding question that can be addressed by live-cell imaging of cells in which the initial segment has been disassembled by RNAi. The finding that disruption of the transport filter is a primary result of initial segment disassembly in mature neurons would support the idea that the two are functionally linked at maturity.

The ankyrinG receptor at the initial segment

It is well established that ankyrinG at the initial segment is required for recruitment of the other initial segment components (Zhou et al., 1998; Jenkins and Bennett, 2001; Pan et al., 2006; Hedstrom et al., 2007; Hedstrom et al., 2008); however, how ankyrinG is enriched at the initial segment remains unknown. The answer will likely come from identification of additional proteins localized to the initial segment that could serve as the ankyrinG receptor. Candidate proteins could be identified by using regions of ankyrinG as bait in yeast-two-hybrid screen for interacting proteins. Alternatively, if initial segment could be isolated, mass spectrometry could be used to identify novel initial segment components. Once ankyrinG receptor candidates are identified, their expression could be knocked down in developing hippocampal neurons, to see if the ankyrinG accumulation at the initial segment was impaired.

The role of ultrastructural studies in understanding selective transport

Electron microscopy studies provide provocative clues about how the transport filter might operate. The microtubule tracks running through the initial segment are grouped into fascicles of closely spaced, parallel bundles containing several microtubules each; a microtubule organization which occurs no other place in neurons (Palay et al., 1968; Peters et al., 1968). How or if this organization of microtubules might account for the selective transport of dendritic vesicles is unknown; however, it is reasonable to suspect that it plays a role. Interestingly, in one EM study, when microtubules in the axon hillock were counted and compared to the number of microtubules in the initial segment, there was a significant discrepancy (Peters et al., 1968). Cross-sections of the axon hillock showed a mixture of single and fasciculated microtubules, amounting to 60-100 microtubules total. However, in cross-sections of initial segments, there were 20-50 microtubules total, all contained in fascicles. Because the authors never saw a microtubule in the hillock loop back towards the cell body, they concluded that some of the microtubules end at the start of the initial segment (Peters et al., 1968).

Due to the laborious process of EM studies such as this, there have not been additional studies corroborating this observation; however, it is worth mentioning here because of the interesting implications for models of selective dendritic transport. Perhaps the fasciculated microtubules are specialized tracks for motors exclusively carrying axonal vesicles (on which motors carrying dendritic

vesicles cannot walk). As the axon hillock tapers toward the opening of the axon, the single microtubule tracks that support transport of dendritic vesicles become fewer and fewer, supporting less and less dendritic transport, until they end at the proximal edge of the initial segment. This would result in fewer dendritic vesicles entering the axon (selective entry). Dendritic vesicles being carried along the single microtubules would simply fall off the end of the microtubule and stop, unable to enter the initial segment due to lack of permissive microtubule tracks (the transport filter). Meanwhile, the fascicles of axonal-vesicle transporting microtubules could increase in number as they approach and enter the axon, which would explain the biased entry of axonal transport vesicles to the axon observed in previously described live-cell imaging studies (Burack et al., 2000; Nakata and Hirokawa, 2003). While this model is speculative, it illustrates the importance ultrastructural studies could play in identifying structural basis of the selective dendritic transport.

Ultrastructural experiments performed in conjunction with conditions that dismantle the initial segment could be informative. For instance, mature cultured neurons treated with RNAi for ankyrinG caused a dismantling of the initial segment membrane complex over several days and gradual conversion of the axon to a dendrite (Hedstrom et al., 2008). Knowing the structural effect of ankyrinG -loss on the initial segment could prove quite informative. For instance, thin section EM of the initial segment at different time-points after ankyrinG-knockdown would show if and when loss of ankyrinG affected the organization of the fasciculated microtubules in the initial segment. This, in conjunction with live-

cell imaging of dendritic transport could help determine if ankyrinG-knockdown had a primary effect on selective transport, and if that effect was accompanied by changes in the structure of initial segment microtubules. How the structure of the microtubules changed could provide clues about how dendritic transport through the initial segment is regulated.

Microtubule polarity and the fate of dendritic vesicles in the proximal axon

In Chapter 2, it was shown that dendritic vesicles that entered the axon paused, reversed out of the axon, or fused with the plasma membrane. To understand how a dendritic vesicle reverses out of the axon, it would be useful to know the microtubule polarity in the axon hillock and initial segment. Currently it is not clear exactly where microtubules in the axon become uniformly plus end out. The microtubule polarity in the axon hillock and initial segment is important to consider when imagining possible models of how dendritic vesicles reverse out of the axon. For instance, if all the microtubules in the axon, starting in the hillock or the very base of the axon, are plus end out, then any reversals of dendritic vesicles in the proximal axon would be dynein-driven. Alternatively, if the microtubules are of mixed polarity, the reversal could be mediated by a kinesin. Live-imaging of GFP-tagged plus-tip tracking proteins, such as EB proteins (Tirnauer and Bierer, 2000), are reliable reporters of microtubule polarity (Stepanova et al., 2003) and could be used to address this question. Such evidence could also be provided by the electron microscopy hook assay, though this approach may be more time consuming (McIntosh and Euteneuer, 1984).

Recent discovery of the first signaling molecule localized to the initial segment

Interestingly, a regulatory subunit of nuclear factor-kappaB (NF-κB), a transcription factor involved in many cellular processes, including cell survival (Karin, 1999), has recently been found to associate with the microtubules in the initial segment (Schultz et al., 2006). This subunit is the phosphorylated form of IκBα (pIκBα), which, when phosphorylated, dissociates from NF-κB, thereby exposing its nuclear localization sequence and allowing translocation of NF-κB to the nucleus, where it mediates gene transcription and promotes neurite growth during neuronal development (Gutierrez et al., 2005).

Activated IκB-kinase (IKK), which phosphorylates IκBα, was also enriched at the membrane of the initial segment (Schultz et al., 2006). Interestingly, ankyrinG failed to localize to the initial segment of developing cultured hippocampal neurons when the phosphorylation of IκBα was blocked pharmacologically by addition of an IKK inhibitor to the culture medium in neurons that had recently specified an axon, suggesting a role for the IKK/IκBα pathway in initial segment assembly (Sanchez-Ponce et al., 2008). Because kinase-blocking drugs can have unintended effects on other kinases, however, more direct confirmation is needed to prove that IKK phosphorylation of IκBα is directly involved in ankyrinG recruitment to the initial segment. Another cause for skepticism is that preliminary immunostaining experiments, in which neurons were doubly-stained for ankyrinG and pIκBα, stained the initial segment of stage 3 neurons for

ankyrinG in the absence of pIκBα (data not shown), suggesting that ankyrinG can accumulate at the initial segment before the accumulation of pIκBα.

Nonetheless, members of the NF-κB signaling complex are the first signaling enzymes found to be specifically enriched at the initial segment, and pIκBα is the first identified initial segment microtubule associated protein. As these discoveries are very recent, it will be exciting to learn how these newly discovered signaling molecules function in the initial segment. In particular, it will be of great interest to see if the activation of IκBα and its localization to initial segment microtubules is truly required for ankyrinG accumulation at the initial segment, which would provide evidence that there is physical link between the microtubules of the initial segment and the initial segment membrane specialization. If the microtubule-binding site of pIκBα was identified, it might be possible to interfere with the localization of pIκBα to initial segment microtubules (by over-expressing a form of IκBα with a mutation in the microtubule binding site, or a peptide corresponding to the microtubule binding site) and see if ankyrinG recruitment to the initial segment is prevented and if the transport filter is affected.

Recent finding suggests mechanism for selective entry

The finding that dendritic vesicles enter the axon with a reduced probability while axonal vesicles enter the axon preferentially (Burack et al., 2000; Nakata and Hirokawa, 2003) suggests that the microtubule tracks in the cell body approaching the axon are different. A recent study in MDCK cells, another polarized cell type, detected the presence of a special population of microtubules

that led from the Golgi to the plasma membrane and had high amounts of bound septin2 (SEPT2)(Spiliotis et al., 2008). Septins are GTP-binding proteins that form polymers, organize polarized membrane domains, and serve as scaffolding complexes (Spiliotis and Nelson, 2006). In the MDCK cells, the specialized population of Golgi-proximal microtubules also had high levels of the posttranslational modification, polyglutamylation. The authors proposed that this specialized group of microtubules formed a “fast-track” for rapid delivery of Golgi-derived transport vesicles during times of rapid growth (Spiliotis et al., 2008). An analogous mechanism may exist in neurons, such that a special population of microtubule tracks is optimized for transport of axonal vesicles from the Golgi to the axon. Likewise, these tracks could be less optimal for dendritic transport, resulting in fewer dendritic vesicles moving into the axon. No such specialized tracks have been detected yet in neurons, but the discovery of new microtubule associated proteins and improved antibodies for detecting microtubule modifications, may lead to new discoveries.

Identifying the kinesin responsible for the transport of dendritic vesicles

Knowing the identity of the kinesin that transports dendritic vesicles could provide valuable insights to how the motor might be regulated as it enters the axon (e.g. any known phosphorylation sites that could regulate the motor, or motor interacting proteins that could be regulated). To date, three motors have been implicated in the transport of dendritic proteins. Immunostaining for the motor KIF21B (a Kinesin-4 family member) showed enrichment in dendrites compared

to the axon, but KIF21B was not linked to the transport of any specific dendritic protein (Marszalek et al., 1999). Furthermore, constitutively-active tailless KIF21B did not selectively accumulate in dendrites, as would be expected if the motor intrinsically preferred trafficking on dendritic microtubules (C.F. Huang, personal communication). Rather, truncated KIF21B accumulated at both axons and dendrites showing no transport selectivity. A second motor, KIF17 (a Kinesin-2 family member) has been linked to the transport of a specific dendritic protein, the NMDA-receptor subunit, NR2B (Guillaud et al., 2003). By live-cell imaging, it was shown that expression of YFP-tagged KIF17 in cultured hippocampal neurons labeled punctate structures in dendrites that moved at rates consistent with kinesin-based transport. Immunostaining for NR2B showed that 30% of non-synaptic NR2B clusters in the dendrites co-localized with mobile puncta labeled by YFP-KIF17, suggesting that KIF17 is responsible for the transport of at least 30% of NR2B subunits. RNAi of KIF17 resulted in a 25% reduction in the number of NR2B-immunolabeled puncta in dendrites. However, the knockdown of KIF17 also caused a 34% reduction in NR2B expression levels (Guillaud et al., 2003). A significant portion of the colocalization observed by KIF17 and NR2B in fixed cells could have resulted from spurious overlap. Also, the reduced expression levels, rather than loss of KIF17-mediated transport might have accounted for the reduced NR2B-labeled puncta in the dendrites; these results therefore need to be further tested by two-color live-cell imaging. Finally, although Kinesin-1 has been implicated in the transport of the dendritic cargo GluR2 (Setou et al., 2002) this study used immunoprecipitation studies and

expression of protein fragments to disrupt localization to demonstrate an interaction between Kinesin-1 and the cargo GluR2 (via the adaptor protein, GRIP1) (Setou et al., 2002). These approaches are indirect and need further confirmation; again, live-cell imaging would provide a much clearer picture.

Although it has proven difficult to identify a dendritic kinesin a promising new candidate, KIF13B, has emerged and is currently being investigated in the Banker lab. When GFP-tagged and expressed in cultured hippocampal neurons, KIF13B labels vesicles that move almost exclusively in the dendrites, and to a much lesser extent in the axon (B. Jenkins, personal communication) suggesting that it may selectively move dendritic proteins. Two-color live-cell imaging of cells co-expressing a dendritic protein and KIF13B will be useful in identifying the population of dendritic vesicles that is labeled by KIF13B. RNAi can then be used to selectively knock-down KIF13 and test its role in the transport of these vesicle populations.

The role of Kinesin-3 motors in the transport of dense core granule proteins

Two-color imaging experiments described in Chapter 3 showed that fluorescently labeled synaptic vesicle proteins and dense core granule components depart the Golgi in a common transport tubule. KIF1A-GFP did not label the common tubule, suggesting that KIF1A is not required for the transport of newly synthesized axonal proteins, including dense core granule proteins. However, later after expression, when the fluorescently tagged dense core granule marker BDNF had reached steady state localization, KIF1A co-labeled spherical vesicles

containing BDNF. The BDNF-KIF1A-labeled vesicles detected at steady state may represent mature dense core granules. To support this notion, fluorescently labeled transferrin could be applied to the extracellular medium to show that the BDNF-KIF1A-labeled vesicles are not endosomes. Also, to show that the BDNF-KIF1A-labeled vesicles undergo regulated secretion, live imaging could be conducted during stimulation. It would also be informative to confirm colocalization of other dense core granule markers, such as phogrin, with BDNF-KIF1A-labeled vesicles to verify their identity as dense core granules.

Further experiments should be done to better characterize the movement of the spherical KIF1A-BDNF labeled vesicles. They appear to move short distances, stop and start frequently, and reverse direction more often than other vesicle populations (Chapter 3, Figure 2L, red line), such as the fast-moving transport tubule. This pattern of movement is similar to that described of GFP-labeled mature dense core granules in Vero cells (Wacker et al., 1997). After characterization of KIF1A-BDNF-labeled vesicle movement, the role of KIF1A in their transport could be directly tested by comparing their transport in cultured hippocampal neurons expressing RNAi against KIF1A and control cells transfected with a scrambled RNAi plasmid. This experimental approach illustrates the point that to detect the effect of impaired motor function on the transport of a specific protein, it is critically important to know which vesicle population to analyze, and at what time after transfection. Because the spherical vesicles labeled by KIF1A-BDNF become labeled 24 hours after transfection, and are a subpopulation of the total population of moving vesicles, the effect of

KIF1A-knockdown on transport of BDNF could easily be overlooked without this information in hand.

The role of KIF1A in the transport of synaptic vesicle proteins

In light of the finding that KIF1A associated with BDNF-containing vesicle population at steady state, it is of great interest to perform the same experiments with GFP-tagged synaptic vesicle proteins to determine if KIF1A associates with a synaptic vesicle protein-containing population at steady state. If a KIF1A-synaptic vesicle protein- labeled vesicle population is identified and its transport characterized, KIF1A expression can be knocked down to directly assess the role of KIF1A in the transport its transport.

The role of KIF1Bβ in the transport of synaptic vesicle proteins and dense core granule proteins

Preliminary dual-color experiments of co-expressed KIF1A-GFP and KIF1Bβ labeled with mCherry revealed that about 70% of the vesicles labeled by KIF1A are co-labeled with KIF1Bβ (data not shown). This suggests that both motors move overlapping populations of transport vesicles. This is supported by reports that both motors transport synaptic vesicle proteins (Okada et al., 1995; Yonekawa et al., 1998; Zhao et al., 2001). This high degree of colocalization of KIF1A and KIF1β on moving vesicles also suggests that KIF1Bβ, like KIF1A, is not associated with the fast moving Golgi-derived transport tubule. However, it is possible that KIF1Bβ does associate with dense core granule- and synaptic vesicle protein-containing organelle populations at later expression times. This raises the possibility that KIF1Bβ could compensate for KIF1A in RNAi

experiments. However, KIF1Bβ did not compensate for loss of KIF1A in KIF1A-knockout mouse, which died within 24 hours of birth and had reduced transport of synaptic proteins to synapses (Yonekawa et al., 1998).

It would also be interesting to test if any of the KIF1Bβ-labeled vesicles (most of which co-label for KIF1A when the motors are co-expressed) stop moving in KIF1A knock-down experiments or vice versa. This would indicate that while both motors are present on the vesicle, one motor is a passenger while the other is the driver. It is possible that the motors attached to vesicles are spatially or temporally regulated, such that different motors become activated in different regions of the cell or at different times.

The identity of the motor moving the post-Golgi common transport tubule

If neither KIF1A nor KIF1Bβ are responsible for the transport of the post-Golgi transport tubule, then which kinesin is? We most likely know the answer to this question: Kinesin-1. Kinesin-1 has been implicated in the transport of tubular post-Golgi vesicles that contain several plasma membrane proteins. Expressed fluorescently tagged axonal plasma membrane proteins were shown to transport along axons in elongated tubular vesicles that arose from the Golgi (Nakata et al., 1998). Another axonal plasma membrane protein, APP, when tagged with YFP also labeled long tubular vesicles in the axon, and the transport of these vesicles was impaired by RNAi-mediated knockdown of the kinesin-1 family member, KIF5B (Kaether et al., 2000). APP was shown to bind to Kinesin-1 by biochemical fractionation and *in vitro* binding assays (Kamal et al., 2000).

Kinesin-1 knockdown by RNAi was also shown to impair the transport of GAP-43, another axonal plasma membrane protein transported in a tubular vesicle in the axon (Nakata and Hirokawa, 2003). The transport of this tubular carrier was also blocked by expression of dominant negative versions of Kinesin-1 (Nakata and Hirokawa, 2003). The tubule described in Chapter 3, which can be labeled by expression of GFP-tagged plasma membrane proteins, synaptic vesicle proteins, and dense core granule components, is almost certainly the tubular axonal transport organelle described in these studies. However, it remains to be directly demonstrated that the transport of tubules containing the axonal plasma membrane proteins, synaptic vesicle proteins, and dense core granule components is impaired following Kinesin-1 knock-down in live-cell imaging studies. Experiments are being designed in the Banker lab to acutely inactivate Kinesin-1 in living neurons while simultaneously imaging transport will address this question.

Bibliography

Ahmari SE, Buchanan J, Smith SJ (2000) Assembly of presynaptic active zones from cytoplasmic transport packets. Nat Neurosci 3:445-451.

Aizawa H, Sekine Y, Takemura R, Zhang Z, Nangaku M, Hirokawa N (1992) Kinesin family in murine central nervous system. J Cell Biol 119:1287-1296.

Angelides KJ, Elmer LW, Loftus D, Elson E (1988) Distribution and lateral mobility of voltage-dependent sodium channels in neurons. J Cell Biol 106:1911-1925.

Ango F, di Cristo G, Higashiyama H, Bennett V, Wu P, Huang ZJ (2004) Ankyrin-based subcellular gradient of neurofascin, an immunoglobulin family protein, directs GABAergic innervation at purkinje axon initial segment. Cell 119:257-272.

Arimura N, Kaibuchi K (2007) Neuronal polarity: from extracellular signals to intracellular mechanisms. Nat Rev Neurosci 8:194-205.

Arvan P, Castle D (1992) Protein sorting and secretion granule formation in regulated secretory cells. Trends Cell Biol 2:327-331.

Arvan P, Castle D (1998) Sorting and storage during secretory granule biogenesis: looking backward and looking forward. Biochem J 332 (Pt 3):593-610.

Arvan P, Kuliawat R, Prabakaran D, Zavacki AM, Elahi D, Wang S, Pilkey D (1991) Protein discharge from immature secretory granules displays both regulated and constitutive characteristics. J Biol Chem 266:14171-14174.

Asbury CL (2005) Kinesin: world's tiniest biped. Curr Opin Cell Biol 17:89-97.

Baas PW, Deitch JS, Black MM, Banker GA (1988) Polarity orientation of microtubules in hippocampal neurons: uniformity in the axon and nonuniformity in the dendrite. Proc Natl Acad Sci U S A 85:8335-8339.

Barkus RV, Klyachko O, Horiuchi D, Dickson BJ, Saxton WM (2008) Identification of an axonal kinesin-3 motor for fast anterograde vesicle transport that facilitates retrograde transport of neuropeptides. Mol Biol Cell 19:274-283.

Bennett V, Baines AJ (2001) Spectrin and ankyrin-based pathways: metazoan inventions for integrating cells into tissues. Physiol Rev 81:1353-1392.

Berghs S, Aggujaro D, Dirkx R, Jr., Maksimova E, Stabach P, Hermel JM, Zhang JP, Philbrick W, Slepnev V, Ort T, Solimena M (2000) betaIV spectrin, a new spectrin localized at axon initial segments and nodes of ranvier in the central and peripheral nervous system. J Cell Biol 151:985-1002.

Boiko T, Vakulenko M, Ewers H, Yap CC, Norden C, Winckler B (2007) Ankyrin-dependent and -independent mechanisms orchestrate axonal compartmentalization of L1 family members neurofascin and L1/neuron-glia cell adhesion molecule. J Neurosci 27:590-603.

Bonanomi D, Benfenati F, Valtorta F (2006) Protein sorting in the synaptic vesicle life cycle. Prog Neurobiol 80:177-217.

Bonnet C, Boucher D, Lazereg S, Pedrotti B, Islam K, Denoulet P, Larcher JC (2001) Differential binding regulation of microtubule-associated proteins MAP1A, MAP1B, and MAP2 by tubulin polyglutamylation. J Biol Chem 276:12839-12848.

Bottenstein JE, Sato GH (1979) Growth of a rat neuroblastoma cell line in serum-free supplemented medium. Proc Natl Acad Sci U S A 76:514-517.

Boucher D, Larcher JC, Gros F, Denoulet P (1994) Polyglutamylation of tubulin as a progressive regulator of in vitro interactions between the microtubule-associated protein Tau and tubulin. Biochemistry 33:12471-12477.

Bowman AB, Kamal A, Ritchings BW, Philp AV, McGrail M, Gindhart JG, Goldstein LS (2000) Kinesin-dependent axonal transport is mediated by the sunday driver (SYD) protein. Cell 103:583-594.

Bradke F, Dotti CG (1997) Neuronal polarity: vectorial cytoplasmic flow precedes axon formation. Neuron 19:1175-1186.
Brady ST (1985) A novel brain ATPase with properties expected for the fast axonal transport motor. Nature 317:73-75.
Burack MA, Silverman MA, Banker G (2000) The role of selective transport in neuronal protein sorting. Neuron 26:465-472.
Burgess TL, Kelly RB (1987) Constitutive and regulated secretion of proteins. Annu Rev Cell Biol 3:243-293.
Burre J, Volknandt W (2007) The synaptic vesicle proteome. J Neurochem 101:1448-1462.
Byrd DT, Kawasaki M, Walcoff M, Hisamoto N, Matsumoto K, Jin Y (2001) UNC-16, a JNK-signaling scaffold protein, regulates vesicle transport in C. elegans. Neuron 32:787-800.
Chamberlain C, Hahn KM (2000) Watching proteins in the wild: fluorescence methods to study protein dynamics in living cells. Traffic 1:755-762.
Ching W, Zanazzi G, Levinson SR, Salzer JL (1999) Clustering of neuronal sodium channels requires contact with myelinating Schwann cells. J Neurocytol 28:295-301.
Cool DR, Normant E, Shen F, Chen HC, Pannell L, Zhang Y, Loh YP (1997) Carboxypeptidase E is a regulated secretory pathway sorting receptor: genetic obliteration leads to endocrine disorders in Cpe(fat) mice. Cell 88:73-83.
Craig AM, Banker G (1994) Neuronal polarity. Annu Rev Neurosci 17:267-310.
Davis JQ, Lambert S, Bennett V (1996) Molecular composition of the node of Ranvier: identification of ankyrin-binding cell adhesion molecules neurofascin (mucin+/third FNIII domain-) and NrCAM at nodal axon segments. J Cell Biol 135:1355-1367.
De Camilli P, Jahn R (1990) Pathways to regulated exocytosis in neurons. Annu Rev Physiol 52:625-645.
Deitch JS, Banker GA (1993) An electron microscopic analysis of hippocampal neurons developing in culture: early stages in the emergence of polarity. J Neurosci 13:4301-4315.
Diefenbach RJ, Mackay JP, Armati PJ, Cunningham AL (1998) The C-terminal region of the stalk domain of ubiquitous human kinesin heavy chain contains the binding site for kinesin light chain. Biochemistry 37:16663-16670.
Dikeakos JD, Reudelhuber TL (2007) Sending proteins to dense core secretory granules: still a lot to sort out. J Cell Biol 177:191-196.
Dixit R, Ross JL, Goldman YE, Holzbaur EL (2008) Differential regulation of dynein and kinesin motor proteins by tau. Science 319:1086-1089.
Dotti CG, Sullivan CA, Banker GA (1988) The establishment of polarity by hippocampal neurons in culture. J Neurosci 8:1454-1468.
Dunn S, Morrison EE, Liverpool TB, Molina-Paris C, Cross RA, Alonso MC, Peckham M (2008) Differential trafficking of Kif5c on tyrosinated and detyrosinated microtubules in live cells. J Cell Sci 121:1085-1095.
Dzhashiashvili Y, Zhang Y, Galinska J, Lam I, Grumet M, Salzer JL (2007) Nodes of Ranvier and axon initial segments are ankyrin G-dependent domains that assemble by distinct mechanisms. J Cell Biol 177:857-870.
Edde B, Rossier J, Le Caer JP, Desbruyeres E, Gros F, Denoulet P (1990) Posttranslational glutamylation of alpha-tubulin. Science 247:83-85.
Faundez V, Horng JT, Kelly RB (1997) ADP ribosylation factor 1 is required for synaptic vesicle budding in PC12 cells. J Cell Biol 138:505-515.

Ferreira A, Niclas J, Vale RD, Banker G, Kosik KS (1992) Suppression of kinesin expression in cultured hippocampal neurons using antisense oligonucleotides. J Cell Biol 117:595-606.
Fukushima N, Furuta D, Hidaka Y, Moriyama R, Tsujiuchi T (2009) Post-translational modifications of tubulin in the nervous system. J Neurochem.
Garrido JJ, Giraud P, Carlier E, Fernandes F, Moussif A, Fache MP, Debanne D, Dargent B (2003) A targeting motif involved in sodium channel clustering at the axonal initial segment. Science 300:2091-2094.
Gennerich A, Vale RD (2009) Walking the walk: how kinesin and dynein coordinate their steps. Curr Opin Cell Biol 21:59-67.
Glover G (2005) Polarized Protein Sorting in Hippocampal Neurons. In: Neuroscience Graduate Program. Portland Oregon Health & Science University.
Gomis-Ruth S, Wierenga CJ, Bradke F (2008) Plasticity of polarization: changing dendrites into axons in neurons integrated in neuronal circuits. Curr Biol 18:992-1000.
Guillaud L, Setou M, Hirokawa N (2003) KIF17 dynamics and regulation of NR2B trafficking in hippocampal neurons. J Neurosci 23:131-140.
Gutierrez H, Hale VA, Dolcet X, Davies A (2005) NF-kappaB signalling regulates the growth of neural processes in the developing PNS and CNS. Development 132:1713-1726.
Hall DH, Hedgecock EM (1991) Kinesin-related gene unc-104 is required for axonal transport of synaptic vesicles in C. elegans. Cell 65:837-847.
Hancock WO, Howard J (1998) Processivity of the motor protein kinesin requires two heads. J Cell Biol 140:1395-1405.
Hannah MJ, Schmidt AA, Huttner WB (1999) Synaptic vesicle biogenesis. Annu Rev Cell Dev Biol 15:733-798.
Hedstrom KL, Rasband MN (2006) Intrinsic and extrinsic determinants of ion channel localization in neurons. J Neurochem 98:1345-1352.
Hedstrom KL, Ogawa Y, Rasband MN (2008) AnkyrinG is required for maintenance of the axon initial segment and neuronal polarity. J Cell Biol 183:635-640.
Hedstrom KL, Xu X, Ogawa Y, Frischknecht R, Seidenbecher CI, Shrager P, Rasband MN (2007) Neurofascin assembles a specialized extracellular matrix at the axon initial segment. J Cell Biol 178:875-886.
Heidemann SR, Landers JM, Hamborg MA (1981) Polarity orientation of axonal microtubules. J Cell Biol 91:661-665.
Hirokawa N, Noda Y (2008) Intracellular transport and kinesin superfamily proteins, KIFs: structure, function, and dynamics. Physiol Rev 88:1089-1118.
Hirokawa N, Pfister KK, Yorifuji H, Wagner MC, Brady ST, Bloom GS (1989) Submolecular domains of bovine brain kinesin identified by electron microscopy and monoclonal antibody decoration. Cell 56:867-878.
Horiuchi D, Collins CA, Bhat P, Barkus RV, Diantonio A, Saxton WM (2007) Control of a kinesin-cargo linkage mechanism by JNK pathway kinases. Curr Biol 17:1313-1317.
Hortsch M (1996) The L1 family of neural cell adhesion molecules: old proteins performing new tricks. Neuron 17:587-593.
Huang TG, Suhan J, Hackney DD (1994) Drosophila kinesin motor domain extending to amino acid position 392 is dimeric when expressed in Escherichia coli. J Biol Chem 269:16502-16507.
Ikegami K, Heier RL, Taruishi M, Takagi H, Mukai M, Shimma S, Taira S, Hatanaka K, Morone N, Yao I, Campbell PK, Yuasa S, Janke C, Macgregor GR, Setou M (2007) Loss of alpha-tubulin polyglutamylation in ROSA22 mice is associated

with abnormal targeting of KIF1A and modulated synaptic function. Proc Natl Acad Sci U S A 104:3213-3218.
Ito M, Yoshioka K, Akechi M, Yamashita S, Takamatsu N, Sugiyama K, Hibi M, Nakabeppu Y, Shiba T, Yamamoto KI (1999) JSAP1, a novel jun N-terminal protein kinase (JNK)-binding protein that functions as a Scaffold factor in the JNK signaling pathway. Mol Cell Biol 19:7539-7548.
Jacobson C, Schnapp B, Banker GA (2006) A change in the selective translocation of the Kinesin-1 motor domain marks the initial specification of the axon. Neuron 49:797-804.
Jenkins SM, Bennett V (2001) Ankyrin-G coordinates assembly of the spectrin-based membrane skeleton, voltage-gated sodium channels, and L1 CAMs at Purkinje neuron initial segments. J Cell Biol 155:739-746.
Kaech S, Banker G (2006) Culturing hippocampal neurons. Nat Protoc 1:2406-2415.
Kaether C, Skehel P, Dotti CG (2000) Axonal membrane proteins are transported in distinct carriers: a two-color video microscopy study in cultured hippocampal neurons. Mol Biol Cell 11:1213-1224.
Kamal A, Stokin GB, Yang Z, Xia CH, Goldstein LS (2000) Axonal transport of amyloid precursor protein is mediated by direct binding to the kinesin light chain subunit of kinesin-I. Neuron 28:449-459.
Kanai Y, Okada Y, Tanaka Y, Harada A, Terada S, Hirokawa N (2000) KIF5C, a novel neuronal kinesin enriched in motor neurons. J Neurosci 20:6374-6384.
Kaplan MR, Meyer-Franke A, Lambert S, Bennett V, Duncan ID, Levinson SR, Barres BA (1997) Induction of sodium channel clustering by oligodendrocytes. Nature 386:724-728.
Karin M (1999) How NF-kappaB is activated: the role of the IkappaB kinase (IKK) complex. Oncogene 18:6867-6874.
Kelkar N, Gupta S, Dickens M, Davis RJ (2000) Interaction of a mitogen-activated protein kinase signaling module with the neuronal protein JIP3. Mol Cell Biol 20:1030-1043.
Keller P, Simons K (1997) Post-Golgi biosynthetic trafficking. J Cell Sci 110 (Pt 24):3001-3009.
Khaliq ZM, Raman IM (2006) Relative contributions of axonal and somatic Na channels to action potential initiation in cerebellar Purkinje neurons. J Neurosci 26:1935-1944.
Kim T, Gondre-Lewis MC, Arnaoutova I, Loh YP (2006) Dense-core secretory granule biogenesis. Physiology (Bethesda) 21:124-133.
Klopfenstein DR, Vale RD (2004) The lipid binding pleckstrin homology domain in UNC-104 kinesin is necessary for synaptic vesicle transport in Caenorhabditis elegans. Mol Biol Cell 15:3729-3739.
Kobayashi T, Storrie B, Simons K, Dotti CG (1992) A functional barrier to movement of lipids in polarized neurons. Nature 359:647-650.
Kole MH, Ilschner SU, Kampa BM, Williams SR, Ruben PC, Stuart GJ (2008) Action potential generation requires a high sodium channel density in the axon initial segment. Nat Neurosci 11:178-186.
Kordeli E, Lambert S, Bennett V (1995) AnkyrinG. A new ankyrin gene with neural-specific isoforms localized at the axonal initial segment and node of Ranvier. J Biol Chem 270:2352-2359.
Kuliawat R, Arvan P (1992) Protein targeting via the "constitutive-like" secretory pathway in isolated pancreatic islets: passive sorting in the immature granule compartment. J Cell Biol 118:521-529.

Kuliawat R, Arvan P (1994) Distinct molecular mechanisms for protein sorting within immature secretory granules of pancreatic beta-cells. J Cell Biol 126:77-86.
Lakamper S, Meyhofer E (2006) Back on track - on the role of the microtubule for kinesin motility and cellular function. J Muscle Res Cell Motil 27:161-171.
Lambert S, Davis JQ, Bennett V (1997) Morphogenesis of the node of Ranvier: co-clusters of ankyrin and ankyrin-binding integral proteins define early developmental intermediates. J Neurosci 17:7025-7036.
Larcher JC, Boucher D, Lazereg S, Gros F, Denoulet P (1996) Interaction of kinesin motor domains with alpha- and beta-tubulin subunits at a tau-independent binding site. Regulation by polyglutamylation. J Biol Chem 271:22117-22124.
Lawrence CJ et al. (2004) A standardized kinesin nomenclature. J Cell Biol 167:19-22.
Lee KD, Hollenbeck PJ (1995) Phosphorylation of kinesin in vivo correlates with organelle association and neurite outgrowth. J Biol Chem 270:5600-5605.
Lemaillet G, Walker B, Lambert S (2003) Identification of a conserved ankyrin-binding motif in the family of sodium channel alpha subunits. J Biol Chem 278:27333-27339.
Leopold PL, McDowall AW, Pfister KK, Bloom GS, Brady ST (1992) Association of kinesin with characterized membrane-bounded organelles. Cell Motil Cytoskeleton 23:19-33.
Liao G, Gundersen GG (1998) Kinesin is a candidate for cross-bridging microtubules and intermediate filaments. Selective binding of kinesin to detyrosinated tubulin and vimentin. J Biol Chem 273:9797-9803.
Lindsey JD, Ellisman MH (1985) The neuronal endomembrane system. III. The origins of the axoplasmic reticulum and discrete axonal cisternae at the axon hillock. J Neurosci 5:3135-3144.
Marszalek JR, Weiner JA, Farlow SJ, Chun J, Goldstein LS (1999) Novel dendritic kinesin sorting identified by different process targeting of two related kinesins: KIF21A and KIF21B. J Cell Biol 145:469-479.
Marx A, Muller J, Mandelkow EM, Hoenger A, Mandelkow E (2006) Interaction of kinesin motors, microtubules, and MAPs. J Muscle Res Cell Motil 27:125-137.
McIntosh JR, Euteneuer U (1984) Tubulin hooks as probes for microtubule polarity: an analysis of the method and an evaluation of data on microtubule polarity in the mitotic spindle. J Cell Biol 98:525-533.
Miki H, Okada Y, Hirokawa N (2005) Analysis of the kinesin superfamily: insights into structure and function. Trends Cell Biol 15:467-476.
Miller KE, DeProto J, Kaufmann N, Patel BN, Duckworth A, Van Vactor D (2005) Direct observation demonstrates that Liprin-alpha is required for trafficking of synaptic vesicles. Curr Biol 15:684-689.
Morfini G, Szebenyi G, Richards B, Brady ST (2001) Regulation of kinesin: implications for neuronal development. Dev Neurosci 23:364-376.
Morfini G, Szebenyi G, Elluru R, Ratner N, Brady ST (2002) Glycogen synthase kinase 3 phosphorylates kinesin light chains and negatively regulates kinesin-based motility. EMBO J 21:281-293.
Morfini G, Pigino G, Szebenyi G, You Y, Pollema S, Brady ST (2006) JNK mediates pathogenic effects of polyglutamine-expanded androgen receptor on fast axonal transport. Nat Neurosci 9:907-916.
Morii H, Takenawa T, Arisaka F, Shimizu T (1997) Identification of kinesin neck region as a stable alpha-helical coiled coil and its thermodynamic characterization. Biochemistry 36:1933-1942.
Nakada C, Ritchie K, Oba Y, Nakamura M, Hotta Y, Iino R, Kasai RS, Yamaguchi K, Fujiwara T, Kusumi A (2003) Accumulation of anchored proteins forms

membrane diffusion barriers during neuronal polarization. Nat Cell Biol 5:626-632.
Nakagawa H, Koyama K, Murata Y, Morito M, Akiyama T, Nakamura Y (2000) EB3, a novel member of the EB1 family preferentially expressed in the central nervous system, binds to a CNS-specific APC homologue. Oncogene 19:210-216.
Nakata T, Hirokawa N (2003) Microtubules provide directional cues for polarized axonal transport through interaction with kinesin motor head. J Cell Biol 162:1045-1055.
Nakata T, Hirokawa N (2007) Neuronal polarity and the kinesin superfamily proteins. Sci STKE 2007:pe6.
Nakata T, Terada S, Hirokawa N (1998) Visualization of the dynamics of synaptic vesicle and plasma membrane proteins in living axons. J Cell Biol 140:659-674.
Nangaku M, Sato-Yoshitake R, Okada Y, Noda Y, Takemura R, Yamazaki H, Hirokawa N (1994) KIF1B, a novel microtubule plus end-directed monomeric motor protein for transport of mitochondria. Cell 79:1209-1220.
Niwa H, Yamamura K, Miyazaki J (1991) Efficient selection for high-expression transfectants with a novel eukaryotic vector. Gene 108:193-199.
Nogales E, Wolf SG, Downing KH (1998) Structure of the alpha beta tubulin dimer by electron crystallography. Nature 391:199-203.
Okada Y, Yamazaki H, Sekine-Aizawa Y, Hirokawa N (1995) The neuron-specific kinesin superfamily protein KIF1A is a unique monomeric motor for anterograde axonal transport of synaptic vesicle precursors. Cell 81:769-780.
Orci L, Ravazzola M, Amherdt M, Perrelet A, Powell SK, Quinn DL, Moore HP (1987) The trans-most cisternae of the Golgi complex: a compartment for sorting of secretory and plasma membrane proteins. Cell 51:1039-1051.
Otsuka AJ, Jeyaprakash A, Garcia-Anoveros J, Tang LZ, Fisk G, Hartshorne T, Franco R, Born T (1991) The C. elegans unc-104 gene encodes a putative kinesin heavy chain-like protein. Neuron 6:113-122.
Pack-Chung E, Kurshan PT, Dickman DK, Schwarz TL (2007) A Drosophila kinesin required for synaptic bouton formation and synaptic vesicle transport. Nat Neurosci 10:980-989.
Palay SL, Sotelo C, Peters A, Orkand PM (1968) The axon hillock and the initial segment. J Cell Biol 38:193-201.
Palmer LM, Stuart GJ (2006) Site of action potential initiation in layer 5 pyramidal neurons. J Neurosci 26:1854-1863.
Pan Z, Kao T, Horvath Z, Lemos J, Sul JY, Cranstoun SD, Bennett V, Scherer SS, Cooper EC (2006) A common ankyrin-G-based mechanism retains KCNQ and NaV channels at electrically active domains of the axon. J Neurosci 26:2599-2613.
Peters A, Proskauer CC, Kaiserman-Abramof IR (1968) The small pyramidal neuron of the rat cerebral cortex. The axon hillock and initial segment. J Cell Biol 39:604-619.
Pigino G, Morfini G, Atagi Y, Deshpande A, Yu C, Jungbauer L, Ladu M, Busciglio J, Brady S (2009) Disruption of fast axonal transport is a pathogenic mechanism for intraneuronal amyloid beta. Proc Natl Acad Sci U S A.
Rahman A, Friedman DS, Goldstein LS (1998) Two kinesin light chain genes in mice. Identification and characterization of the encoded proteins. J Biol Chem 273:15395-15403.
Rao S, Lang C, Levitan ES, Deitcher DL (2001) Visualization of neuropeptide expression, transport, and exocytosis in Drosophila melanogaster. J Neurobiol 49:159-172.

Reed NA, Cai D, Blasius TL, Jih GT, Meyhofer E, Gaertig J, Verhey KJ (2006) Microtubule acetylation promotes kinesin-1 binding and transport. Curr Biol 16:2166-2172.

Regnier-Vigouroux A, Tooze SA, Huttner WB (1991) Newly synthesized synaptophysin is transported to synaptic-like microvesicles via constitutive secretory vesicles and the plasma membrane. EMBO J 10:3589-3601.

Rivera J, Chu PJ, Lewis TL, Jr., Arnold DB (2007) The role of Kif5B in axonal localization of Kv1 K(+) channels. Eur J Neurosci 25:136-146.

Rosenbaum J (2000) Cytoskeleton: functions for tubulin modifications at last. Curr Biol 10:R801-803.

Rudolf R, Salm T, Rustom A, Gerdes HH (2001) Dynamics of immature secretory granules: role of cytoskeletal elements during transport, cortical restriction, and F-actin-dependent tethering. Mol Biol Cell 12:1353-1365.

Sabo SL, Gomes RA, McAllister AK (2006) Formation of presynaptic terminals at predefined sites along axons. J Neurosci 26:10813-10825.

Sakamoto R, Byrd DT, Brown HM, Hisamoto N, Matsumoto K, Jin Y (2005) The Caenorhabditis elegans UNC-14 RUN domain protein binds to the kinesin-1 and UNC-16 complex and regulates synaptic vesicle localization. Mol Biol Cell 16:483-496.

Salzer JL (2003) Polarized domains of myelinated axons. Neuron 40:297-318.

Sampo B, Kaech S, Kunz S, Banker G (2003) Two distinct mechanisms target membrane proteins to the axonal surface. Neuron 37:611-624.

Sanchez-Ponce D, Tapia M, Munoz A, Garrido JJ (2008) New role of IKK alpha/beta phosphorylated I kappa B alpha in axon outgrowth and axon initial segment development. Mol Cell Neurosci 37:832-844.

Sato-Yoshitake R, Yorifuji H, Inagaki M, Hirokawa N (1992) The phosphorylation of kinesin regulates its binding to synaptic vesicles. J Biol Chem 267:23930-23936.

Schlierf B, Fey GH, Hauber J, Hocke GM, Rosorius O (2000) Rab11b is essential for recycling of transferrin to the plasma membrane. Exp Cell Res 259:257-265.

Scholey JM, Heuser J, Yang JT, Goldstein LS (1989) Identification of globular mechanochemical heads of kinesin. Nature 338:355-357.

Schultz C, Konig HG, Del Turco D, Politi C, Eckert GP, Ghebremedhin E, Prehn JH, Kogel D, Deller T (2006) Coincident enrichment of phosphorylated IkappaBalpha, activated IKK, and phosphorylated p65 in the axon initial segment of neurons. Mol Cell Neurosci 33:68-80.

Seiler S, Kirchner J, Horn C, Kallipolitou A, Woehlke G, Schliwa M (2000) Cargo binding and regulatory sites in the tail of fungal conventional kinesin. Nat Cell Biol 2:333-338.

Setou M, Hayasaka T, Yao I (2004) Axonal transport versus dendritic transport. J Neurobiol 58:201-206.

Setou M, Seog DH, Tanaka Y, Kanai Y, Takei Y, Kawagishi M, Hirokawa N (2002) Glutamate-receptor-interacting protein GRIP1 directly steers kinesin to dendrites. Nature 417:83-87.

Shahani N, Brandt R (2002) Functions and malfunctions of the tau proteins. Cell Mol Life Sci 59:1668-1680.

Shaner NC, Campbell RE, Steinbach PA, Giepmans BN, Palmer AE, Tsien RY (2004) Improved monomeric red, orange and yellow fluorescent proteins derived from Discosoma sp. red fluorescent protein. Nat Biotechnol 22:1567-1572.

Silverman MA, Kaech S, Jareb M, Burack MA, Vogt L, Sonderegger P, Banker G (2001) Sorting and directed transport of membrane proteins during development of hippocampal neurons in culture. Proc Natl Acad Sci U S A 98:7051-7057.

Song AH, Wang D, Chen G, Li Y, Luo J, Duan S, Poo MM (2009) A selective filter for cytoplasmic transport at the axon initial segment. Cell 136:1148-1160.
Spiliotis ET, Nelson WJ (2006) Here come the septins: novel polymers that coordinate intracellular functions and organization. J Cell Sci 119:4-10.
Spiliotis ET, Hunt SJ, Hu Q, Kinoshita M, Nelson WJ (2008) Epithelial polarity requires septin coupling of vesicle transport to polyglutamylated microtubules. J Cell Biol 180:295-303.
Srinivasan Y, Elmer L, Davis J, Bennett V, Angelides K (1988) Ankyrin and spectrin associate with voltage-dependent sodium channels in brain. Nature 333:177-180.
Stagi M, Gorlovoy P, Larionov S, Takahashi K, Neumann H (2006) Unloading kinesin transported cargoes from the tubulin track via the inflammatory c-Jun N-terminal kinase pathway. FASEB J 20:2573-2575.
Stepanova T, Slemmer J, Hoogenraad CC, Lansbergen G, Dortland B, De Zeeuw CI, Grosveld F, van Cappellen G, Akhmanova A, Galjart N (2003) Visualization of microtubule growth in cultured neurons via the use of EB3-GFP (end-binding protein 3-green fluorescent protein). J Neurosci 23:2655-2664.
Sullivan KF, Cleveland DW (1986) Identification of conserved isotype-defining variable region sequences for four vertebrate beta tubulin polypeptide classes. Proc Natl Acad Sci U S A 83:4327-4331.
Takamori S et al. (2006) Molecular anatomy of a trafficking organelle. Cell 127:831-846.
Thomas-Reetz AC, De Camilli P (1994) A role for synaptic vesicles in non-neuronal cells: clues from pancreatic beta cells and from chromaffin cells. FASEB J 8:209-216.
Tirnauer JS, Bierer BE (2000) EB1 proteins regulate microtubule dynamics, cell polarity, and chromosome stability. J Cell Biol 149:761-766.
Tooze SA, Huttner WB (1990) Cell-free protein sorting to the regulated and constitutive secretory pathways. Cell 60:837-847.
Tripet B, Vale RD, Hodges RS (1997) Demonstration of coiled-coil interactions within the kinesin neck region using synthetic peptides. Implications for motor activity. J Biol Chem 272:8946-8956.
Tsukita S, Ishikawa H (1980) The movement of membranous organelles in axons. Electron microscopic identification of anterogradely and retrogradely transported organelles. J Cell Biol 84:513-530.
Vale RD (2003) The molecular motor toolbox for intracellular transport. Cell 112:467-480.
Vale RD, Reese TS, Sheetz MP (1985) Identification of a novel force-generating protein, kinesin, involved in microtubule-based motility. Cell 42:39-50.
Vallee RB, Williams JC, Varma D, Barnhart LE (2004) Dynein: An ancient motor protein involved in multiple modes of transport. J Neurobiol 58:189-200.
Valtorta F, Fesce R, Grohovaz F, Haimann C, Hurlbut WP, Iezzi N, Torri Tarelli F, Villa A, Ceccarelli B (1990) Neurotransmitter release and synaptic vesicle recycling. Neuroscience 35:477-489.
Verhey KJ, Meyer D, Deehan R, Blenis J, Schnapp BJ, Rapoport TA, Margolis B (2001) Cargo of kinesin identified as JIP scaffolding proteins and associated signaling molecules. J Cell Biol 152:959-970.
Vershinin M, Carter BC, Razafsky DS, King SJ, Gross SP (2007) Multiple-motor based transport and its regulation by Tau. Proc Natl Acad Sci U S A 104:87-92.
von Zastrow M, Castle JD (1987) Protein sorting among two distinct export pathways occurs from the content of maturing exocrine storage granules. J Cell Biol 105:2675-2684.

Wacker I, Kaether C, Kromer A, Migala A, Almers W, Gerdes HH (1997) Microtubule-dependent transport of secretory vesicles visualized in real time with a GFP-tagged secretory protein. J Cell Sci 110 (Pt 13):1453-1463.

Wasmeier C, Hutton JC (1996) Molecular cloning of phogrin, a protein-tyrosine phosphatase homologue localized to insulin secretory granule membranes. J Biol Chem 271:18161-18170.

Westermann S, Weber K (2003) Post-translational modifications regulate microtubule function. Nat Rev Mol Cell Biol 4:938-947.

Winckler B, Forscher P, Mellman I (1999) A diffusion barrier maintains distribution of membrane proteins in polarized neurons. Nature 397:698-701.

Winkler H (1997) Membrane composition of adrenergic large and small dense cored vesicles and of synaptic vesicles: consequences for their biogenesis. Neurochem Res 22:921-932.

Wisco D, Anderson ED, Chang MC, Norden C, Boiko T, Folsch H, Winckler B (2003) Uncovering multiple axonal targeting pathways in hippocampal neurons. J Cell Biol 162:1317-1328.

Woehlke G, Ruby AK, Hart CL, Ly B, Hom-Booher N, Vale RD (1997) Microtubule interaction site of the kinesin motor. Cell 90:207-216.

Yang JT, Laymon RA, Goldstein LS (1989) A three-domain structure of kinesin heavy chain revealed by DNA sequence and microtubule binding analyses. Cell 56:879-889.

Yang Y, Ogawa Y, Hedstrom KL, Rasband MN (2007) betaIV spectrin is recruited to axon initial segments and nodes of Ranvier by ankyrinG. J Cell Biol 176:509-519.

Yonekawa Y, Harada A, Okada Y, Funakoshi T, Kanai Y, Takei Y, Terada S, Noda T, Hirokawa N (1998) Defect in synaptic vesicle precursor transport and neuronal cell death in KIF1A motor protein-deficient mice. J Cell Biol 141:431-441.

Zahn TR, Angleson JK, MacMorris MA, Domke E, Hutton JF, Schwartz C, Hutton JC (2004) Dense core vesicle dynamics in Caenorhabditis elegans neurons and the role of kinesin UNC-104. Traffic 5:544-559.

Zhang X, Bennett V (1998) Restriction of 480/270-kD ankyrin G to axon proximal segments requires multiple ankyrin G-specific domains. J Cell Biol 142:1571-1581.

Zhao C, Takita J, Tanaka Y, Setou M, Nakagawa T, Takeda S, Yang HW, Terada S, Nakata T, Takei Y, Saito M, Tsuji S, Hayashi Y, Hirokawa N (2001) Charcot-Marie-Tooth disease type 2A caused by mutation in a microtubule motor KIF1Bbeta. Cell 105:587-597.

Zhou D, Lambert S, Malen PL, Carpenter S, Boland LM, Bennett V (1998) AnkyrinG is required for clustering of voltage-gated Na channels at axon initial segments and for normal action potential firing. J Cell Biol 143:1295-1304.

Zhou HM, Brust-Mascher I, Scholey JM (2001) Direct visualization of the movement of the monomeric axonal transport motor UNC-104 along neuronal processes in living Caenorhabditis elegans. J Neurosci 21:3749-3755.